# VISUAL CHANNELS IN AGING

# THE EFFECT OF AGING ON VISUAL ORIENTATION AND SPATIAL FREQUENCY CHANNELS

By

STANLEY W. GOVENLOCK, BSc

A Thesis

Submitted to the School of Graduate Studies

In Partial Fulfillment of the Requirements

for the Degree

Doctor of Philosophy

McMaster University

DOCTOR OF PHILOSOPHY (2010)
(Psychology)
McMaster University
Hamilton, Ontario

TITLE: The effect of aging on visual orientation and spatial frequency channels
AUTHOR: Stanley W. Govenlock, BSc (University of Lethbridge)
SUPERVISORS: Professor Patrick J. Bennett and Professor Allison B. Sekuler
NUMBER OF PAGES: xii, 130

# Abstract

Although nearly one third of the Canadian population is projected to be over the age of 65 by the year 2030, we know relatively little about how aging affects brain function generally, let alone how aging affects visual perception. The current dissertation was conducted as part of a research programme designed to better characterize how aging affects visual perception.

Older persons exhibit a variety of deficits for perception of complex visual forms. The perception of these complex forms—including everyday forms such as faces and objects—is subserved by low-level channels that are selective, or tuned, for the orientation and spatial frequency of luminance-defined contours in the visual scene. The bandwidth of these channels is inversely related to the amount of information that they can pass on to higher visual processes; narrowly-tuned channels are better. Single-cell physiological investigations of primates suggest that visual cortex neurons thought to subserve these channels exhibit broader tuning in senescence. If these channels become broadly-tuned in older aging, this could explain age-related deficits for complex form perception. In Chapters 2 and 3 of the current thesis, I measured the tuning of these channels in otherwise healthy, older humans using psychophysical masking techniques. In Chapters 4 and 5, I measured the average tuning of the neurons thought to underlie these channels in older human adults, physiologically, using electroencephalography (EEG). Despite the aforementioned reports of functional decline in senescent neurons, psychophysical and physiological orientation and spatial frequency tuning did not differ between younger and older adults. One explanation for this discrepancy is that there is a methodological issue in the single-cell primate literature wherein anesthetics interact with senescence to produce seemingly broader neural tuning. Another explanation is that older humans do have otherwise detuned neurons and channels, but are able to tune their neurons and channels by the action of consciousness, attention, or age-related compensatory brain reorganization.

# Preface

This thesis comprises six chapters. Chapters 2 through 5, presenting the research, are written in journal article format. After I wrote initial drafts, Chapters 2 and 3 were revised collaboratively with my supervisors, Patrick J Bennett (PJB), and Allison B Sekuler (ABS), and a senior grad student, Christopher P Taylor (CPT). Chapters 2 and 3 have been published in the journal, Vision Research, published by Elsevier. After being reformatted to suit McMaster thesis guidelines, Chapters 2 and 3 have been reproduced here with full permission from Elsevier: As stated under, "Author's Rights," authors retain the "right to include the journal article, in full or in part, in a thesis or dissertation." As of August 20, 2010 this policy could be found at the following website:

http://www.elsevier.com/wps/find/authorsview.authors/copyright#whatrights

After I wrote initial drafts, Chapters 4 and 5 were revised collaboratively with my supervisors, and are manuscripts being prepared for journal submission.

For all chapters, as the primary author, I oversaw all aspects of the research. The programming for Chapters 2 and 4 was primarily done by CPT and PJB, respectively. I adapted their code for Chapters 3 and 5. I was assisted in the data collection for Chapters 2 and 3 by our research assistant, Donna Waxman. I was assisted in the data collection for Chapters 4 and 5 by various undergraduate students. I was primarily responsible for the data analysis in all chapters.

This research was supported by a grant from the Canadian Institutes of Health Research (CIHR) to PJB and ABS, the Canada Research Chairs program, which supports PJB and ABS, and the now inactive CIHR Strategic Training Grant on Communication and Social Interaction in Healthy Aging, of which PJB and ABS were mentors and I was a trainee. This research was also supported by a Natural Sciences and Engineering Research Council (NSERC) of Canada Postgraduate Scholarship M(asters) to myself for Year 1 and Year 2 of my postgraduate studies, an Ontario Graduate Scholarship: Science and Technology in Year 3, and second NSERC Postgraduate Scholarship P(hD) in Years 4 and 5. Portions of this work were presented at the 6th, 8th, and 10th annual meetings of the Vision Sciences Society, and at the McMaster Department of Psychology Cognition/Perception Seminar in November, 2006, October, 2008, and January, 2010.

# Acknowledgements

First, thanks to Pat and Allison for teaching me programming, design, analysis, writing, and critical thinking skills that will serve me well in the future, no matter what field I end up in. Thanks to Donna Waxman for being the greatest possible research assistant, a most generous friend, and a baker of fine treats. Thanks to all my labmates for being great friends and colleagues. Thanks to my parents, Alice and Gerald, my brothers, Paul and William, and our dogs, Heidi, Rosie, Missie, and, I suppose, Pebbles too, for their love and support. Thanks to Nikki Benevides also for her love and support during my time in graduate school. And finally, thanks to John Vokey for fostering my intellectual growth.

# Contents

# List of Tables

# List of Figures

# Chapter 1

# General Introduction

This dissertation concerns the interaction between healthy aging and low-level spatial vision mechanisms. Spatial vision — also called pattern vision — concerns low-level visual processes that, during the act of seeing, operate after the visual scene is registered by the photoreceptors of the retina, but before higher-level cortical visual areas that complete the perception of complex, everyday forms such as objects, faces, and the many other components of visual scenes. After the visual scene is initially registered in an approximately point-by-point fashion by the photoreceptors of the retina, these low-level mechanisms begin to integrate that information across space to yield information about how luminance changes across the visual scene. Many classic studies in vision research suggest that these low-level mechanisms are particularly concerned with the orientation and the spatial scale (i.e., spatial frequency) at which these luminance changes occur (for a review, see DeValois and DeValois, 1988). Insofar as the visual system is organized as a processing hierarchy (Felleman and Van Essen, 1991), these mechanisms — which I shall refer to as orientation and spatial frequency channels, filters, or -selective mechanisms — pass the results of their computations on to intermediate and higher-level visual processes that integrate localized samples of orientation and spatial frequency information into contours, curvature, textures, shapes, features, and, eventually, whole objects and scenes, which can then be interfaced with memory to serve visual cognition and recognition.

These low-level mechanisms can be conceptualized as spatially-localized banks of orientation-selective channels, each channel selective for luminance changes at different orientations, and spatially-localized banks of spatial frequency-selective channels, each channel selective for luminance changes at a different spatial scale or frequency (Campbell

and Kulikowski, 1966; Campbell and Robson, 1968; Pantle and Sekuler, 1968; Gilinsky, 1968; Graham and Nachmias, 1971; Kelly and Magnuski, 1975). A particular channel responds most strongly if a stimulus is presented at its preferred orientation or spatial frequency, and its response drops-off as a stimulus is moved away from the channel's preferred value along either the orientation or spatial frequency dimension. An observer monitoring the output of these channels (i.e., higher-level visual processes) can know something about the orientation and spatial frequency content of luminance-changes in the visual scene based on the relative responses of these channels. For example, if the visual scene consists only of a horizontal edge, such as a horizon, channels selective for horizontal will respond strongly, whereas channels selective for vertical will not, thereby providing information about the visual scene to the observer. Complex visual forms are broadband with respect to their orientation and spatial frequency content, they contain energy at many orientations and spatial frequencies. Therefore, when performing complex form perception, higher level visual centers must simultaneously consider the relative responses of many channels, whose passbands cumulatively span the orientation and spatial frequency dimensions.

The computations that these orientation- and spatial frequency-selective mechanisms perform are instantiated in the electrophysiological functioning of neurons in the retina (i.e., retinal ganglion cells), in the relay nucleus between the eyes and the cerebral cortex, the lateral geniculate nucleus (LGN), and, perhaps most significantly, in the primary and secondary visual cortices (areas V1 and V2). Although the entirety of the processing done by the retina — the most well-studied neural structure — is far from understood (Dacey, 2000), retinal ganglion cells tend to exhibit circularly-symmetric, antagonistic, center-surround receptive fields (Kuffler, 1953; Barlow et al., 1964; Barlow and Levick, 1965). In turn, at least to a first approximation, neurons in the lateral geniculate nucleus seem to inherit and relay these center-surround spatial response properties from the retina to the primary visual cortex. These retinal and geniculate neurons, having receptive fields of different sizes, perform the beginnings of the spatial frequency analysis of the visual scene: some neurons respond to very fine luminance changes (i.e., high spatial frequencies, at which luminance changes rapidly over some retinal angle), and other neurons respond to very coarse luminance changes (i.e., low spatial frequencies). Neuronal orientation-selectivity first arises in V1 neurons (e.g., Hubel and Wiesel, 1962; DeValois et al., 1982). V1 neurons are also selective for particular spatial frequencies (Blakemore and Campbell, 1969; De Valois et al., 1982, e.g.,). The degree of selectivity that V1 neurons exhibit for orientation and spatial frequency is thought to be due to the spatial arrangement of their

geniculate input (Hubel and Wiesel, 1962) in conjunction with non-linearities arising via spike-thresholding (e.g., Gillespie et al., 2001; Priebe and Ferster, 2008) and/or the effects of lateral intracortical inhibitory activity (e.g., Sillito, 1975a,b; Eysel et al., 1998; Xing et al., 2005).

Because of response variability in these channels for any given input — attributable to the stochastic nature of neuronal firing — the selectivity of these channels is positively related to the amount of information that they can convey to higher level visual processes[1]. A channel, or neuron, selective for horizontal luminance contours is informative (i.e., dependable or reliable) only insofar as its response to horizontal contours can be distinguished from its response to non-horizontal contours. In the example, above, of an observer trying to detect the presence of a horizon in the visual scene, if the channel formerly selective for horizontal contours were to, for whatever reason, become less selective such that it responded as strongly, or nearly as strongly, to vertical contours, then that channel could no longer be used by the observer to reliably signal the presence of the horizon. This scenario brings us to the issue of the aging visual system.

## 1.1 Aging and Pattern Vision

Seniors — persons aged 65 years or older[2], whom I shall synonymously refer to as seniors, elderly persons, older persons, older adults, older observers, older participants, and older subjects — constitute an increasing portion of the general Canadian population. As of the most recent census projections (Statistics Canada - Catalogue No. 97-551, 2006),

[1]If an observer monitored the state of the world through one or more *noiseless* Gaussian-like channels, then the bandwidth of those channels could be arbitrarily broad and the channels would still convey a high degree of information to the observer. In other words, even out on the asymptotes of this channel's response profile, the small difference in response given some constant change in the input along the dimension to which the channel is selective would still be a dependable and useful difference that could be used to detect that change in the input. However, channels that are instantiated in physical media (i.e., real channels) inevitably involve some element of response variability (i.e., internal noise). Because of this variability, Gaussian-like channels are most informative along their flanks where their response profile changes at the greatest rate given some constant change in the input (i.e., at the maxima of their first derivative). The sharper the tuning of such a channel—the more selective it is—the steeper its flanks will be and the more informative it will be. There is a trade-off, of course: one might desire an arbitrarily large number of channels with an infinitely narrow bandwidth to detect arbitrarily small changes in the input along some stimulus dimension (e.g., orientation), but physically instantiating an arbitrarily large number of channels is impractical for many reasons. Presumably, the human visual system has evolved to achieve some sort of compromise between channel narrowness and number.

[2]In our lab, we actually use 60 as the minimum age for our our older participants. However, the great majority of our older participants are more than 65 years of age.

1 in every 7 Canadians were over 65 years of age in the year 2006, but by the year 2030 this ratio is predicted to be about 1 in every 3.5 Canadians. Despite the growth of this subset of the population, we know relatively little about how aging affects brain function, let alone how aging affects visual perception. The current dissertation is part of a general research agenda that aims to better understand how brain and behaviour change, or are maintained, during the course of healthy older aging.

Relative to young adults, otherwise healthy older adults exhibit a variety of deficits for complex visual form perception (e.g., Stanford and Pollack, 1984; Herbert et al., 2002; Boutet and Faubert, 2006; Del Viva and Agostini, 2007; Habak et al., 2008; Roudaia et al., 2008; Ruffman et al., 2009). These forms range from curvature and textures, to the perception of entire faces, bodies, and other everyday 3-dimensional objects. These visual forms can all be considered to be complex insofar as they require the integration of output from more than one spatially-localized orientation or spatial frequency-selective mechanism. Some portion of these changes in complex form perception is attributable to well-known age-related changes in the optical quality of the eye, including yellowing of the lens, constriction and inflexibility of the pupil (i.e., senile meiosis), opacification of the lens, and a build-up of debris suspended in the intra-ocular media (Weale, 1992). However, some substantial remaining portion of these declines are attributable to declines in post-optical structures (i.e., photoreceptors and neurons) that have yet to be fully characterized (Sekuler and Sekuler, 2000).

Anatomically, there is little evidence that age affects the visual pathway after the optics of the eye. There does seem to be some attrition of photoreceptors during the course of normal aging, but this loss primarily affects rods as opposed to cones (Curcio et al., 1993; Jackson et al., 2002), which explains complaints of poor night-time (i.e., scotopic conditions) vision by seniors, but does not explain age-related declines for vision in photopic (i.e., typical lighting conditions indoors, or brighter) conditions, when cones are primarily relied upon. Along the geniculostriate pathway (LGN and V1), several post-mortem studies have reported no significant change in cell number or morphology (e.g., dendritic branching) in humans or primates as a function of older age (for a review, see Spear, 1993).

Physiologically, the stimulus-response properties of retinal and geniculate neurons are not noticeably affected by older age (Spear, 1993; Spear et al., 1994). However, marked functional declines do seem to take place in senescence in cortical neurons. A series of single-cell studies from Leventhal and colleagues have shown that spontaneous

firing rates increase and orientation-selectivity decreases significantly in senescent primate (Schmolesky et al., 2000) and feline (Hua et al., 2006) V1 and primate V2 (Yu et al., 2006) neurons. Additional experiments implicate an age-related decline in the efficacy of GABAergic intracortical inhibitory activity, which previous research has suggested is necessary for the degree of stimulus selectivity exhibited by V1 neurons (e.g., Sillito, 1975a; Nelson et al., 1994), as the cause for this detuning and increase in spontaneous firing rates (Leventhal et al., 2003; Hua et al., 2008). Further, although an assay of neuronal spatial frequency-selectivity in senescence has not yet been directly reported, Zhang et al. (2008) found that the preferred spatial frequency of senescent V1 neurons in a primate model declines, as does the spatial resolution of those neurons (i.e., the highest spatial frequency to which they will respond). Taking the difference, in octaves, of preferred spatial frequency to spatial resolution as a measure of the selectivity of those neurons, we suggest that Zhang et al. (2008)'s results support the conclusion that spatial frequency-selectivity declines in senescent V1 neurons (see Discussion in Chapter 3).

## 1.2 Thesis Overview

The aforementioned declines in selectivity reported for senescent macaque visual cortex neurons raise the possibility that low-level visual mechanisms tuned for orientation and spatial frequency become less selective in older age[3]. Because these lower-level mechanisms convey information to higher-level visual processes, the selectivity, or informativeness, of these lower-level mechanisms determines the fidelity of higher-level visual perception. If these lower-level mechanisms selective for orientation and spatial frequency become detuned during the course of normal, older aging, this could explain some portion of age-related declines for complex visual form perception (e.g., Habak et al., 2008; Roudaia et al., 2008). Therefore, in the current dissertation I sought to characterize the selectivity of these lower-level mechanisms as a function of healthy, older aging in humans.

In Chapter 2 I employed two psychophysical masking techniques to assess the tuning of orientation-selective mechanisms in normal aging. Subjects were tasked with detecting a horizontal orientation signal (a Gaussian-damped sinewave grating, or a 2D "Gabor") that

[3]Even if there were no published reports, to date, of physiological detuning for orientation- and spatial frequency-selective neurons, an investigation of the selectivity of these lower-level spatial vision mechanisms would still be warranted given age-related deficits for the perception of complex visual forms as part of a reductive research programme seeking to explain higher-level perception first in terms of the performance of lower-level mechanisms.

was masked with either a variably-oriented sine wave grating, a method first employed by Campbell and Kulikowski (1966), or 2D visual noise that was variably notch-filtered in orientation-space, a technique first used by Patterson (1976) to measure auditory critical bands. Assuming that subjects detect the signal by monitoring the output of an orientation-selective mechanism that is centered on the signal, then as the mask's orientation content is moved toward that of the signal, it will progressively fall within the passband of this channel, masking the presence of the signal, and necessitating a stronger signal (i.e., of higher contrast) in order for the subject to achieve some fixed level of detection performance. The rate at which subjects' signal contrast detection threshold rises as the mask's orientation content is brought nearer that of the signal is a proxy for the selectivity of the channel used to detect that signal. Given the aforementioned reports of marked detuning of senescent orientation-selective V1 (e.g., Schmolesky et al., 2000) and V2 (Yu et al., 2006) neurons, as well as various reports of decline for complex form-perception, I anticipated broader psychophysical orientation tuning in older persons. Surprisingly, however, I found no effect of age on psychophysical orientation tuning.

In Chapter 3 I employed the same two psychophysical masking techniques that were used in Chapter 2, but masking was done along the spatial-frequency dimension instead of the orientation dimension. These two masking experiments enabled us to characterize the effect of age on the tuning of spatial frequency-selective mechanisms. As was the outcome for the experiments in Chapter 2, despite reported functional decline in senescent primate spatial frequency-selective V1 neurons (Zhang et al., 2008), older subjects yielded psychophysical spatial frequency tuning that was on par with younger subjects.

One possible explanation for the discrepancy between reports of functional decline in senescent orientation- and spatial frequency-selective neurons and the lack of an effect of older age on psychophysical orientation- and spatial frequency-selectivity that we found in Chapters 2 and 3 is as follows: Although the aforementioned physiological studies (e.g., Schmolesky et al., 2000) found neurons to be detuned *on average*, there were some outlying senescent cells that retained the selectivity that is typical of neurons in younger animals. Thus, if visual neurons become detuned in older age, on average, but if older adults' psychophysical tuning relies on such a finely-tuned subset of neurons — either because adults' psychophysical tuning relies on such a subset throughout life, or because the older brain compensates for declining average tuning by preferentially monitoring such a subset — then we ought not expect an effect of age on psychophysical tuning. Empirical support for this notion comes from studies that have found that, for some perceptual tasks, performance may rely on a surprisingly small number of neurons (for a

review, see Parker and Newsome, 1998; Gold and Shadlen, 2007).

I examined this idea in the experiments described in Chapters 4 and 5, in which I employed an electroencephalographic (EEG) technique suggested by Regan and Regan (1987, 1988) that is thought to measure the orientation or spatial frequency tuning of the population response of visual cortex neurons. The steady-state visually-evoked potential (ssVEP) is the EEG response to one or more stimuli that are temporally periodically-modulated in some fashion. In Chapter 4 I flickered (counterphase-modulated) two sine-wave gratings at independent frequencies and, in different experimental conditions, I varied the orientation difference between the two flickering gratings. To the extent that the two gratings fall within the passband of a full-wave rectifying unit — ostensibly, a spatially phase-insensitive complex cell, or two spatially-antiphase phase-sensitive simple cells — intermodulation frequencies will be produced and recordable at scalp EEG electrodes. These intermodulation frequencies include `mF1 +/- nF2`, where `m` and `n` are small, positive integers, `F1` is the flicker-rate of one grating, and `F2` is the flicker rate of the other grating. Much intermodulation activity is produced when the gratings are of similar orientations, and as the orientation difference is increased, the intermodulation activity drops off. This rate of drop-off is a proxy for the tuning of the population response of orientation-selective neurons in visual cortex. In Chapter 5 I performed the analogous ssVEP experiment to quantify the spatial frequency tuning of the population response in older humans.

If the population response of visual cortex neurons is detuned in older humans, this would lend support to the notion that the aged brain is able to compensate for orientation and spatial frequency detuning by selectively monitoring a subset of neurons that remain highly selective into older age, or, that the aging brain is impervious to this detuning because the brain monitors such a subset of neurons throughout life. Conversely, if the population response is not detuned in older humans, this suggests that there is no effect of older age on the tuning of visual cortex neurons, or that there is an effect of older age age on tuning, but that the aged brain is able to tune those neurons in a compenstory, ad hoc fashion. The results of Chapters 4 and 5 provided no evidence that orientation and spatial frequency tuning are broader in older age in awake, behaving humans.

Altogether, the results from this dissertation suggest that the selectivity of low-level visual mechanisms selective for orientation and spatial frequency remains intact in awake, attending older humans. A more detailed exposition of the experiments involved follow in the next four chapters. A discussion of how these results can be reconciled with the aforementioned single-cell reports of detuning in primate models, and ideas for future

research directions, can be found in the Discussion sections of those four chapters, as well as in Chapter 6, the General Discussion of this dissertation.

# References

Barlow, H. B., Hill, R. M., Levick, W. R., 1964. Retinal ganglion cells responding selectively to direction and speed of image motion in the rabbit. J Physiol 173, 377–407.

Barlow, H. B., Levick, W. R., 1965. The mechanism of directionally selective units in rabbit's retina. J Physiol 178 (3), 477–504.

Bennett, P. J., Sekuler, A. B., McIntosh, A. R., Della-Maggiore, V., 2001. The effects of aging on visual memory: Evidence for functional reorganization of cortical networks. Acta Psychologica 107 (1-3), 249–273.

Blakemore, C., Campbell, F. W., 1969. On the existence of neurones in the human visual system selectively sensitive to the orientation and size of retinal images. Journal of Physiology 203, 237–260.

Boutet, I., Faubert, J., 2006. Recognition of faces and complex objects in younger and older adults. Memory and Cognition 34 (4), 854–864.

Campbell, F. W., Kulikowski, J. J., 1966. Orientational selectivity of the human visual system. Journal of Physiology 187, 437–445.

Campbell, F. W., Robson, J. G., 1968. Application of fourier analysis to the visibility of gratings. Journal of Physiology 197 (551–566).

Curcio, C. A., Millican, C. L., Allen, K. A., Kalina, R. E., 1993. Aging of the human photoreceptor mosaic: evidence for selective vulnerability of rods in central retina. Investigative Ophthalmology and Vision Science 34 (3278–3296).

Dacey, D. M., 2000. Parallel pathways for spectral coding in primate retina. Annu Rev Neurosci 23, 743–75.

De Valois, R. L., Albrecht, D. G., Thorell, L. G., 1982. Spatial frequency selectivity of cells in macaque visual cortex. Vision Res 22 (5), 545–59.

Del Viva, M. M., Agostini, R., 2007. Visual spatial integration in the elderly. Investigative Ophthalmology and Vision Science 48 (6), 2940–2946.

DeValois, R. L., DeValois, K. K., 1988. Spatial Vision. Oxford University Press.

DeValois, R. L., Yund, W., Hepler, N., 1982. The orientation and direction selectivity of cells in macaque visual cortex. Vision Research 22 (5), 531–544.

Eysel, U. T., Shevelev, I. A., Lazareva, N. A., Sharaev, G. A., May 1998. Orientation tuning and receptive field structure in cat striate neurons during local blockade of intracortical inhibition. Neuroscience 84 (1), 25–36.

Felleman, D. J., Van Essen, D. C., 1991. Distributed hierarchical processing in the primate cerebral cortex. Cereb Cortex 1 (1), 1–47.

Gilinsky, A. S., Jan 1968. Orientation-specific effects of patterns of adapting light on visual acuity. J Opt Soc Am 58 (1), 13–8.

Gillespie, D. C., Lammpl, I., Anderson, J. S., Ferster, D., 2001. Dynamics of the orientation-tuned membrane potential response in cat primary visual cortex. Nature Neuroscience 4 (10), 1014–1019.

Gold, J. I., Shadlen, M. N., 2007. The neural basis of decision making. Annual Review of Neuroscience 30, 535–74.

Graham, N., Nachmias, J., 1971. Detection of grating patterns containing two spatial frequencies: A comparison of single-channel and multiple-channel models. Vision Research 11 (3), 251–259.

Habak, C., Wilkinson, F., Wilson, H. R., 2008. Aging disrupts the neural transformations that link facial identity across views. Vision Res 48 (1), 9–15.

Herbert, A. M., Overbury, O., Singh, J., Faubert, J., 2002. Aging and bilateral symmetry detection. Journal of Gerontology Series B: Psychological Science and Social Sciences 57, P241–P245.

Hua, T., Kao, C., Sun, Q., Li, X., Zhou, Y., Jan 2008. Decreased proportion of gaba neurons accompanies age-related degradation of neuronal function in cat striate cortex. Brain Res Bull 75 (1), 119–25.

Hua, T., Li, X., He, L., Zhou, Y., Wang, Y., Leventhal, A. G., 2006. Functional degradation of visual cortical cells in old cats. Neurobiology of Aging 27, 155–162.

Hubel, D. H., Wiesel, T. N., 1962. Receptive fields, binocular interaction and functional architecture in the cat's visual cortex. J Physiol 160, 106–54.

Jackson, G. R., Owsley, C., Curcio, C. A., 2002. Photoreceptor degeneration and dysfunction in aging and age-related maculopathy. Ageing Research Reviews 1, 381–396.

Kelly, D. H., Magnuski, H. S., 1975. Pattern detection and the two-dimensional fourier transform: circular targets. Vision Res 15, 911–5.

Kuffler, S. W., 1953. Discharge patterns and functional organization of mammalian retina. J Neurophysiol 16 (1), 37–68.

Leventhal, A. G., Wang, Y., Pu, M., Zhou, Y., Ma, Y., 2003. GABA and its agonists improved visual cortical function in senescent monkeys. Science 300, 812–815.

McIntosh, A. R., Sekuler, A. B., Penpeci, C., Rajah, M. N., Grady, C. L., Sekuler, R., Bennett, P. J., 1999. Recruitment of unique neural systems to support visual memory in normal aging. Current Biology 9, 1275–1278.

Nelson, S., Toth, L., Sheth, B., Sur, M., Aug 1994. Orientation selectivity of cortical neurons during intracellular blockade of inhibition. Science 265 (5173), 774–7.

Pantle, A., Sekuler, R., Dec 1968. Size-detecting mechanisms in human vision. Science 162 (858), 1146–8.

Parker, A. J., Newsome, W. T., 1998. Sense and the single neuron: Proving the physiology of perception. Annual Review of Neuroscience 21, 227–277.

Patterson, R. D., 1976. Auditory filter shapes derived with noise stimuli. Journal of the Acoustical Society of America 59, 640–654.

Priebe, N. J., Ferster, D., 2008. Inhibition, spike threshold, and stimulus selectivity in primary visual cortex. Neuron 57, 482–497.

Regan, D., Regan, M., 1988. Objective evidence for phase-independent spatial frequency analysis in the human visual pathway. Vision Rsearch 28 (1), 187–191.

Regan, D., Regan, M. P., 1987. Nonlinearity in human visual resonses to two-dimensional patterns, and a limitation of fourier methods. Vision Rsearch 27 (12), 2181–2183.

Reuter-Lorenz, P. A., Lustig, C., 2005. Brain aging: Reorganizing discoveries about the aging mind. Curr Opin Neurobiol 15 (2), 245–251.

Roudaia, E., Bennett, P., Sekuler, A., 2008. The effect of aging on contour integration. Vision Research 48, 2767–2774.

Ruffman, T., Halberstadt, J., Murray, J., Nov 2009. Recognition of facial, auditory, and bodily emotions in older adults. J Gerontol B Psychol Sci Soc Sci 64 (6), 696–703.

Schmolesky, M. T., Wang, Y., Pu, M., Leventhal, A. G., 2000. Degradation of stimulus selectivity of visual cortical cells in senescent rhesus monkeys. Nature Neuroscience 3, 384–390.

Sekuler, R., Sekuler, A. B., 2000. Visual perception and cognition. In: Evans, J. G., Williams, T. F., Beattie, B. L., Michel, J. P., Wilcock, G. K. (Eds.), Oxford Textbook of Geriatric Medicine. Oxford University Press, New York, pp. 874–880.

Sillito, A. M., Sep 1975a. The contribution of inhibitory mechanisms to the receptive field properties of neurones in the striate cortex of the cat. J Physiol 250 (2), 305–29.

Sillito, A. M., Sep 1975b. The effectiveness of bicuculline as an antagonist of gaba and visually evoked inhibition in the cat's striate cortex. J Physiol 250 (2), 287–304.

Spear, P. D., 1993. Neural bases of visual deficits during aging. Vision Research 33 (18), 2589–2609.

Spear, P. D., Moore, R. J., Kim, C. B., Xue, J. T., Tumosa, N., Jul 1994. Effects of aging on the primate visual system: spatial and temporal processing by lateral geniculate neurons in young adult and old rhesus monkeys. J Neurophysiol 72 (1), 402–20.

Stanford, T., Pollack, R. H., 1984. Configuration color vision tests: the interaction between aging and the complexity of figure-ground segregation. Journal of Gerontology 39 (5), 568–571.

Statistics Canada - Catalogue No. 97-551, 2006. Martel, L. and Caron-Malenfant, E., `www12.statcan.gc.ca/census-recensement/2006/as-sa/97-551/index-eng.cfm`

Weale, R. A., 1992. The senescence of human vision. Oxford University Press.

Xing, D., Shapley, R. M., Hawken, M. J., Ringach, D. L., 2005. Effect of stimulus size on the dynamics of orientation selectivity in macaque v1. J Neurophysiol 94 (1), 799–812.

Yu, S., Wang, Y., Li, X., Zhou, Y., Leventhal, A. G., 2006. Functional degradation of extrastriate visual cortex in senescent rhesus monkeys. Neuroscience 140, 1023–1029.

Zhang, J., Wang, X., Wang, Y., Fu, Y., Liang, Z., Ma, Y., Leventhal, A. G., 2008. Spatial and temporal sensitivity degradation of primary visual cortical cells in senescent rhesus monkeys. European Journal of Neuroscience 28, 201–207.

# Chapter 2

# The effect of aging on the orientational selectivity of the human visual system

**Abstract**

Leventhal *et al.* (*Science*, 2003, 300(5620), 812-15) reported that orientation selectivity of V1 neurons was significantly reduced in older macaque monkeys, which suggests that mechanisms that encode orientation in humans may become more broadly tuned in old age. We examined this hypothesis in two experiments that used sine-wave masking and notched-noise masking to estimate the bandwidth of orientation-selective mechanisms in younger (age $\approx$ 23 years) and older (age $\approx$ 68 years) human adults. In both experiments, the orientation selectivity of masking was essentially identical in younger and older subjects.

## 2.1 Introduction

Many aspects of vision decline in old age (Sekuler and Sekuler, 2000). Some of the effects of aging can be attributed to changes in the optical quality of the eye (Weale, 1961), but optical changes alone cannot explain all of the age-related changes in vision (e.g., Bennett et al. 1999; Sekuler et al. 2000). Although non-sensory factors may affect performance in visual tasks, generally it is thought that impaired visual performance

in older adults is due, at least in part, to changes in the anatomical or physiological characteristics of visual neurons (Bennett et al., 1999; Delahunt et al., 2008; Sekuler and Sekuler, 2000). Consistent with this view, Leventhal et al. (2003) and Schmolesky et al. (2000) reported that senescent macaque V1 neurons are less selective for orientation than neurons in younger adult macaques. These physiological findings raise the possibility that mechanisms that encode orientation are degraded in older human adults.

Recently, Delahunt et al. (2008) investigated the tuning properties of orientation-selective mechanisms in younger and older adults by measuring detection thresholds for a Gabor pattern that was presented simultaneously with a sine wave mask that varied in orientation. The shape of the masking functions were similar in both age groups, which suggests that the bandwidth of orientation-selective mechanisms does not change significantly with age. This psychophysical result differs significantly from the physiological reports, and therefore we thought it would be worthwhile to reexamine the issue of age differences in orientation selectivity in two masking experiments. Experiment 1 used a sine wave mask like Delahunt et al. (2008). Experiment 2 used a notched-filtered noise mask.

## 2.2 Experiment 1: Sine-wave grating masking

Orientation tuning curves were obtained by measuring detection thresholds for a Gaussian-damped sine wave grating embedded in a sine wave mask (Campbell and Kulikowski, 1966). The spatial frequency and contrast of the mask was fixed, but its orientation varied across conditions.

### 2.2.1 Methods

For all of the experiments reported here, the research protocol was approved by McMaster University's Research Ethics Board and informed consent was obtained from each subject prior to the start of the study.

Table 2.1: Age, acuity, and Mini-Mental State Exam (MMSE).

| Experiment | Number of subjects | Age ($\mu$, $\sigma$) | Near logMAR acuity ($\mu$, $\sigma$) | Far logMAR acuity ($\mu$, $\sigma$) | MMSE ($\mu$, $\sigma$) |
|---|---|---|---|---|---|
| 1 | 12 older | 68.75 (4.18) | 0.00 (0.12) | -0.04 (0.09) | 29.08 (1.16) |
| | 12 younger | 23.67 (3.63) | -0.15 (0.07) | -0.10 (0.11) | |
| 1 (control) | 4 younger | 22.5 (0.58) | -0.14 (0.04) | -0.18 (0.06) | |
| 2 | 12 older | 66.50 (3.58) | -0.02 (0.10) | -0.03 (0.09) | 29.25 (1.22) |
| | 12 younger | 23.00 (3.72) | -0.15 (0.09) | -0.13 (0.08) | |
| 2 (control) | 5 younger | 22.4 (0.56) | -0.14 (0.03) | -0.17 (0.06) | |

### Subjects

Twelve older and 12 younger paid subjects participated in the main experiment. An additional group of four younger subjects participated in a control experiment that measured the effect of reduced retinal illuminance on masking. All subjects completed vision and general health questionnaires to screen for visual pathology, such as cataracts, macular degeneration, glaucoma, and amblyopia. Near and far decimal logMAR acuities were measured for all subjects with CSV-100EDTRS eye charts (Precision Vision, LaSalle, Illinois, USA). When measuring acuity, subjects wore their normal optical correction for each distance. Older subjects completed the Mini-Mental State Examination (MMSE; Folstein et al., 1975) to screen for age-related dementia. All older subjects scored within the normal range for their age groups on the MMSE (Crum et al., 1993). The means and standard deviations of age, near and far acuities, and MMSE scores are presented in Table 2.1. All subjects had normal or corrected-to-normal acuity and no known vision health problems (see Table 2.1 for details).

### Stimuli and Apparatus

The experiment was programmed in MatLab v5.2.1 (The Mathworks) using the Psychophysics and Video Toolboxes (Brainard 1997; Pelli 1997) running on an Apple G4 PowerMac computer. The stimuli were displayed on a 21-inch Apple Studio Display.

Display size was 1024 x 768 pixels, which subtended visual angles of 19.1 deg horizontally and 14.4 deg vertically from the viewing distance of 114 cm. The frame rate was 75 Hz, noninterlaced. Calibration was done using a PhotoResearch PR-650 spectracolorimeter, and the calibration data were used to build a 1779-element look-up table (Tyler et al., 1992). When constructing the stimuli used on each trial, the computer software selected appropriate luminance values from the calibrated look-up table and stored them in the 8-bit look-up table of the display. Average luminance of the display was 32 $cd/m^2$ and was constant throughout the experiment. The monitor was the only source of light in the experimental room during testing. Viewing was binocular through natural pupils, and a chin/forehead rest was used to stabilize viewing position.

The visual target – 256 x 256 pixels, or 4.8 x 4.8 deg, in size – was a horizontal (0 deg), 2.9 $c/deg$ sine-wave grating. Target contrast was modulated by a radially-symmetric Gaussian window ($2\sigma$ = 1.2 deg). The spatial phase of the grating, relative to the center of the Gaussian window, was 0 deg (i.e., cosine phase). The target was masked by a 256 x 256 pixel sine-wave grating. Mask contrast was 0.2, and was modulated by a circular aperture (diameter = 256 pixels). The addition of the target to sine wave mask introduces a spatial pattern of beats which could be used to detect the target (Nachmias, 1993). To make it more difficult for subjects to learn to use a *specific* pattern of beats to detect the target, on each interval of every trial the phase of the mask was randomized and the spatial frequency of the mask was uniformly jittered ± 0.1 log units around the target frequency of 2.9 $c/deg$. In different conditions, the mask orientation was offset from the target's orientation by 0, ±15, ±30, ±45, ±60, ±75, or ±85 deg.

A separate control experiment was conducted to measure the effects of retinal illuminance on orientation masking. Four young subjects were each tested in two conditions. Stimuli in the High Luminance condition were the same as those described in the previous paragraphs. In the Low Luminance condition, subjects viewed the display through neutral density filters that reduced average luminance from 32 $cd/m^2$ to about 4 $cd/m^2$. This difference in stimulus luminance corresponds to a reduction of retinal illuminance of approximately 0.65 log units in young subjects (Betts et al., 2007), which is slightly larger than Weale's (1961) estimate of the reduction in retinal illuminance that occurs between the ages of 20 and 60 years. The order of luminance conditions was counter-balanced across subjects.

### Procedure

Thresholds were measured with a two-interval forced-choice (2-IFC) task. A circular (diameter = 6 pixels) high-contrast fixation spot was presented in the center of the display. After fixating on the spot, the subject began a trial by pressing the space bar on a standard computer keyboard. The fixation point then was erased, and, after a delay of 500 ms, followed by two successive stimulus intervals. The duration of each stimulus interval was 200 ms, and the inter-stimulus interval was 500 ms. Each stimulus interval contained a 1-pixel wide high-contrast circle (diameter = 256 pixels) that served to mark the spatial and temporal extent of the stimulus. One interval contained the target-plus-mask, the other contained the mask alone, and the subject's task was to select the interval that contained the target by pressing one of two response keys. An auditory tone provided feedback after incorrect responses; no sound followed a correct response. Subjects were informed that the probability of the target appearing in the first stimulus interval was 0.5.

Target contrast was varied across trials using QUEST (Watson and Pelli, 1983). The seven mask orientation conditions were intermixed, and the direction of the orientation offset (i.e., clockwise vs. counter-clockwise) was selected randomly on each interval of each trial. A session ended when each staircase had accumulated 45 trials.

## 2.2.2 Results

All statistical analyses were done with R (R Development Core Team, 2007). When appropriate, the Huynh-Feldt correction, $\tilde{\epsilon}$, was used to adjust the degrees-of-freedom to correct for violations of the sphericity assumption underlying $F$ tests for within-subject variables (Maxwell and Delaney, 2004). In cases where the Huynh-Feldt correction is used, the reported $p$ values are the adjusted $p$ values. Effect size was expressed as Cohen's $f$ (Cohen, 1988), and was calculated using formulae described by Kirk (1995). When $F < 1$, the effect size was assumed to be zero (see Kirk, 1995, page 180). Between-group $t$ tests assumed unequal group variances and used the Welch-Satterthwaite formula to adjust the degrees-of-freedom: $p$ values listed for such tests are the adjusted $p$ values.

The psychometric function was defined as

$$p = 1 - (1 - \gamma) \exp\left(-10^{\beta \log_{10}(c/\alpha)}\right) \tag{2.1}$$

where $p$ is proportion correct, $\gamma$ is the guessing rate, $c$ is stimulus contrast, $\beta$ governs the

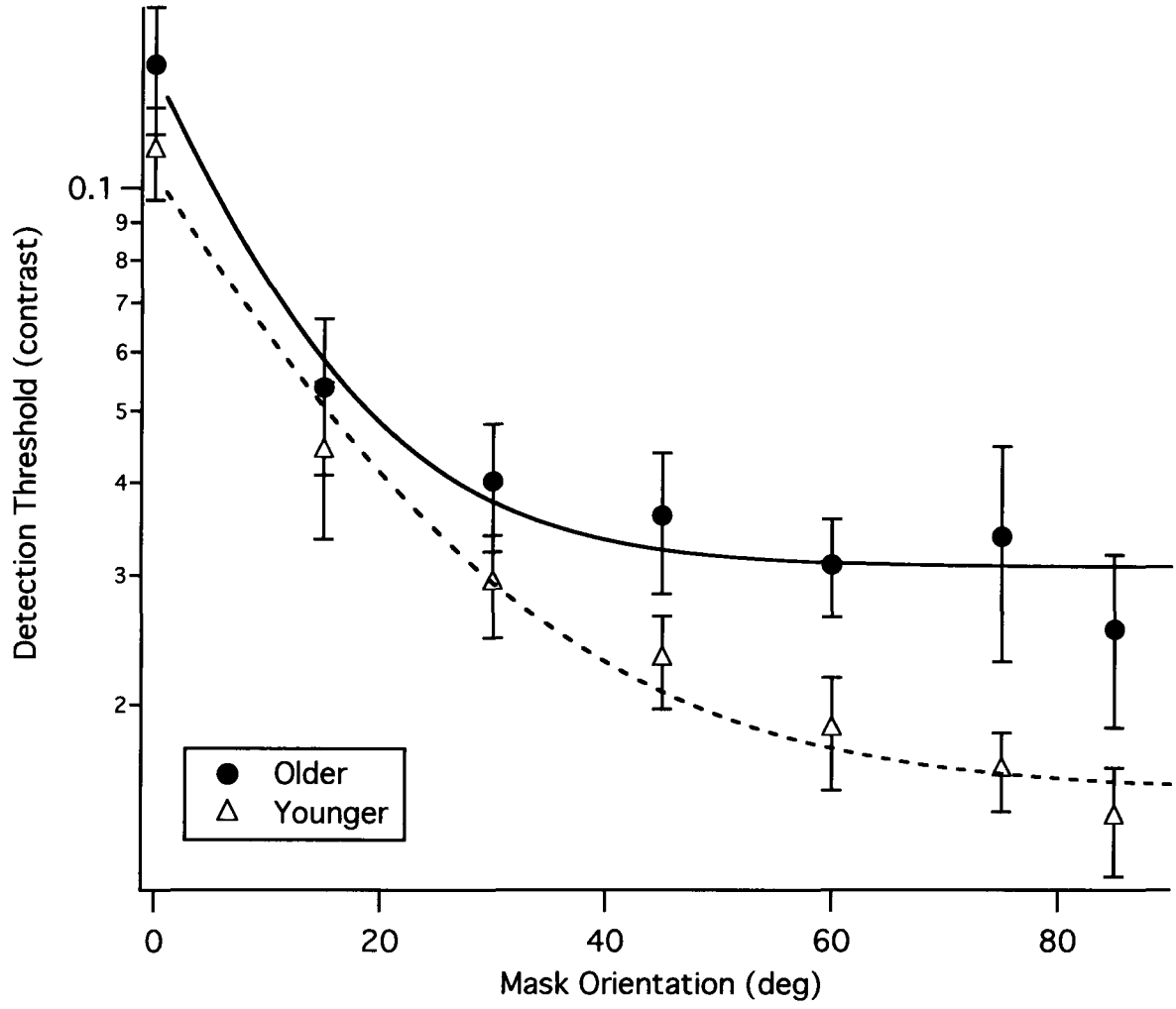


Figure 2.1: Sine wave masking data. Mean detection thresholds for older and younger subjects are plotted as a function of mask orientation. The orientation of the target grating was 0 deg. Error bars represent the 95% confidence interval of the mean. Equation 2.2 was fit to the average thresholds from each age group. The solid and dashed curves represent the results for older and younger subjects, respectively.

slope of the psychometric function, and $\alpha$ corresponds to threshold (i.e., the stimulus contrast that yields a response accuracy of 81.6% correct). The guessing rate was set to 0.5, and a maximum likelihood curve fitting procedure was used to estimate $\beta$ and $\alpha$ for each subject in each condition.

One older subject in the main experiment had thresholds that were 3-3.4 standard deviations higher than the group mean when the mask orientation was 0, 15, and 30 deg. These thresholds were deemed outliers, and therefore thresholds from this subject were discarded prior to analyzing the data.

The grand mean of $\beta$ was 3.5. An ANOVA on the log-transformed values of $\beta$ found that the main effects of group, $F(1, 21) = 1.60$, $f = 0.06$, $p = 0.22$, and mask orientation, $F(6, 126) = 0.73$, $\tilde{\epsilon} = 0.91$, $p = 0.61$, as well as the group x orientation interaction, $F(6, 126) = 0.97$, $\tilde{\epsilon} = 0.91$, $p = 0.44$, were not significant. Hence, we did not find any evidence that the slope of the psychometric function varied systematically across conditions or groups.

Detection thresholds from the main experiment are presented in Figure 2.1 as a function of mask orientation and age. Thresholds declined with increasing mask orientation in both age groups, but thresholds from older subjects reached a lower asymptote more quickly than thresholds from younger subjects. Consequently, the difference between groups increased slightly as mask orientation increased. An ANOVA on log-transformed thresholds found significant main effects of age, $F(1, 21) = 20.21$, $f = 0.35$, $p = 0.0002$, and mask orientation, $F(6, 126) = 162.44$, $f = 2.45$, $\tilde{\epsilon} = 0.86$, $p < 0.0001$, and a significant age x orientation interaction, $F(6, 126) = 2.79$, $f = 0.26$, $\tilde{\epsilon} = 0.86$, $p < 0.019$.

Table 2.2: Parameters $k$, $a$, $b$, and $\theta_{1/2}$ estimated in the sine-wave masking experiment.

| | younger subjects $\hat{\mu} \pm \hat{\sigma}_{\mu}$ | older subjects $\hat{\mu} \pm \hat{\sigma}_{\mu}$ |
|---|---|---|
| $k$ | $1.43 \pm 0.15$ $(\times 10^{-2})$ | $2.82 \pm 0.36$ $(\times 10^{-2})$ |
| $a$ | $0.90 \pm 0.08$ $(\times 10^{-1})$ | $1.14 \pm 0.15$ $(\times 10^{-1})$ |
| $b$ | $16.79 \pm 1.79$ | $14.36 \pm 3.25$ |
| $\theta_{1/2}$ | $14.41 \pm 1.16$ | $14.33 \pm 3.09$ |

Thresholds were fit with the equation

$$T(x) = k + a \cdot \exp\left(-\frac{x}{b}\right) \tag{2.2}$$

where $T$ is threshold, $x$ is the mask's orientation offset, $k$ is the lower asymptote, $a$ is the difference between the maximum and the lower asymptote, and $b$ governs the rate of decline from the maximum threshold, $(k + a)$, to the minimum threshold, $k$. Equation 2.2 was first fit to the average thresholds in each age group, and the resulting parameters were used to draw the smooth curves in Figure 2.1. It can be seen that Equation 2.2 provided reasonably good fits to the data in both age groups. Next, Equation 2.2 was fit to the data from each subject. The means and standard errors of the best-fitting parameters are listed in Table 2.2. Separate $t$-tests found that the value of $k$ differed significantly between age groups, $CI_{95\%} = (0.028, 0.014)$, $t(21) = 3.53$, $p = 0.003$, whereas $a$, $CI_{95\%} = (-0.013, 0.061)$, $t(21) = 1.35$, $p = 0.19$, and $b$, $CI_{95\%} = (-10.31, 5.45)$, $t(21) = -0.65$, $p = 0.52$, did not. The difference in $k$ reflects the fact that the lower asymptote of the masking function was significantly higher in older subjects.

Previous estimates of the orientation selectivity of masking often have been expressed in terms of half-amplitude half-bandwidth, $\theta_{1/2}$, defined as the orientation at which threshold drops to one-half of its peak value. Equation 2.2 was used to estimate $\theta_{1/2}$ for each subject. The overall mean of $\theta_{1/2}$ was 14.4 deg, $CI_{95\%} = (11.1,\ 17.6)$. The difference between the group means, listed in Table 2.2, was not statistically significant, $CI_{95\%} = (-7.23, 7.07)$, $t(21) = -0.024$, $p = 0.98$.

The grand mean of $\beta$ measured in the control experiment was 3.6, and a 2 (luminance) x 7(orientation) ANOVA on log-transformed values of $\beta$ found no significant effects ($F \leq 1.93$, $f \leq 0.13$, $p \geq 0.26$ in all cases). Detection thresholds from the control experiment are shown in Figure 2.2. Thresholds were higher in the low luminance condition at all mask orientations. A within-subjects ANOVA on log-transformed thresholds revealed significant main effects of luminance, $F(1, 3) = 47.95$, $f = 0.92$, $p = 0.006$, and mask orientation, $F(6, 18) = 76.71$, $f = 2.84$, $\tilde{\epsilon} = 0.30$, $p = 0.0001$. The interaction between luminance and orientation was not significant, $F(6, 18) = 1.20$, $f = 0.15$, $\tilde{\epsilon} = 0.41$, $p = 0.364$, but a more focussed test of the linear trend of threshold across conditions did reveal a significant group x trend interaction, $F(1, 3) = 11.83$, $f = 1.64$, $p = 0.041$. This interaction suggests that the slope of the masking function was shallower in the low luminance condition. Equation 2.2 was fit to data from each subject in each luminance condition, and the best-fitting parameters, averaged across subjects, are shown in Table 2.3. Separate $t$ tests found that $k$ differed across luminance levels, $CI_{95\%} = (-0.010, -0.002)$,

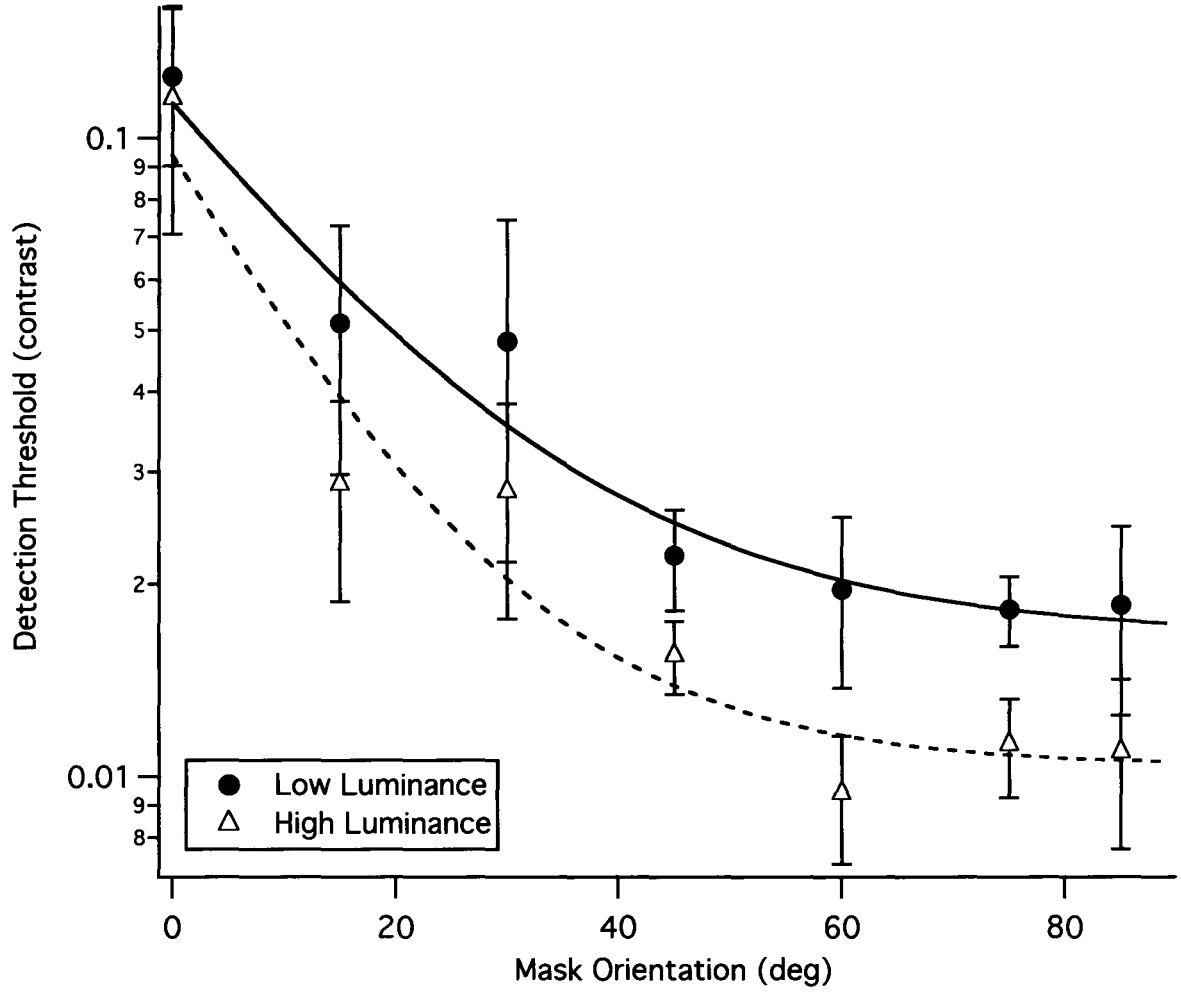


Figure 2.2: Low luminance control experiment using a sine wave mask. Mean detection thresholds measured at two average luminances for four younger subjects are plotted as a function of mask orientation. The orientation of the target grating was 0 deg. Error bars represent the 95% confidence interval of the mean. Equation 2.2 was fit to the average thresholds in each condition. The solid and dashed curves represent the results for low and high luminance conditions, respectively.

$t(3) = -4.75$, $p = 0.017$, but that $a$, $CI_{95\%} = (-0.089, 0.086)$, $t(3) = -0.05$, $p = 0.959$, and $b$, $CI_{95\%} = (-13.96, 5.01)$, $t(3) = -1.50$, $p = 0.23$, did not. The masking bandwidth ($\theta_{1/2}$) also did not vary significantly between luminance conditions, $CI_{95\%} = (-12.83, 3.44)$, $t(3) = -1.84$, $p = 0.16$.

Table 2.3: Parameters $k$, $a$, $b$, and $\theta_{1/2}$ estimated in the sine-wave masking control experiment.

| | high luminance $\hat{\mu} \pm \hat{\sigma}_{\mu}$ | low luminance $\hat{\mu} \pm \hat{\sigma}_{\mu}$ |
|---|---|---|
| $k$ | $1.08 \pm 0.06$ $(\times 10^{-2})$ | $1.68 \pm 0.10$ $(\times 10^{-2})$ |
| $a$ | $1.02 \pm 0.23$ $(\times 10^{-1})$ | $1.03 \pm 0.16$ $(\times 10^{-1})$ |
| $b$ | $12.62 \pm 3.13$ | $17.10 \pm 2.11$ |
| $\theta_{1/2}$ | $10.43 \pm 2.67$ | $15.13 \pm 1.92$ |

### 2.2.3 Discussion

Experiment 1 measured detection thresholds for a Gabor pattern embedded in a sine wave mask whose orientation was variably offset from that of the target. As has been found previously, thresholds in both age groups were highest when the target and mask had the same orientation, and declined rapidly and significantly as the difference between orientations increased (Anderson et al., 1991; Blake and Holopigian, 1985; Campbell and Kulikowski, 1966; Delahunt et al., 2008; Phillips and Wilson, 1984). There was no evidence that the selectivity of orientation masking, as indexed by $\theta_{1/2}$, was broader in older results. In this regard, our results are consistent with the human behavioral findings of Delahunt et al. (2008), but differ from predictions based on single cell electrophysiology in macaques (Schmolesky et al., 2000; Leventhal et al., 2003).

Estimates of $\theta_{1/2}$ from a subset of conditions in several previous masking experiments are shown in Table 2.4. The values of $\theta_{1/2}$ listed for Anderson et al. (1991) and Phillips and Wilson (1984) were estimated directly from the published masking curves, and are not the bandwidths of the underlying orientation-selective mechanisms that the authors derived from the masking data. All of the studies listed in the table used a static sine wave target, but the spatial frequency of the target varied over a ten-fold range. The masks

were all narrow band in terms of spatial frequency, but differed in other ways: Phillips and Wilson used a static, high-contrast sine wave grating; Campbell and Kulikowski (1966) used static high-contrast sine wave gratings and narrow-band dynamic noise; Anderson et al. used a high-contrast sine wave grating whose spatial phase was jittered randomly at 50 Hz; Delahunt et al. (2008) used a static sine wave grating set to a contrast equal to two times detection threshold; Blake and Holopigian (1985) used a narrow-band dynamic noise that consisted of two orientations that were rotated symmetrically about the target's orientation. Despite these differences across experiments, the estimates of $\theta_{1/2}$ all fall within the range of 11-30 deg, and the mean value of 17.5 deg is only 3 deg greater than current estimate of $\theta_{1/2}$. Hence, our estimate of orientation masking bandwidth is similar to those reported previously.

Table 2.4: Estimates of $\theta_{1/2}$ derived from masking functions in several experiments.

| Source | target (c/deg) | $\theta_{1/2}$ (deg) |
|---|---|---|
| Campbell and Kulikowski (1966) | 10 | 12 |
| Phillips and Wilson (1984) | 2 | 14.6 |
| | 8 | 16.4 |
| Blake and Holopigian (1985) | 1.25 | 30 |
| | 8 | 23 |
| Anderson et al. (1991) | 3 | 15.2 |
| Delahunt et al. (2008) | | |
| – older & younger subjects | 1 & 4 | 11.5 |
| Mean Value: | | 17.5 |

A high-contrast mask that is oriented orthogonally to a target grating can produce masking (Burbeck and Kelly, 1981; Burr and Morrone, 1987; Foley, 1994), and an increase in such masking in older subjects could explain why the lower asymptote of the masking function was higher in those subjects. To test this idea, we measured masking functions in five older and four younger subjects using the same methods as Experiment 1, except that a no-mask condition was added to the experimental conditions. For younger subjects, thresholds in the no-mask condition were $\approx 0.18$ log units lower than thresholds measured with a $\pm 85$ deg mask. For older subjects, the threshold difference was $\approx 0.11$ log units. Hence, there was no evidence that orthogonal masks produced greater masking in older subjects. The luminance control experiment found that reducing retinal illuminance in

younger subjects raised $k$. It is likely, therefore, that age differences in retinal illuminance (Weale, 1961) contributed to the age differences in the asymptotic level of the masking functions.

## 2.3 Experiment 2: Notched-noise masking

Adding a Gabor target to a sine wave mask that differs in orientation produces spatial beats. In Experiment 1, the spatial phase and frequency of the mask varied slightly across trials to make it difficult to detect the target based on the presence of a *particular* pattern of spatial beats. Nevertheless, subjects may have detected the target on the basis of the presence of spatial beats or other local spatial distortions in the mask (Nachmias, 1993). Experiment 2 minimized the possibility that subjects used such cues by measuring detection thresholds for a Gabor pattern embedded in static noise that was broadband in terms of spatial frequency.

The spatial frequency selectivity of visual mechanisms has been estimated in experiments that used noise masks that were band-pass filtered (e.g., Stromeyer and Julesz, 1972) or low- and high-pass filtered (e.g., Henning et al., 1981). The current experiment used a notch filter to vary the orientation content of a noise mask: the notch was centered on the target's orientation, and the width of the notch varied across conditions (see Figure 2.3). Notched noise has been used to investigate contrast discrimination (Henning and Wichmann, 2007), to estimate the frequency selectivity of auditory channels (e.g., Patterson 1976), the spatial frequency tuning of luminance and chromatic visual mechanisms (Losada and Mullen, 1995; Mullen and Losada, 1999), and the orientation tuning of binocular (i.e., cyclopean) mechanisms (Hibbard, 2005). In this experiment the notched-noise method was used to compare the orientation-selectivity of masking in younger and older subjects.

### 2.3.1 Methods

#### Subjects

Twelve older and 12 younger subjects were paid for participating in this experiment. An additional group of five younger subjects participated in a control experiment that

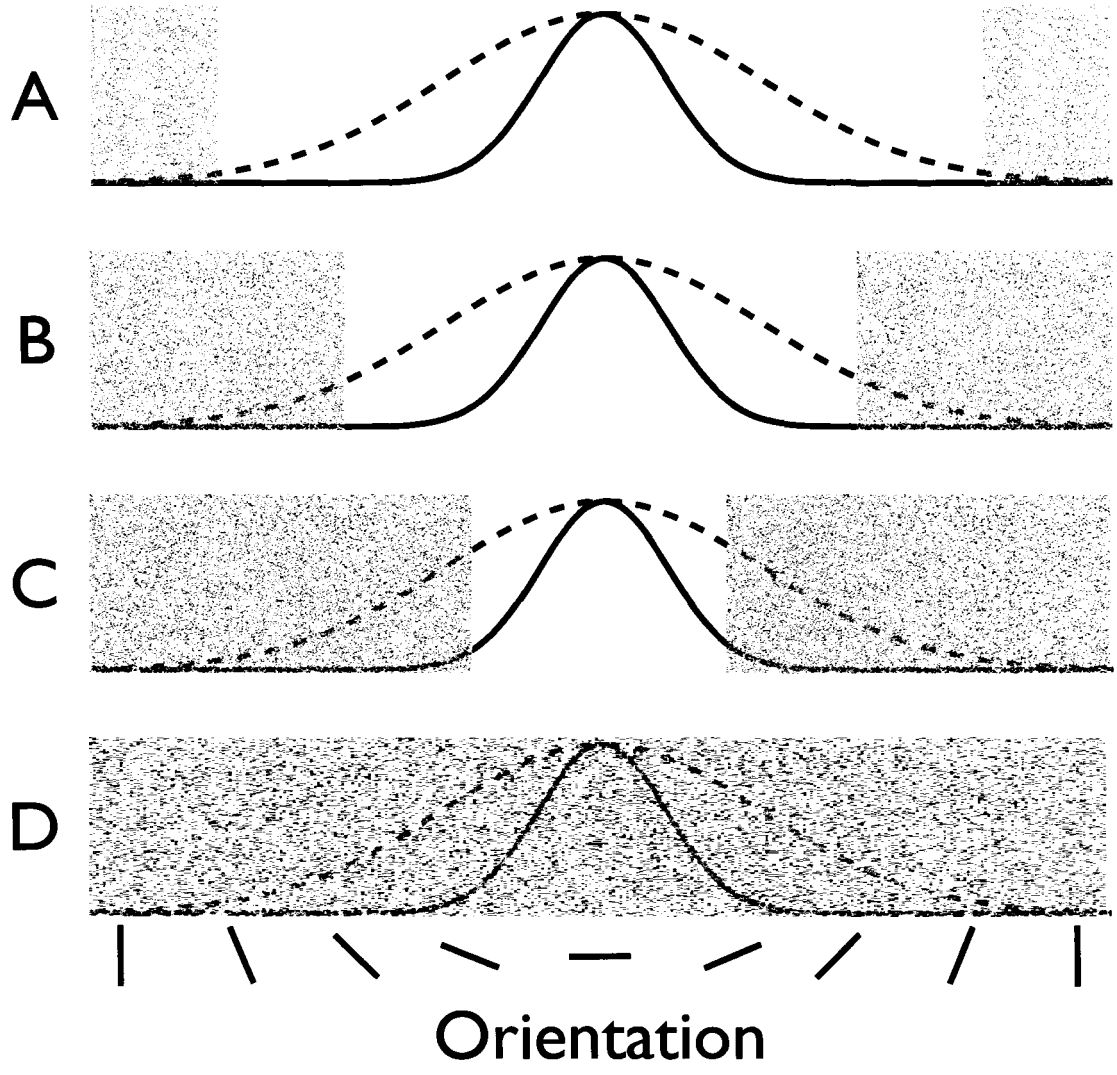


Figure 2.3: Illustration of the notched-noise masking paradigm. The solid and dashed lines in each panel illustrate hypothetical orientation tuning functions that differ in bandwidth. The orientation content of the external noise is illustrated by the shaded regions. Panel A illustrates the orientation spectrum of a noise that has been filtered with a wide notch filter centered on the horizontal orientation. The notch width is progressively narrower in Panels B and C, and is zero in Panel D. Noise falling within the pass band of the orientation filters will increase response variability, and lower the signal-to-noise ratio. Notice that, in B and C, more noise falls within the pass band of the broader orientation filter.

measured the effect of reduced retinal illuminance on masking. The subjects were screened with the same protocol used in Experiment 1. The ages, acuities, and MMSE scores for these subjects are listed in Table 2.1. As before, all older subjects scored within the normal range for their age groups on the MMSE (Crum et al., 1993). All subjects had normal or corrected-to-normal acuity and no known vision health problems (see Table 2.1 for details).

### Stimuli and Apparatus

The experimental apparatus was the same as in Experiment 1.

The visual target was a horizontally-oriented (i.e., 0 deg) 2.9 $c/deg$ Gabor pattern with the same parameters as in Experiment 1. Two-dimensional static noise fields (256 x 256 pixels in size) were constructed by digitally filtering white Gaussian noise. Prior to filtering, the value of each noise pixel was drawn randomly from a Gaussian distribution with a mean of 0 and a variance of 0.16. Noise values beyond $\pm 2$ standard deviations from the mean were discarded and replaced by random samples from the remaining contrast values.

Orientation filtering was done in the Fourier domain using Matlab's `fft2` function and custom software. In different conditions, the filtering procedure removed all Fourier components within $\pm 15$, $\pm 30$, $\pm 45$, $\pm 60$, $\pm 75$, and $\pm 80$ deg of the target orientation. In addition, there was one condition in which no orientation filtering was performed. Thus, the filtering can be thought of as notch filtering along the orientation dimension, with the notch centered on 0 deg and seven notch widths ranging from 0 to 160 deg. We did not include a no-mask condition because because pilot experiments showed that such thresholds are very similar to thresholds measured with a notch width of 160 deg. A different noise field was constructed for each interval of every trial. Noise contrast was modulated by a circular window (diameter = 256 pixels). Example stimuli are shown in Figure 2.4.

A separate control experiment was conducted to measure the effects of retinal illuminance. Five young subjects were each tested in High and Low Luminance conditions. Stimuli in the High Luminance condition were the same as those described in the previous paragraphs. In the Low Luminance condition, subjects viewed the display through neutral density filters that reduced average luminance from 32 $cd/m^2$ to about 4 $cd/m^2$. The order of luminance conditions was counter-balanced across subjects.

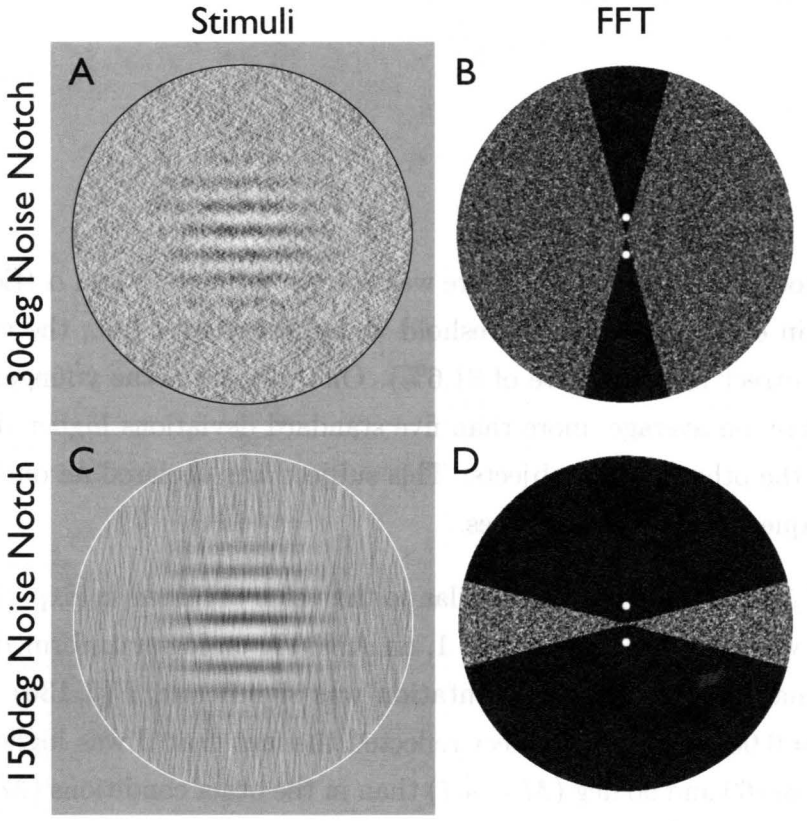


Figure 2.4: Example of the stimuli used in the notched-noise masking experiment. (A) The target is shown at supra-threshold contrast embedded in noise having only a small orientation notch (30 deg). (B) The Fourier transform of the stimulus in (A). Orientation is represented radially, and spatial frequency is represented by distance from the origin. The two bright points are the frequency components of the target. Note that, in this type of plot, a horizontal grating is represented by two vertically-aligned points, whereas a vertical grating would be represented as two horizontally-aligned points. The broadband noise mask contains non-zero amplitudes at all frequency components except those falling within 30 deg of the target's orientation. (C) and (D) show an example of a stimulus constructed with a notch bandwidth of 150 deg.

### Procedure

The same 2-IFC task that was employed in Experiment 1 was used here. Target contrast was varied across trials using QUEST. Staircases from all seven notch noise conditions were intermixed randomly, and a session ended when each staircase had accumulated 45 trials.

## 2.3.2 Results

A maximum likelihood curve fitting procedure was used to estimate $\beta$ and $\alpha$ (Equation 3.1) for each subject in each condition. Threshold was defined as $\alpha$ (i.e., the contrast needed to produce a correct response rate of 81.6%). One subject in the younger group had thresholds that were, on average, more than five standard deviations higher than the mean thresholds from the other young subjects. This subject was declared an outlier and was not used in subsequent statistical analyses.

The mean value of $\beta$ was 3.8, which was similar to the value obtained in Experiment 1. However, unlike what was found in Experiment 1, an ANOVA on log-transformed values of $\beta$ found that the main effect of mask orientation was significant, $F(6, 136) = 3.26$, $f = 0.33$, $\tilde{\epsilon} = 0.90$, $p = 0.007$. This main effect reflected the fact that $\beta$ was higher when the noise notch width was 60 and 90 deg ($M = 4.7$) than in the other conditions ($M = 3.5$). This result means that the shapes of the masking curves will not be invariant with changes in the threshold criterion. This point is elaborated in the Discussion. Importantly, however, the slope of the psychometric function did not vary across groups: Both the main effect of group, $F(1, 21) = 1.84$, $f = 0.08$, $p = 0.19$, as well as the group x orientation interaction, $F(6, 126) = 0.47$, $\tilde{\epsilon} = 0.90$, $p = 0.81$, were not significant. Therefore, the magnitude of any observed group differences in threshold do not depend on the threshold criterion.

Detection thresholds varied significantly with notch bandwidth, but were similar in the two age groups (Figure 2.5). An ANOVA on log-transformed thresholds found that the main effect of notch bandwidth was significant, $F(6, 126) = 189.89$, $f = 2.65$, $\tilde{\epsilon} = 0.88$, $p < 0.0001$, but that the main effect of age, $F(1, 21) = 0.18$, $p = 0.67$, and the age x notch bandwidth interaction, $F(6, 126) = 2.12$, $f = 0.20$, $\tilde{\epsilon} = 0.88$, $p = 0.065$, were not. Although the overall interaction between age and notch bandwidth was not significant, a more focussed statistical test did find that the linear effect of notch bandwidth was

smaller in older subjects, $F(1, 21) = 4.12$, $f = 0.14$, $p = 0.05$. This age x linear trend interaction is due primarily to the fact that thresholds in the widest notch conditions were higher in older subjects.

Table 2.5: Parameters $k$, $a$, $b$, and $\theta_{1/2}$ estimated in the notched-noise masking experiment.

| | younger subjects $\hat{\mu} \pm \hat{\sigma}_{\mu}$ | older subjects $\hat{\mu} \pm \hat{\sigma}_{\mu}$ |
|---|---|---|
| $k$ | $0.96 \pm 0.19$ $(\times 10^{-2})$ | $1.06 \pm 0.08$ $(\times 10^{-2})$ |
| $a$ | $0.67 \pm 0.14$ $(\times 10^{-1})$ | $0.49 \pm 0.31$ $(\times 10^{-1})$ |
| $b$ | $43.70 \pm 3.16$ | $44.56 \pm 3.25$ |
| $\theta_{1/2}$ | $40.62 \pm 2.43$ | $43.51 \pm 3.06$ |

Preliminary analyses indicated that Equation 2.2 provided a poor fit to the data from the current experiment. A much better fit was provided by the function

$$T(x) = k + a \cdot \exp\left(-\left(\frac{0.5x}{b}\right)^2\right) \tag{2.3}$$

where $T$ is threshold, $x$ is the full width of the noise notch, $k$ is the lower asymptote, $a$ is the difference between the maximum value and $k$, and $b$ governs the rate of decline from the maximum, $(k+a)$, to the minimum, $k$. Equation 2.3 was first fit to average thresholds in each age group by adjusting the values of $k$, $a$, and $b$ to minimize the sum of the squared log differences between the observed and predicted thresholds across conditions. The resulting parameters were used to draw the smooth curves in Figure 2.5, which fit the data in both age groups reasonably well. Next, Equation 2.3 was fit to the data from each subject. The value of $b$ for one subject was more than two standard deviations below the mean, and therefore was declared an outlier and not included in subsequent analyses. The means and standard errors of the best-fitting parameters are listed in Table 2.5. Separate $t$ tests indicated that none of the parameters differed significantly across age ($k$: $CI_{95\%} = (-0.0002, 0.0055)$, $t(21) = 1.94$, $p = 0.069$; $a$: $CI_{95\%} = (-0.015, 0.006)$, $t(21) = -0.9$, $p = 0.38$; $b$: $CI_{95\%} = (-8.60, 10.33)$, $t(20) = 0.19$, $p = 0.85$). The statistical test on $b$ remained non-significant when the outlier was included.

For each subject, the best-fitting version of Equation 2.3 was used to estimate $\theta_{1/2}$, which was defined as *one-half* of the notch width at which threshold fell to half of the maximum threshold. We used one-half of the notch width, rather than the full width, to

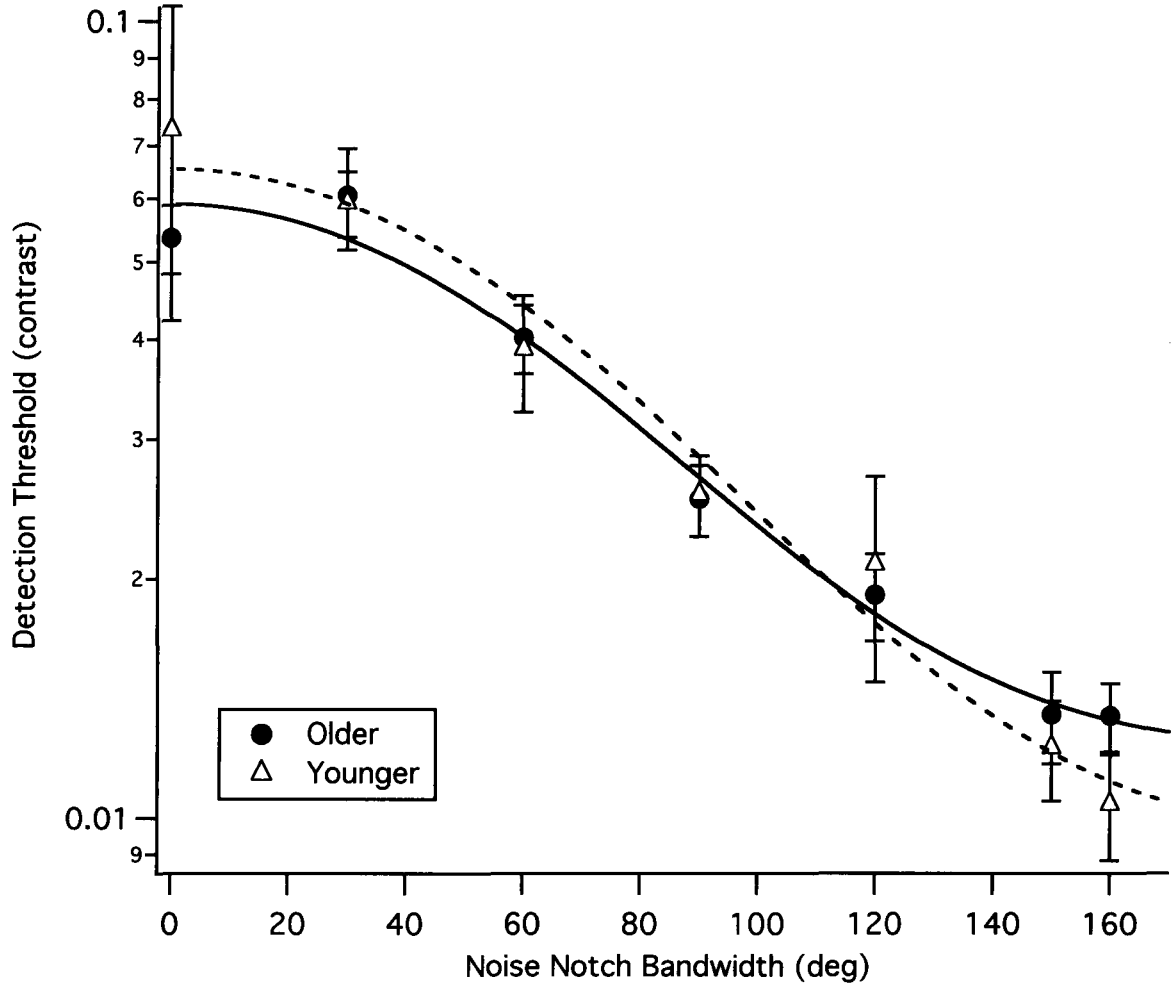


Figure 2.5: Notched-noise masking. Mean detection thresholds for older and younger subjects plotted as a function of the full width of the orientation notch bandwidth. The notch was centered on the orientation of the target grating (i.e, 0 deg). Error bars represent the 95% confidence interval of the mean. Equation 2.3 was fit to the average thresholds from each age group. The solid and dashed curves represent the results for older and younger subjects, respectively.

enable comparisons between $\theta_{1/2}$ in the current Experiment with the values calculated in Experiment 1. The overall mean of $\theta_{1/2}$ was 42.2 deg, $CI_{95\%} = (38.1,\ 46.4)$; the mean value for each age group is listed in Table 2.5. The difference between age groups was not statistically significant, $CI_{95\%} = (-5.27, 11.04)$, $t(20) = 0.74$, $p = 0.47$.

The grand mean of $\beta$ measured in the low-luminance control experiment was 3.5. Interestingly, a 2 (luminance) x 7(orientation) ANOVA on log-transformed values of $\beta$ found no significant effects (luminance: $F(1,4) = 0.08$, $p = 0.78$; notch width: $F(6,24) = 0.69$, $\tilde{\epsilon} = 1$, $p = 0.66$; luminance x notch width: $F(6,24) = 1.92$, $f = 0.28$, $\tilde{\epsilon} = 1$, $p = 0.12$). Hence, unlike what was found in the main experiment, there was no evidence that $\beta$ varied systematically across conditions. Thresholds obtained in the control experiment are shown in Figure 2.6. A within-subjects ANOVA performed on log-transformed thresholds found that the main effect of luminance was not significant, $F(1,4) = 6.13$, $f = 0.27$, $p = 0.7$, but that the main effect of notch bandwidth, $F(6,24) = 84.6$, $f = 2.67$, $\tilde{\epsilon} = 1$, $p < 0.0001$, and the luminance x notch bandwidth interaction, $F(6,24) = 9.75$, $f = 0.87$, $\tilde{\epsilon} = 1$, $p < 0.0001$, were significant.

Equation 2.3 provided reasonably good fits to the average thresholds in each luminance condition (Figure 2.6) as well as to the individual sets of data. The means and standard errors of the best-fitting parameters are shown in Table 2.6. Separate $t$ tests indicated that $k$ was significantly lower in the high luminance condition, $CI_{95\%} = (-0.010, -0.002)$, $t(4) = -4.32$, $p = 0.012$; $b$ was significantly higher in the high luminance condition, $CI_{95\%} = (3.11, 7.43)$, $t(4) = 6.78$, $p = 0.002$; and $a$ did not differ between luminance conditions, $CI_{95\%} = (-0.011, 0.026)$, $t(4) = 1.16$, $p = 0.31$. The bandwidth of orientation masking, $\theta_{1/2}$, was 35.19 and 34.97 deg in the high and low luminance conditions, respectively, a difference that was not statistically significant, $CI_{95\%} = (-4.85, 5.29)$, $t(4) = 0.12$, $p = 0.91$.

### 2.3.3 Discussion

Experiment 2 measured thresholds for a Gabor pattern embedded in notched-filtered noise to reduce the possibility that subjects could detect the target on the basis of spatial beats or other local spatial distortions in the mask. We found that thresholds in most conditions were very similar in older and younger subjects, and that the parameters of the masking function (Equation 2.3) did not differ across age groups (Table 2.5). A test for linear trend suggested that threshold declined more slowly in older subjects than

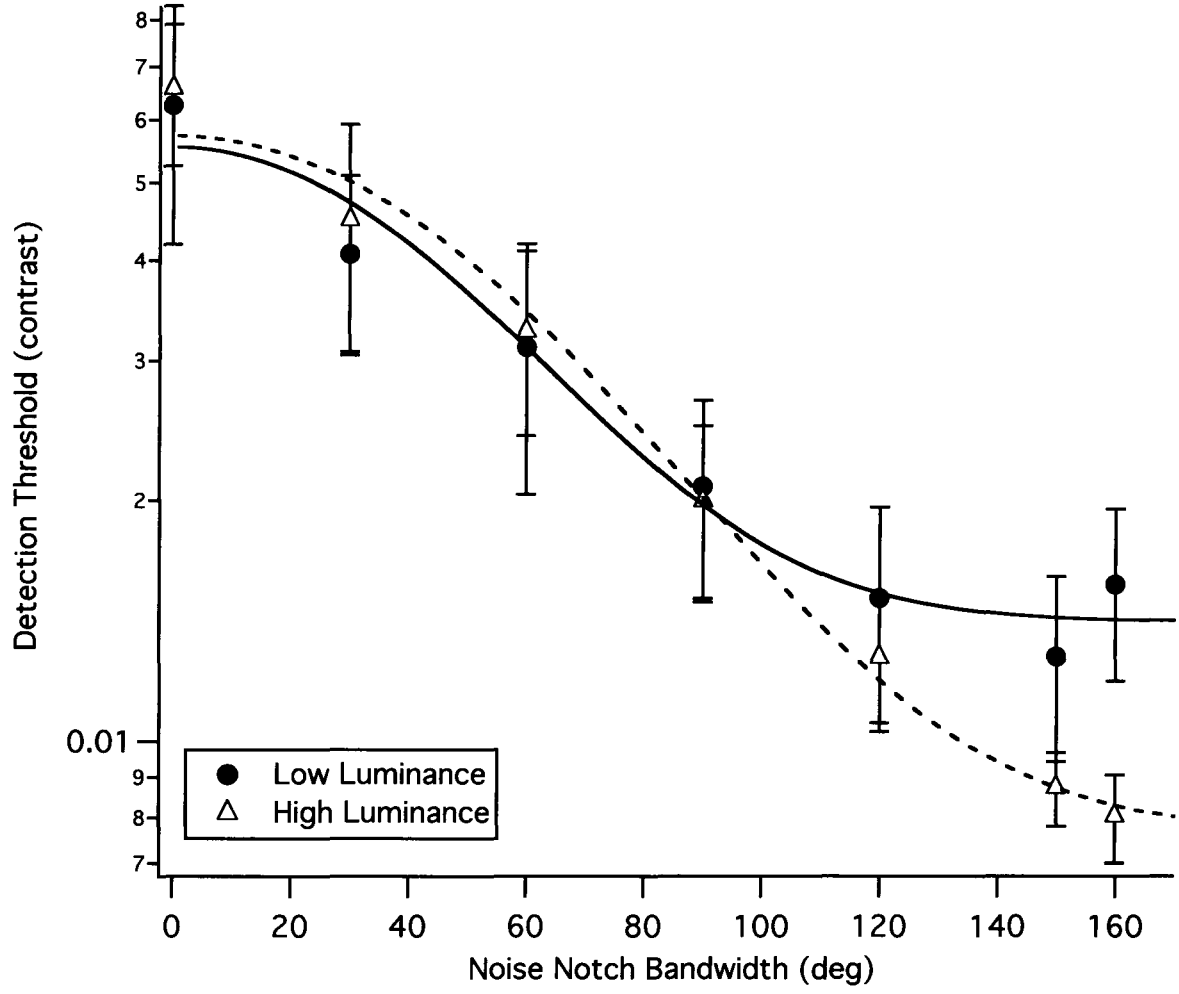


Figure 2.6: Low luminance control experiment using notched-noise masking. Mean detection thresholds measured at two average luminances for five younger subjects are plotted as a function of the full notch bandwidth. The notch was centered on the orientation of the target grating (i.e., 0 deg). Error bars represent the 95% confidence interval of the mean. Equation 2.3 was fit to the average thresholds in each condition; the solid and dashed curves represent the results for low and high luminance conditions, respectively.

Table 2.6: Parameters $k$, $a$, $b$, and $\theta_{1/2}$ estimated in the notched-noise luminance control experiment.

| | high luminance $\hat{\mu} \pm \hat{\sigma}_{\mu}$ | low luminance $\hat{\mu} \pm \hat{\sigma}_{\mu}$ |
|---|---|---|
| $k$ | $0.75 \pm 0.02$ $(\times 10^{-2})$ | $1.38 \pm 0.15$ $(\times 10^{-2})$ |
| $a$ | $0.50 \pm 0.06$ $(\times 10^{-1})$ | $0.42 \pm 0.07$ $(\times 10^{-1})$ |
| $b$ | $37.80 \pm 2.36$ | $35.52 \pm 2.96$ |
| $\theta_{1/2}$ | $35.19 \pm 2.22$ | $34.97 \pm 3.87$ |

in younger subjects with increasing notch width. The results of the luminance control experiment, however, suggest that this slight difference in the shape of the masking function may simply be due to age differences in retinal illuminance. The key result for the present investigation, however, is the fact that there was no evidence for reduced orientation selectivity of masking in older subjects. In this regard, the results of the current experiment are similar to the behavioral results obtained in Experiment 1 and by Delahunt et al. (2008), but, again, are inconsistent with results from single cell electrophysiology (Schmolesky et al., 2000; Leventhal et al., 2003).

In the main experiment, the slope of the psychometric function was higher in conditions that used notch widths of 60 and 90 deg. This difference in slope means that the shape of the masking function would change if a different threshold criterion (e.g., 70% correct) were used. However, such changes in the function's shape would be small. For example, defining threshold as the 70% correct point on the psychometric function (Equation 3.1) would lower threshold by 0.097 log units if $\beta = 3$, and by 0.053 log units if $\beta = 5.5$. In other words, if the slopes in two conditions were 3 and 5.5, then changing the definition of threshold from 81.6% to 70% correct would introduce a *relative* change in threshold equal to $0.097 - 0.053 = 0.044$ log units or $\approx 10\%$. Smaller changes in the threshold criterion (e.g., from 81.6% to 75% correct) would produce smaller relative changes in threshold across conditions. In our experiment, $\beta$ ranged from approximately 3 to 5.5, so using a different criterion for threshold would have only minor effects on the shape of the masking function. Therefore, variation of $\beta$ across conditions cannot account for the finding that the masking function was much broader in Experiment 2 than Experiment 1. This point is reinforced by the the fact that broad masking functions were obtained in the notched-noise luminance control experiment even though $\beta$ did *not* vary significantly

across conditions.

Our estimate of $\theta_{1/2}$ from Experiment 2 (42 deg) is similar to the value of 45 deg reported by Tootell et al. (1998) in an fMRI analysis of orientation tuning in V1 in humans. Of all the values listed in Table 2.4, our estimate of $\theta_{1/2}$ is closest to the value of 30 deg reported by Blake and Holopigian (1985), who used a two-component noise mask, but it is considerably larger than the other values in Table 2.4 as well as the estimate obtained in Experiment 1. It is not clear why $\theta_{1/2}$ was so much larger in Experiment 2. One possibility is that the broader orientation bandwidth was the result of using a noise mask that eliminated spatial beats as a potential cue for detecting the target. Such cues have been shown to be important for detecting and discriminating supra-threshold spatial patterns in several contexts, including masking experiments (Badcock, 1988; Derrington and Badcock, 1986; Hess and Pointer, 1987; Nachmias, 1993). In Experiment 1, such cues may have made it easier to detect the target in conditions where the orientations of the target and mask differed, and therefore decreased $\theta_{1/2}$. A related idea, suggested by a reviewer, is that the narrower masking functions obtained in Experiment 1 were due to the way beats and local distortions affected spatial probability summation (see Baker and Meese, 2007, p. 3102).

Another possibility is that the value of $\theta_{1/2}$ obtained with sine wave masks is unusually low because of the effects of off-channel looking (Blake and Holopigian, 1985; Henning and Wichmann, 2007; Henning et al., 1981; Patterson and Nimmo-Smith, 1980; Solomon and Pelli, 1994). If a subject can detect a target by monitoring one of several channels tuned to different orientations, then an efficient strategy would be to monitor the channel with the highest signal-to-noise ratio. In Experiment 1, the mask was asymmetrical: it consisted of a single orientation rotated clockwise or counter-clockwise relative to the target. Therefore, off-channel looking would enable a subject to minimize the effects of the mask by monitoring the responses of channels that responded best to orientations that differed from the target orientation, and therefore lead to narrower estimates of $\theta_{1/2}$. If the mask was rotated counter-clockwise relative to the target, for example, then the signal-to-noise ratio would be highest in a channel tuned to an orientation that is clockwise relative to the target. Off-channel looking would not produce much benefit in Experiment 2 because the noise contained orientations that were placed symmetrically about the target's orientation. Hence, off-channel looking would produce smaller values of $\theta_{1/2}$ in Experiment 1 than in Experiment 2.

Blake and Holopigian (1985) estimated the effects of off-channel looking on the

bandwidth of orientation masking by measuring masking with one- and two-component masks in a single subject, and found that $\theta_{1/2}$ was 6 deg larger when the mask contained two components oriented symmetrically about the target. So Blake and Holopigian obtained evidence that off-channel looking occurred, but the effect probably is too small to account for the difference between $\theta_{1/2}$ obtained in Experiments 1 and 2. On the other hand, Derrington and Henning (1989) found that the masking produced by a plaid pattern – composed of two sine wave gratings oriented symmetrically about the target grating – was much greater than the sum of the component masking effects (also see Meese et al., 2007; Ross and Speed, 1991). Moreover, Derrington and Henning obtained significant masking with plaids composed of orientations that differed significantly from the target's orientation (e.g., ±45 and ±67 deg). At least under some conditions, therefore, the orientation bandwidth of masking is greatly increased when the mask is a plaid rather than a sine wave grating. The same mechanism that produces this excess masking with plaids – be it off-channel looking or some other non-linearity – may have contributed to the broader pattern of masking found in Experiment 2. The current results suggests that these mechanisms operate similarly in older and younger subjects.

## 2.4 General discussion

Orientation selectivity is reduced significantly in V1 cells in senescent cats (Hua et al., 2006) and monkeys (Schmolesky et al., 2000), but there is little evidence that the perception of orientation is impaired by normal aging. Betts et al. (2007) reported that sensitivity to orientation differences was reduced in older subjects when stimulus contrast was low, but not when stimulus contrast was high. Although Delahunt et al. (2008) found age differences in orientation discrimination thresholds at all stimulus contrasts, they attributed this effect to age differences in contrast sensitivity, rather than to orientation discrimination *per se*: When stimulus contrast was expressed in terms of multiples of detection threshold, orientation discrimination thresholds in older and younger subjects did not differ. In addition, Delahunt et al. reported that the orientational selectivity of sine wave masking did not differ across age groups. Experiment 1 replicated Delahunt et al.'s finding: $\theta_{1/2}$ was approximately 14 deg in both age groups. The bandwidth of masking was considerably broader in Experiment 2 ($\theta_{1/2} \approx 42$ deg), but again did not differ in older and younger subjects. These findings suggest that orientation tuning may be preserved across the life span.

What might account for the apparent discrepancy between the physiological studies of the effects of aging on orientation coding (Hua et al., 2006; Schmolesky et al., 2000) and the psychophysical results reported here and elsewhere (Betts et al., 2007; Delahunt et al., 2008)? One possible explanation for the difference is that the physiological effects are caused by age differences in the effects of anesthesia, rather than visual processing *per se*. Evidence against this explanation comes from Wang et al. (2005), who found that large variations in the level of anesthetic did not significantly alter the age differences in the physiological responses of V1 and V2 neurons. Another possibility is that older human subjects in our experiments, but not the anesthetized monkeys in the physiological studies, were able to use focussed attention to compensate for age-related physiological changes in V1 neurons. In monkeys, focussed attention alters the response properties of single neurons in many visual cortical areas (Maunsel, 2003); in humans, attention modulates the steady-state visually-evoked potential (ss-VEP; Di Russo and Spinelli 1999) and the BOLD response in V1 (Smith et al., 2006). Thus, it is plausible to suggest that visual attention may have boosted the signal-to-noise ratio of orientation-selective mechanisms in our older subjects, or perhaps allowed older subjects to use different functional neural networks for extracting the signal from visual neurons, as has been shown for a spatial frequency discrimination task (Bennett et al., 2001; Della-Maggiore et al., 2000; McIntosh et al., 1999). However, there is as yet little evidence that attention significantly alters the tuning of cortical neurons, and at least one study has found that attention has no effect on orientation selectivity in V4 neurons (McAdams and Maunsel, 1999). Hence, the effect of attention on orientation selectivity remains unclear.

Another way of reconciling the physiological and psychophysical results is to consider which subset of cortical neurons might contribute to behaviour. The physiological difference in orientation selectivity between cells in young and old animals reflects the difference between *average* cells. However, a small number of cells in older cats (Hua et al., 2006) and monkeys Schmolesky et al. (2000) remained highly selective for orientation. If psychophysical orientation judgments were most closely related to the responses of this relatively small group of highly-selective cells (Parker and Newsome, 1998), then we would not expect to find large age differences in orientation bandwidth. One way of testing this idea would be to use the steady-state visually evoked potential (ss-VEP) to measure orientation-tuning (Regan and Regan, 1987). Because ss-VEP represents the average response of a large population of neurons, rather than just the most selective neurons, it might be more sensitive than psychophysical methods to age-related changes in the average orientation bandwidth of cortical mechanisms.

**Acknowledgements**

This research was supported by the Canada Research Chairs program, of which PJB and ABS are members, a grant from the Canadian Institutes of Health Research to PJB and ABS, and by NSERC-PGS and CIHR-STIHR awards to SWG. Portions of this work were presented at the annual meeting of the Vision Sciences Society (Sarasota, FL U.S.A, May 2006). The authors would like to thank Donna Waxman for her help with collecting the data.

# References

Anderson, S. J., Burr, D. C., Morrone, M. C., 1991. Two-dimensional spatial and spatial-frequency selectivity of motion-sensitive mechanisms in human vision. Journal of the Optical Society of America. A, Optics, Image science, and Vision 8 (8), 1340–1351.

Badcock, D. R., 1988. Discrimination of spatial phase changes: contrast and position codes. Spat Vis 3 (4), 305–322.

Baker, D. H., Meese, T. S., 2007. Binocular contrast interactions: dichoptic masking is not a single process. Vision Res 47 (24), 3096–3107.

Bennett, P. J., Sekuler, A. B., McIntosh, A. R., Della-Maggiore, V., 2001. The effects of aging on visual memory: Evidence for functional reorganization of cortical networks. Acta Psychologica 107 (1-3), 249–273.

Bennett, P. J., Sekuler, A. B., Ozin, L., 1999. Effects of aging on calculation efficiency and equivalent noise. Journal of the Optical Society of America. A, Optics, Image science, and Vision 16, 654–658.

Betts, L. R., Sekuler, A. B., Bennett, P. J., 2007. The effects of aging on orientation discrimination. Vision Research 47, 1769–1780.

Blake, R., Holopigian, K., 1985. Orientation selectivity in cats and humans assessed by masking. Vision Research 25 (10), 1459–1467.

Brainard, D. H., 1997. The psychophysics toolbox. Spatial Vision 10, 443–446.

Burbeck, C. A., Kelly, D. H., 1981. Contrast gain measurements and the transient/sustained. J Opt Soc Am 71 (11), 1335–1342.

Burr, D. C., Morrone, M. C., 1987. Inhibitory interactions in the human vision system revealed in pattern-evoked potentials. J Physiol 389, 1–21.

Campbell, F. W., Kulikowski, J. J., 1966. Orientational selectivity of the human visual system. Journal of Physiology 187, 437–445.

Cohen, J., 1988. Statistical power analysis for the behavioral sciences, 2nd Edition. L. Erlbaum Associates, Hillsdale, N.J.

Crum, R. M., Anthony, J. C., Bassett, S. S., Folstein, M. F., 1993. Population-based norms for the mini-mental state examination by age and education level. Journal of the American Medical Association 269, 2386–2391.

Delahunt, P., Hardy, J., Werner, J., 2008. The effect of sensescence on orientation discrimination and mechanism tuning. Journal of Vision 8 (3), 1–9.

Della-Maggiore, V., Sekuler, A. B., Grady, C. L., Bennett, P. J., Sekuler, R., McIntosh, A. R., 2000. Corticolimbic interactions associated with performance on a short-term memory task are modified by age. Journal of Neuroscience 20, 8410–8416.

Derrington, A. M., Badcock, D. R., 1986. Detection of spatial beats: non-linearity or contrast increment detection? Vision Res 26 (2), 343–348.

Derrington, A. M., Henning, G. B., 1989. Some observations on the masking effects of two-dimensional stimuli. Vision Res 29 (2), 241–246.

Di Russo, F., Spinelli, D., 1999. Electrophysiological evidence for an early attentional mechanism in visual processing in humans. Vision Research 39 (18), 2975–85.

Foley, J. M., 1994. Human luminance pattern-vision mechanisms: masking experiments require a new model. J Opt Soc Am A Opt Image Sci Vis 11 (6), 1710–1719.

Folstein, M. F., Folstein, S. E., McHugh, P. R., 1975. "mini-mental state." a practical method for grading the cognitive state of patients for the clinician. Journal of Psychiatric Research 12, 189–198.

Henning, G. B., Hertz, B. G., Hinton, J. L., 1981. Effects of different hypothetical detection mechanisms on the shape of spatial-frequency filters inferred from masking experiments: I. noise masks. J Opt Soc Am 71 (5), 574–581.

Henning, G. B., Wichmann, F. A., 2007. Some observations on the pedestal effect. J Vis 7 (1), 3.

Hess, R. F., Pointer, J. S., 1987. Evidence for spatially local computations underlying discrimination of periodic patterns in fovea and periphery. Vision Res 27 (8), 1343–1360.

Hibbard, P., 2005. The orientation bandwidth of cyclopean channels. Vision Research 45 (21), 2780–2785.

Hua, T., Li, X., He, L., Zhou, Y., Wang, Y., Leventhal, A. G., 2006. Functional degradation of visual cortical cells in old cats. Neurobiology of Aging 27, 155–162.

Kirk, R. E., 1995. Experimental design: procedures for the behavioral sciences, 3rd Edition. Brooks/Cole, Pacific Grove, Calif.

Leventhal, A. G., Wang, Y., Pu, M., Zhou, Y., Ma, Y., 2003. GABA and its agonists improved visual cortical function in senescent monkeys. Science 300, 812–815.

Losada, M. A., Mullen, K. T., 1995. Color and luminance spatial tuning estimated by noise masking in the absense of off-frequency looking. Journal of the Optical Society of America. A, Optics, Image science, and Vision 12, 250–260.

Maunsel, J., 2003. The role of attention in visual cerebral cortex. In: Chalupa, L., Werner, J. (Eds.), The Visual Neurosciences. Vol. 2. MIT Press, Cambridge, Mass., Ch. 103, pp. 1538–1545.

Maxwell, S., Delaney, H., 2004. Designing Experiments and Analyzing Data: A Model Comparison Approach, 2nd Edition. Lawrence Erlbaum Associates, Mahwah, New Jersey.

McAdams, C., Maunsel, J., 1999. Effects of attention on orientation-tuning functions of single neurons in macaque cortical area v4. Journal of Neuroscience 19, 431–441.

McIntosh, A. R., Sekuler, A. B., Penpeci, C., Rajah, M. N., Grady, C. L., Sekuler, R., Bennett, P. J., 1999. Recruitment of unique neural systems to support visual memory in normal aging. Current Biology 9 (21), 1275–1278.

Meese, T. S., Holmes, D. J., Challinor, K. L., 2007. Remote facilitation in the fourier domain. Vision Res 47 (8), 1112–1119.

Mullen, K. T., Losada, M. A., 1999. The spatial tuning of color and luminance peripheral vision measured with notch filtered noise masking. Vision Research 39, 721–731.

Nachmias, J., 1993. Masked detection of gratings: the standard model revisited. Vision Res 33 (10), 1359–1365.

Parker, A. J., Newsome, W. T., 1998. Sense and the single neuron: Proving the physiology of perception. Annual Review of Neuroscience 21, 227–277.

Patterson, R. D., 1976. Auditory filter shapes derived with noise stimuli. Journal of the Acoustical Society of America 59, 640–654.

Patterson, R. D., Nimmo-Smith, I., 1980. Off-frequency listening and auditory-filter asymmetry. Journal of the Acoustical Society of America 67 (1), 229–245.

Pelli, D. G., 1997. The videotoolbox software for visual psychophysics: Transforming numbers into movies. Spatial Vision 10, 437–442.

Phillips, G., Wilson, H., 1984. Orientation bandwidths of spatial mechanisms measured by masking. Journal of the Optical Society of America. A, Optics, Image science, and Vision 1 (2), 226–232.

R Development Core Team, 2007. R: A Language and Environment for Statistical Computing. R Foundation for Statistical Computing, Vienna, Austria.
URL `http://www.R-project.org`

Regan, D., Regan, M. P., 1987. Nonlinearity in human visual responses to two-dimensional patterns, and a limitation of fourier methods. Vision Research 27 (12), 2181–2183.

Ross, J., Speed, H. D., 1991. Contrast adaptation and contrast masking in human vision. Proc Biol Sci 246 (1315), 61–69.

Schmolesky, M. T., Wang, Y., Pu, M., Leventhal, A. G., 2000. Degradation of stimulus selectivity of visual cortical cells in senescent rhesus monkeys. Nature Neuroscience 3, 384–390.

Sekuler, A. B., Bennett, P. J., Mamelak, M., 2000. Effects of aging on the useful field of view. Experimental Aging Research 26, 103–120.

Sekuler, R., Sekuler, A. B., 2000. Visual perception and cognition. In: Evans, J. G., Williams, T. F., Beattie, B. L., Michel, J. P., Wilcock, G. K. (Eds.), Oxford Textbook of Geriatric Medicine. Oxford University Press, New York, pp. 874–880.

Smith, A., Cotillon-Williams, N., Williams, A., 2006. Attentional modulation in the human striate cortex: The time-course of the bold response and its implications. Neuroimage 29, 328–334.

Solomon, J. A., Pelli, D. G., 1994. The visual filter mediating letter identification. Nature 369 (6479), 395–397.

Stromeyer, C. F. r., Julesz, B., 1972. Spatial-frequency masking in vision: critical bands and spread of masking. J Opt Soc Am 62 (10), 1221–1232.

Tootell, R., Hadjikhani, N., Vanduffel, W., Liu, A., Mendola, J., Sereno, M., Dale, A., 1998. Functional analysis of primary visual cortex (v1) in humans. Proceedings of the National Academy of Sciences USA 95, 811–817.

Tyler, C., Chan, H., Liu, L., McBride, B., Kontsevich, L., 1992. Bit-stealing: How to get 1786 or more grey levels from an 8-bit color monitor. In: Rogowitz, B. (Ed.), SPIE Proceedings: Human vision, visual processing, and digital display III. Vol. 1666. pp. 351–364.

Wang, Y., Zhou, Y., Ma, Y., Leventhal, A., 2005. Degradation of signal timing in cortical areas V1 and V2 of senescent monkeys. Cerebral Cortex 15 (15), 403–408.

Watson, A. B., Pelli, D. G., 1983. Quest: A bayesian adaptive psychophysical method. Perception & Psychophysics 33, 113–120.

Weale, R. A., 1961. Retinal illumination and age. Transactions of the Illuminating Engineering Society 26, 95–100.

# Chapter 3

# The effect of aging on the spatial frequency selectivity of the human visual system

**Abstract**

Changes in the physiological properties of senescent V1 neurons suggest that the mechanisms encoding spatial frequency in primate cortex may become more broadly tuned in old age (Zhang et al., *Eur J Neurosci*, 2008, 28, 201-07). We examined this possibility in two psychophysical experiments that used masking to estimate the bandwidth of spatial frequency-selective mechanisms in younger (age $\approx$ 22 years) and older (age $\approx$ 65 years) human adults. Contrary to predictions from physiological studies, in both experiments, the spatial frequency selectivity of masking was essentially identical in younger and older subjects.

## 3.1 Introduction

The visual system encodes the visual scene with spatial filters selective for spatial frequency, orientation, and motion (see DeValois and DeValois, 1988, for a review). The fidelity with which the visual scene is encoded presumably depends, in part, on the bandwidth of these filters, and the bandwidth of these mechanisms may increase with normal, healthy aging. For example, compared to visual neurons in young adult macaque

monkeys, neurons in the primary visual cortex in senescent macaques have markedly reduced selectivity for spatial frequency, orientation, and direction of motion (Schmolesky et al., 2000; Leventhal et al., 2003; Zhang et al., 2008).

Previous psychophysical studies have examined the effects of aging on orientation (Delahunt et al., 2008; Govenlock et al., 2009) and motion (Bennett et al., 2007) selectivity in humans, with mixed results; psychophysical estimates of the bandwidth of orientation tuning change little as a function of age, whereas psychophysical results from motion discrimination tasks are consistent with an age-related broadening of the bandwidth of direction-selective mechanisms. To the best of our knowledge, however, there are no estimates of the effects of aging on the selectivity of spatial frequency-tuned mechanisms of human adults. Detuning of older humans' lower-level spatial scale mechanisms could explain a variety of higher level age-related visual deficits related to form (Norman et al., 2003; Del Viva and Agostini, 2007; Legault et al., 2007; Andersen and Ni, 2008; Habak et al., 2008; Roudaia et al., 2008) and the interaction of motion and form (Andersen and Atchley, 1995; Norman et al., 2003; Billino et al., 2008; Pilz et al., in press). In the current study, therefore, we used two psychophysical masking techniques to examine whether the spatial frequency selectivity of masking — which is thought to reflect the tuning of underlying spatial frequency channels (DeValois and DeValois, 1988) — is affected by normal aging.

## 3.2 Experiment 1: Sine-wave grating masking

The presence of one or more high-contrast sine wave masks elevates threshold for a sine wave target pattern, provided that the mask(s) and target have similar spatial frequencies and orientations. The relation between the strength of masking and the difference between mask and target spatial frequencies has been used to infer the spatial frequency bandwidth of the mechanisms used to detect the target in younger observers. The earliest studies using this method utilized only one sine wave mask (e.g., Stromeyer and Julesz 1972; Stromeyer and Klein 1974; Legge and Foley 1980). One potential problem with these studies is that the estimates of channel bandwidth may have been affected by off-channel, or off-frequency, looking (Gaspar et al., 2008; Patterson and Nimmo-Smith, 1980; Solomon and Pelli, 1994). If a target can be detected by monitoring the response one of several spatial frequency channels, then the optimal strategy would be to pick the channel that responds well to the target and very poorly to the noise. In cases where the mask consists

Table 3.1: Mean values for age (years), logMAR acuity, and Mini-Mental State Exam (MMSE). Values in parentheses are standard deviations.

| Experiment | $N$ | Age | Near acuity | Far acuity | MMSE |
|---|---|---|---|---|---|
| 1 | 13 older | 68.9 (3.3) | -0.02 (0.08) | -0.05 (0.11) | 29.46 (1.13) |
| | 13 younger | 21.8 (1.4) | -0.15 (0.07) | -0.10 (0.08) | |
| 2 | 12 older | 69.8 (4.3) | -0.00 (0.11) | -0.04 (0.10) | 28.67 (1.30) |
| | 12 younger | 21.8 (3.5) | -0.16 (0.08) | -0.15 (0.06) | |

of spatial frequencies that are higher than the target, then the signal to noise ratio might be increased by monitoring the response of a channel whose peak frequency is below the target frequency. On the other hand, if the mask consists of frequencies below the target frequency, then it might be better to monitor the response of a channel tuned to frequencies that are slightly higher than the target frequency. Off-frequency looking essentially reduces the amount of masking produced by frequencies close to the target frequency, and therefore results in a lower estimate of channel bandwidth.

To reduce the effects of off-frequency looking, masking studies have used two symmetrically-offset masks (Patterson and Nimmo-Smith, 1980; Henning et al., 1981; Solomon and Pelli, 1994; Henning and Wichmann, 2007), which makes it more likely that the channel centered on the target frequency is the one with the highest signal to noise ratio in all mask conditions. In Experiment 1 we measured detection thresholds for a Gaussian-damped sine wave grating (i.e., the target) embedded in a mask consisting of two sine wave gratings that had frequencies that were symmetrically offset from the target frequency to determine whether the spatial frequency selectivity of masking changes as a function of aging (see Figure 3.1).

### 3.2.1 Methods

For all of the experiments reported here, the research protocol was approved by McMaster University's Research Ethics Board, and informed consent was obtained from each subject before the start of the experiment.

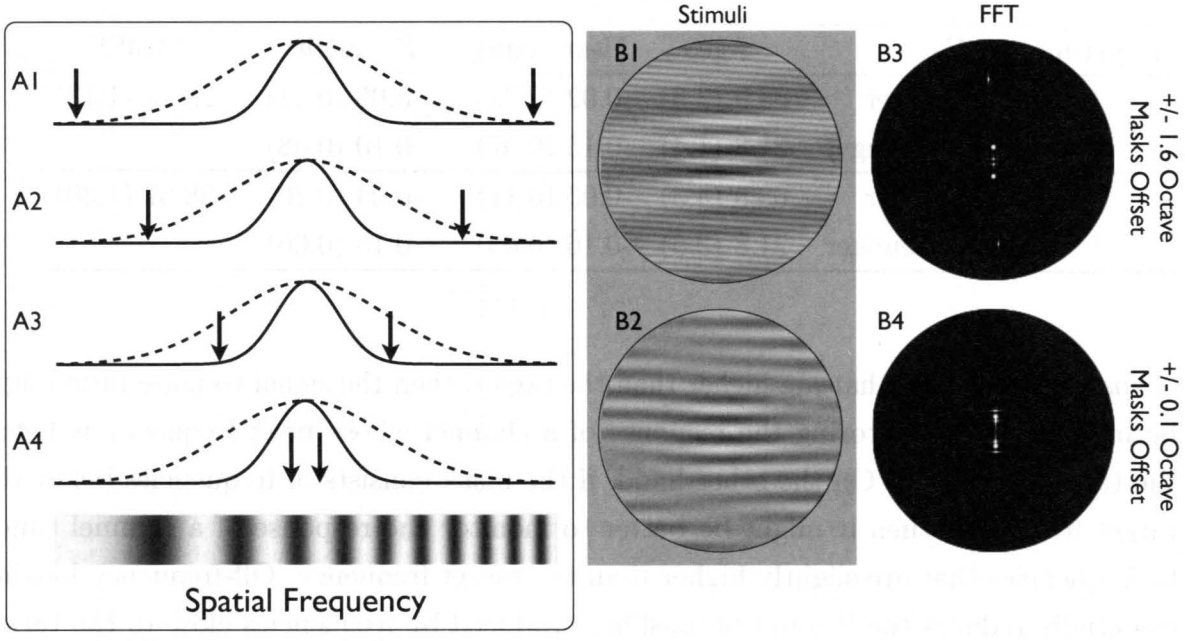


Figure 3.1: An illustration of the sine wave grating masking paradigm, as well as example stimuli and their Fourier transforms from two conditions. Panel A: the solid and dashed lines illustrate hypothetical tuning functions of two spatial frequency filters that are centered on the same (target) frequency but differ in bandwidth. In A1 the arrows, representing two masking frequencies, are far removed from the target frequency and will not affect the response of either filter. As the mask frequencies move toward the target frequency (A2-A4), they fall within the passband of the filters and will elevate target detection threshold. In some conditions, the mask frequencies affect only the broader filter (A3). Panel B: B1 and B2 show example stimuli constructed with large and small masks' offset, respectively. B3 and B4 show the respective 2D Fourier transforms for these stimuli. In these polar plots, a horizontal grating is represented by a pair of vertically-aligned dots, whereas a vertical grating would be represented by two horizontal dots. Spatial frequency is represented by the distance from the dots to the center of the graph. The two brightest points in each transform represent the horizontal, 3 c/deg target Gabors, and the remaining two pairs of dots represent the mask frequencies.

**Subjects** Thirteen older and 13 younger paid subjects participated in this experiment. All subjects completed vision and general health questionnaires to screen for visual pathology, such as cataracts, macular degeneration, glaucoma, and amblyopia. Near and far decimal logMAR acuities were measured for all subjects with CSV-100EDTRS eye charts (Precision Vision, LaSalle, Illinois, USA). When measuring acuity, subjects wore their normal optical correction for each distance. Older subjects completed the Mini-Mental State Examination (MMSE) (Folstein et al., 1975) to screen for age-related dementia. All older subjects scored within the normal range for their age groups on the MMSE (Crum et al., 1993). The means and standard deviations of age, near and far acuities, and MMSE scores appear in Table 3.1. All subjects had normal or corrected-to-normal acuity and no known vision health problems.

**Stimuli and Apparatus** The experiment was programmed in MatLab v5.2.1 (The Mathworks) using the Psychophysics and Video Toolboxes (Brainard 1997; Pelli 1997) running on an Apple G4 PowerMac computer. The stimuli were displayed on a 21-inch Apple Studio Display. Display size was 1024 × 768 pixels, which subtended visual angles of 19.1 ° horizontally and 14.4 ° vertically from the viewing distance of 114 cm. The frame rate was 75 Hz, noninterlaced. Calibration was done using a PhotoResearch PR-650 spectracolorimeter, and the calibration data were used to build a 1779-element look-up table (Tyler et al., 1992). When constructing the stimuli used on each trial, the computer software selected appropriate luminance values from the calibrated look-up table and stored them in the 8-bit look-up table of the display. Average luminance of the display was 32 cd/m$^2$ and was constant throughout the experiment. The monitor was the only source of light in the room during testing. Viewing was binocular through natural pupils, and a chin/forehead rest was used to stabilize viewing position.

The visual target – 256 × 256 pixels, or 4.8 ° × 4.8 ° – was a horizontal, 3 c/deg sine wave grating. Target contrast was modulated by a radially-symmetric Gaussian window ($2\sigma$ = 1.2 °). The spatial phase of the target, relative to the center of the Gaussian window, was fixed at 0 ° (i.e., cosine phase). The target was masked by two 4.8 ° × 4.8 ° sine wave gratings. The contrast of each mask component grating was 0.14, and was modulated by a circular aperture (diameter = 4.8 °). To make it more difficult for subjects to learn to use a *specific* pattern of beats to detect the target (Nachmias, 1993), on each interval of every trial the phase of each mask component was randomized and the orientation of each mask component was selected randomly from a uniform distribution that extended from ± 5 ° around the target orientation. The spatial frequencies of the

mask components differed from the target spatial frequency by 0, ±0.1, ±0.2, ±0.5, ±0.8, ±1.6, or ±3 octaves. In conditions that used a non-zero frequency offset, one mask component had a spatial frequency that was higher than the target frequency and the other had a frequency that was lower than the target frequency, and both components differed from the target frequency by an equal number of octaves (Figure 3.1).

**Procedure** Thresholds were measured with a two-interval forced-choice (2-IFC) task. A circular (diameter = 6.7 arcmin) high-contrast fixation spot was presented in the center of the display. The subject began a trial by fixating the spot and pressing the space bar on a standard computer keyboard. The fixation point then was erased, and, after a delay of 500 ms, followed by two successive 200 ms stimulus intervals separated by an inter-stimulus interval of 500 ms. Each stimulus interval contained a high-contrast outline of a circle (diameter = 4.8 °; outline width = 1 pixel) that served to mark the spatial and temporal extent of the stimulus. One interval contained the target-plus-mask, the other contained the mask alone, and the subject's task was to select the interval that contained the target by pressing one of two response keys. An auditory tone provided feedback after incorrect responses; no sound followed a correct response. Subjects were informed that the probability of the target appearing in the first stimulus interval was 0.5. Target contrast was varied across trials using QUEST (Watson and Pelli, 1983). The seven mask spatial frequency conditions were blocked and randomly ordered. A session ended when each staircase had accumulated 45 trials.

### 3.2.2 Results

All statistical analyses were done with R (R Development Core Team, 2007). Where appropriate, the Huynh-Feldt correction, $\tilde{\epsilon}$, was used to adjust the degrees-of-freedom to correct for violations of the sphericity assumption underlying $F$ tests for within-subject variables (Maxwell and Delaney, 2004). In cases where the Huynh-Feldt correction is used, the reported $p$ values are the adjusted $p$ values. Effect size was expressed as Cohen's $f$ (Cohen, 1988), and was calculated using formulae described by Kirk (1995). When $F < 1$, the effect size was assumed to be zero (see Kirk, 1995, page 180). Between-group $t$ tests assumed unequal group variances and used the Welch-Satterthwaite formula to adjust the degrees-of-freedom: $p$ values listed for such tests are the adjusted $p$ values.

The psychometric function was defined as

$$p = 1 - (1 - \gamma) \exp\left(-10^{\beta \log_{10}(c/\alpha)}\right) \tag{3.1}$$

where $p$ is proportion correct, $\gamma$ is the guessing rate, $c$ is stimulus contrast, $\beta$ governs the slope of the psychometric function, and $\alpha$ corresponds to threshold (i.e., the stimulus contrast that yields a response accuracy of 81.6% correct). The guessing rate was set to 0.5, and a maximum likelihood curve fitting procedure was used to estimate $\beta$ and $\alpha$ for each subject in each condition. One older and one younger subject had thresholds that were, on average, more than two standard deviations higher than the group mean for each condition for their respective age group. These subjects were deemed outliers, and their data were not included in subsequent analyses.

First, an analysis was conducted to determine if the slope of the psychometric function was approximately constant across age and mask conditions. The grand mean of $\beta$ was 3.62 (SEM = 0.14). An ANOVA on the log-transformed values of $\beta$ found no effect of age, $F(1, 20) = 3.55$, $f = 0.09$, $p = 0.074$, mask condition, $F(6, 120) = 0.839$, $\tilde{\epsilon} = 1$, $f = 0$, $p = 0.542$, or an age $\times$ mask condition interaction, $F(6, 120) = 0.339$, $\tilde{\epsilon} = 1$, $f = 0$, $p = 0.915$. These results mean that the magnitude of any observed group difference in threshold does not depend on the threshold criterion.

Figure 3.2 shows mean detection thresholds for each group plotted as a function of mask offset. An ANOVA on log-transformed thresholds found a significant main effect of age, $F(1, 20) = 5.92$, $f = 0.13$, $p = 0.024$, and a significant effect of mask condition, $F(6, 120) = 198.70$, $f = 1.96$, $\tilde{\epsilon} = 0.64$, $p < 0.0001$, but no significant age $\times$ condition interaction, $F(6, 120) = 2.32$, $f = 0.16$, $\tilde{\epsilon} = 0.64$, $p = 0.067$. Hence, the ANOVA found no evidence that the frequency selectivity of masking differed in older and younger subjects.

Thresholds were fit with the equation

$$T(x) = k + a \cdot \exp\left(-\frac{x}{b}\right) \tag{3.2}$$

where $T$ is threshold, $x$ is the mask components' spatial frequency offset, $k$ is the lower asymptote, $a$ is the difference between the maximum and the lower asymptote, and $b$ governs the rate of decline from the maximum threshold, $(k + a)$, to the lower asymptote, $k$. Equation 3.2 was then used to calculate the half-amplitude half-bandwidth of masking, $\theta_{1/2}$, which was defined as the mask spatial frequency offset, in octaves, at which threshold dropped to one-half of its peak value.

Equation 3.2 was first fit to the average thresholds in each age group, and the resulting

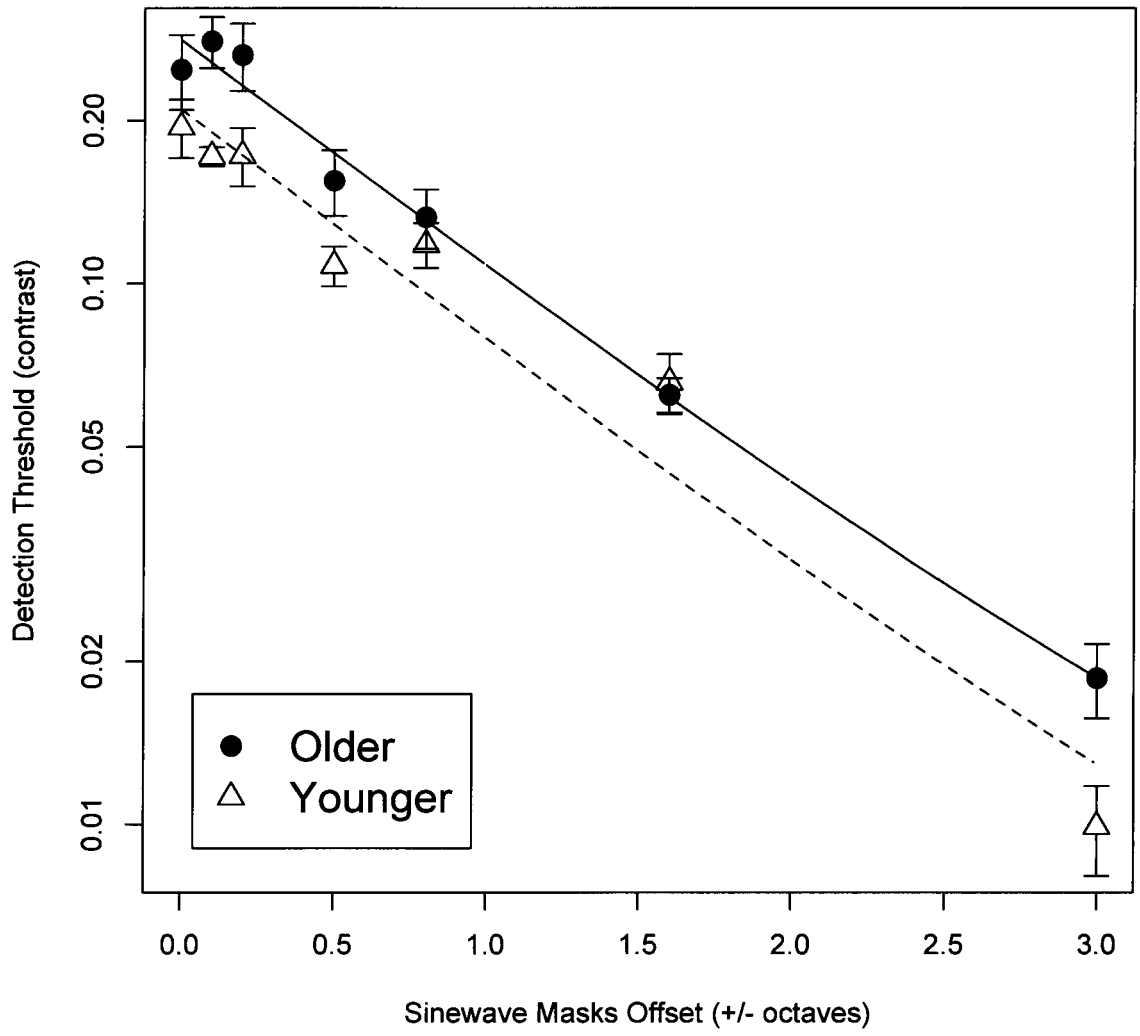


Figure 3.2: Experiment 1: Sine wave grating masking. Mean detection thresholds for older and younger subjects are plotted as a function of the mask spatial frequency offset relative to that of the 3 c/deg target. Error bars represent ±1 SEM. Equation 3.2 was fit to the average thresholds from each age group; the solid and dashed curves represent the results for older and younger subjects, respectively.

Table 3.2: Masking bandwidths ($\theta_{1/2}$) estimated from Experiments 1 and 2.

| | younger subjects $\hat{\mu} \pm \hat{\sigma}_{\mu}$ | older subjects $\hat{\mu} \pm \hat{\sigma}_{\mu}$ |
|---|---|---|
| Experiment 1 | $0.70 \pm 0.050$ | $0.71 \pm 0.060$ |
| Experiment 2 | $0.89 \pm 0.068$ | $0.95 \pm 0.133$ |

parameters were used to draw the smooth curves in Figure 3.2; Equation 3.2 provided reasonably good fits to the data in both age groups. Next, Equation 3.2 was fit to the data from each subject. During curve-fitting, the value of $k$, which determines the lower asymptote of the function, and therefore constrains the estimate of a subject's unmasked target contrast threshold, was restricted to have a psychophysically plausible lower limit of 0.0025. For each subject, the best-fitting version of Equation 3.2 was used to estimate $\theta_{1/2}$. As seen in Table 3.2, the mean $\theta_{1/2}$ was 0.70 for younger subjects and 0.71 for older subjects. The difference in masking bandwidth between age groups was not statistically significant, $CI_{95\%} = (-0.18, 0.16)$, $t(20) = -0.13$, $p = 0.90$.

### 3.2.3 Discussion

Experiment 1 measured detection thresholds for a Gabor pattern embedded in a mask consisting of two sine wave gratings whose spatial frequencies were symmetrically offset from that of the target. Thresholds in both age groups were highest when the target and mask had the same spatial frequency, and declined as the difference between target and mask spatial frequencies increased. An ANOVA on the detection thresholds showed that the age $\times$ condition interaction approached statistical significance. This nearly-significant effect reflects the fact that age differences in the 0.8 and 1.6 octave mask offset conditions were smaller than in the other conditions, and might suggest that the shapes of the threshold vs. mask curves differ slightly between groups. Nevertheless, Experiment 1 found no evidence that the selectivity of spatial frequency masking was broader in older adults.

## 3.3 Experiment 2: Notched-noise masking

In Experiment 1 we randomized the phase and randomly jittered the orientation for each of the masking sine wave components by ±5 ° on each trial. These measures ensured that the subjects could not use a *particular* pattern of spatial beats, as a cue for detecting the target. However, the *presence* of spatial beats or other local spatial distortions still may have been used by subjects to detect the target (Thomas, 1985; Derrington and Badcock, 1986; Hess and Pointer, 1987; Badcock, 1988). Experiment 2 minimized the possibility that subjects used such strategies by measuring detection thresholds for a Gabor pattern embedded in static, broadband noise.

To estimate the spatial frequency selectivity of masking, the frequency content of the masking noise was notched-filtered: the notch was centered on the target's spatial frequency, and the width of the notch varied across conditions (see Figure 3.3). This procedure has been used to estimate the frequency selectivity of auditory channels (e.g., Patterson 1976), the spatial frequency tuning of luminance and chromatic visual mechanisms (Losada and Mullen, 1995; Mullen and Losada, 1999), and the orientation tuning of visual mechanisms (Hibbard, 2005; Govenlock et al., 2009).

### 3.3.1 Methods

**Subjects** Twelve naive older and 12 naive younger subjects were paid for participating in this experiment. The subjects were screened with the same protocol used in Experiment 1. The ages, acuities, and MMSE scores for these subjects are listed in Table 2.1. All older subjects scored within the normal range for their age groups on the MMSE (Crum et al., 1993). All subjects had normal or corrected-to-normal acuity and no known vision health problems (see Table 2.1 for details).

**Stimuli and Apparatus** The apparatus was the same as in Experiment 1. The visual target was a 3 c/deg Gabor pattern with the same parameters as in Experiment 1. Two-dimensional static noise fields (4.8 ° × 4.8 ° in size) were constructed by digitally filtering white Gaussian noise. Prior to filtering, the value of each noise pixel was drawn randomly from a Gaussian distribution with a mean of 0 and a variance of 0.16. Noise values beyond ±2 standard deviations from the mean were discarded and replaced by random samples from the remaining contrast values. A new sample of noise was created for each interval

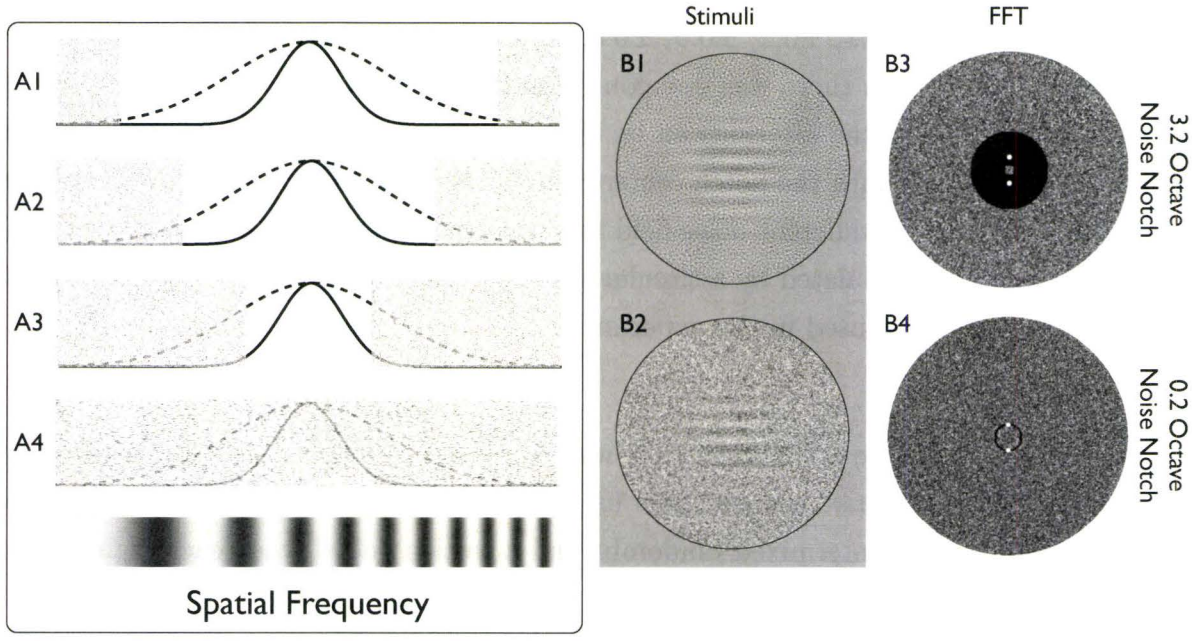


Figure 3.3: Illustration of the notched-noise masking paradigm, and example stimuli and their Fourier transforms from two conditions. Panel A: Shaded regions depict spatial frequency content of the external noise; solid and dashed lines represent hypothetical tuning functions of two filters. In A1–A3, the spatial frequency spectrum of the noise has been filtered with progressively narrower notches. The notch width is zero in A4. Noise falling within the passband of the spatial frequency filters increases response variability and lowers the signal-to-noise ratio. Notice that, in B and C, more noise falls within the passband of the broader spatial frequency filter. Panel B: In B1 the target appears at supra-threshold contrast embedded in noise having a wide (3.2 octaves) spatial frequency notch. B3 is the Fourier transform of the stimulus in B1. The broadband noise mask contains non-zero amplitudes at all frequency components except those falling within 1.6 octaves of the target spatial frequency. B2 and B4 show an example of a stimulus constructed with a narrow notch bandwidth (0.2 octaves). Note that the scale of the spatial frequency axis in the Fourier transform plots differs from the scale used in Figure 3.1.

of every trial.

Spatial frequency filtering was done in the Fourier domain using Matlab's `fft2` function and custom software. In different conditions, the filtering procedure removed all Fourier components within ±0.1, ±0.2, ±0.5, ±0.8, ±1.6, or ±3.0 octaves of the target spatial frequency. In addition, there was one condition in which no spatial frequency filtering was performed. Thus, the filtering can be thought of as notch filtering along the spatial frequency dimension, with the notch centered on 3 c/deg and seven notch widths ranging from 0 to 6 octaves. A different noise field was constructed for each interval of every trial. Noise contrast was modulated by a circular window (diameter = 4.8 °). Figure 3.3 shows example of the stimuli used in the experiment.

**Procedure** The same 2-IFC task that was employed in Experiment 1 was used here, and target contrast varied across trials using QUEST. Staircases from all seven noise notch conditions were intermixed randomly, and a session ended when each staircase had accumulated 45 trials.

### 3.3.2 Results

Thresholds obtained from one older subject in 3 of the 7 conditions were more than 2.9 standard deviations away from the mean of the other older subjects in those conditions. This subject was deemed an outlier, and his data were not included in subsequent analyses.

Subjects' responses were fit with the psychometric function defined by Equation 3.1. The mean value of $\beta$—the slope—was 4.18. A 2 (age groups) × 7 (mask conditions) ANOVA on log-transformed values of $\beta$ found that there were no significant main effects of age $F(1,21) = 1.686$, $f = 0.046$, $p = 0.208$, or condition, $F(6,126) = 1.266$, $f = 0.070$, $\tilde{\epsilon} = 0.96$, $p = 0.279$, and no age × condition interaction $F(6,126) = 0.499$, $f = 0$, $\tilde{\epsilon} = 0.96$, $p = 0.802$. The fact that the slopes of the psychometric functions did not vary significantly across age or condition implies that age differences in masking do not depend on the criterion used to define threshold.

As seen in Figure 3.4, thresholds for old and young subjects were quite similar to one another in most conditions. An ANOVA on log-transformed thresholds found that there was no significant effect of age $F(1,21) = 2.475$, $f = 0.068$, $p = 0.131$, but there was a significant effect of condition, $F(6,126) = 114.561$, $f = 1.45$, $\tilde{\epsilon} = 0.617$, $p < 0.001$, and a

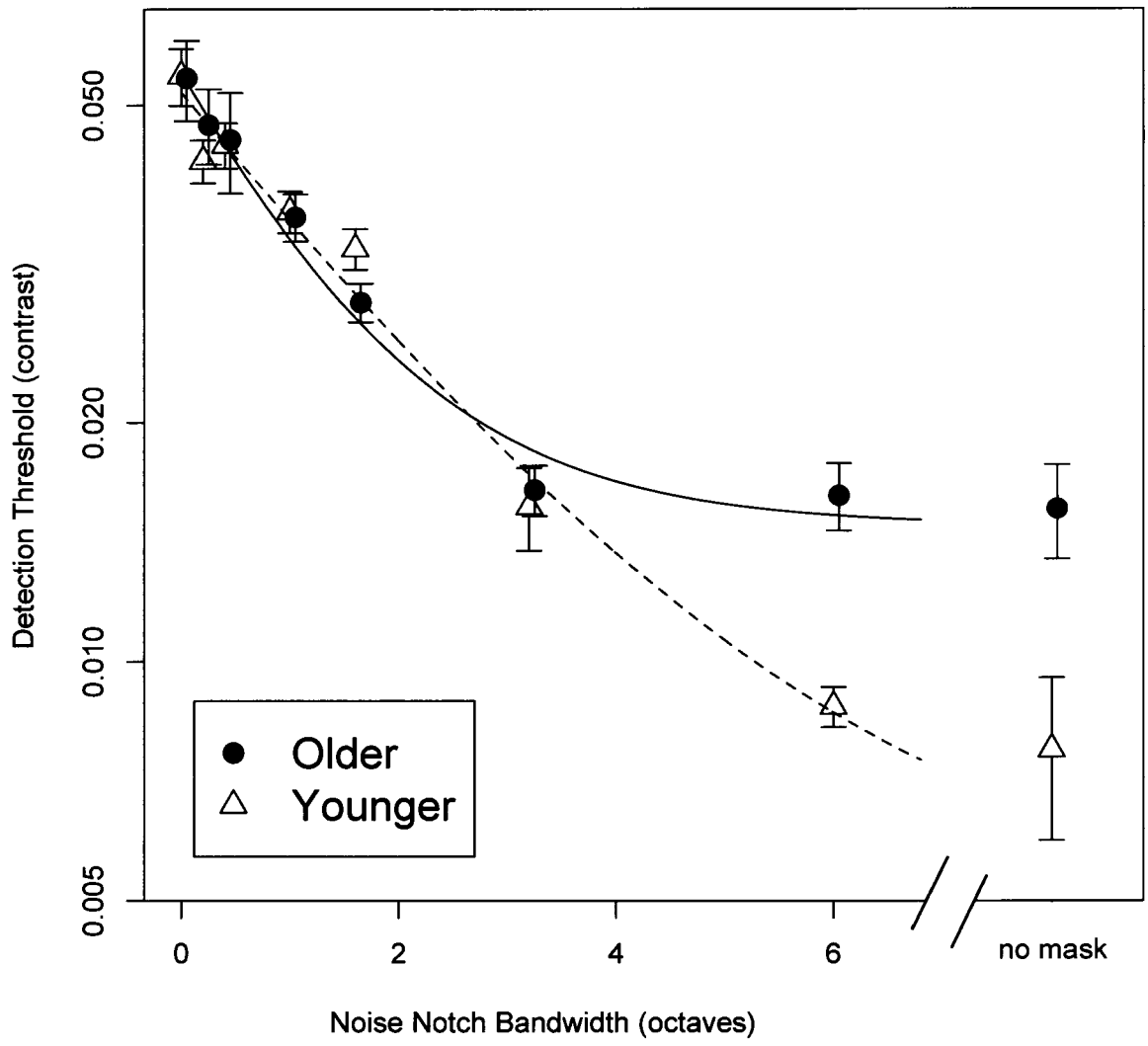


Figure 3.4: Experiment 2: Notched-noise masking. Mean detection thresholds for older and younger subjects plotted as a function of the full width of the spatial frequency notch. The notch was centered on the spatial frequency of the target grating, which was 3 c/deg . The data points for the two groups have been slightly horizontally offset from one another for the purposes of visualization only. Equation 3.2 was fit to the average thresholds from each age group; the solid and dashed curves represent the results for older and younger subjects, respectively. Unmasked thresholds (i.e., the no mask condition) were obtained on two additional groups of subjects (see Results section for details). Error bars represent $\pm 1$ SEM.

significant age × condition interaction $F(6, 126) = 4.836$, $f = 0.267$, $\tilde{\epsilon} = 0.617$, $p = 0.002$. The interaction effect was caused by the divergence of thresholds at the widest notch width.

To obtain a measure of the spatial frequency selectivity of masking, thresholds were analyzed using Equation 3.2. Equation 3.2 was first fit to the average thresholds in each age group, and the resulting parameters were used to draw the smooth curves in Figure 3.4. It can be seen that Equation 3.2 provided reasonably good fits to the data in both age groups. Next, Equation 3.2 was fit to the data from each subject. As in Experiment 1, the value of $k$, which corresponds to the lower asymptote of the masking function, and estimates detection threshold without a mask, was restricted to have a lower limit of 0.0025.

For each subject, the best-fitting version of Equation 3.2 was used to estimate $\theta_{1/2}$. To make the values of $\theta_{1/2}$ comparable across experiments, $\theta_{1/2}$ for the current experiment was defined as *one-half* of the notch width at which threshold fell to half of the maximum threshold. The mean value of $\theta_{1/2}$ for each age group is listed in Table 3.2. The difference between age groups was not statistically significant, $CI_{95\%} = (-0.385, 0.253)$, $t(21) = -0.442$, $p = 0.665$. Also noteworthy is the fact that the values of $\theta_{1/2}$ differed by only $\approx 0.2$ octaves across experiments, despite the fact that the strength of masking, as well as the shape of the masking function, varied considerably across experiments (*cf.*, Figures 3.2 and 3.4).

The lower asymptotes of the masking curves in Figure 3.4 differed across age groups. We attribute this age difference to the well-established age difference in contrast sensitivity for gratings presented without noise (e.g., Owsley et al. 1983). To test this idea, we measured *unmasked* contrast detection thresholds for the same 3 c/deg target used here with two new groups of young ($n = 13$) and older ($n = 12$) subjects who had not participated in Experiments 1 or 2. One younger subject yielded a threshold that was more than 2.5 standard deviations from their respective group mean; that subject was deemed an outlier and was not included in subsequent analyses.

Mean thresholds obtained in older ($M = 0.016$) and younger ($M = 0.007$) subjects are plotted on the right side of Figure 3.4. A t-test on the log-transformed threshold values found that thresholds were significantly higher in older subjects, $CI_{95\%} = (0.077, 0.567)$, $t(22) = 2.73$, $p < 0.010$, one-tailed, a result that is consistent with previous reports of age differences in contrast sensitivity (e.g., Owsley et al. 1983). Furthermore, these unmasked thresholds were similar to the thresholds obtained with wide notched noise

masks, and therefore support the hypothesis that the age difference obtained with the widest noise mask notch simply reflects the fact that contrast sensitivity for unmasked 3 c/deg patterns is reduced in older subjects.

Finally, we examined whether the bandwidth of masking, $\theta_{1/2}$, varied among older subjects as a function of age. When the data from both experiments were combined, the slope of the linear regression line relating $\theta_{1/2}$ to age did not not differ significantly from zero (slope = 0.023, $CI_{95\%} = [-0.015,\ 0.062]$), and the correlation between $\theta_{1/2}$ and age in older subjects was not significant ($r = 0.25$, $t(20) = 1.17$, $p = 0.25$). The correlations also were not significant when the two experiments were analyzed separately (Experiment 1: $r = -0.05$, $t(9) = 0.168$, $p = 0.87$; Experiment 2: $r = 0.34$, $t(10) = 1.03$, $p = 0.33$).

### 3.3.3 Discussion

In Experiment 2 we measured thresholds for a Gabor pattern embedded in notched-filtered noise. We found that thresholds at all but the widest noise-notch condition were very similar in older and younger subjects, and that the selectivity of masking, as indexed by $\theta_{1/2}$, did not differ with age. Furthermore, we found that $\theta_{1/2}$ was not linearly associated with age among our older subjects.

Estimates of $\theta_{1/2}$ for a subset of conditions from several published masking studies are shown in Table 3.3. Anderson and Burr (1985) measured detection thresholds for a drifting 3 c/deg target grating masked with a 25% contrast grating whose phase was randomized on each temporal screen frame. Legge and Foley (1980) used a static 2 c/deg grating target masked with a static 20% contrast grating. Stromeyer and Julesz (1972) used a static 2.5 c/deg target and a band-pass filtered noise mask. The estimates of $\theta_{1/2}$ fall within a range of 0.6 to 0.9, with a mean estimate of about 0.7 octaves. Averaged across age groups and experiments, our current estimate of $\theta_{1/2}$ is 0.81, which falls within this previously reported range.

## 3.4 General Discussion

In Experiment 1 we employed a masking plaid composed of two high contrast sine wave gratings that, on a log-frequency axis, were positioned symmetrically on either side of a spatially co-extensive Gabor target. In both age groups, target detection thresholds

Table 3.3: Estimates of $\theta_{1/2}$ from various masking studies.

| Source | target frequency (c/deg ) | $\theta_{1/2}$ (octaves) |
|---|---|---|
| Anderson and Burr (1985) | 3 | 0.6 |
| Legge and Foley (1980) | 2 | 0.9 |
| Stromeyer and Julesz (1972) | 2.5 | 0.5 — 0.75 |
| Experiment 1 | 3 | .71 |
| Experiment 2 | 3 | .92 |

decreased as the difference between mask and target spatial frequencies increased, and the shape of the masking function did not differ significantly across groups. Similar results were obtained in Experiment 2, which used a static, notch-filtered noise mask: In both age groups, detection thresholds were highest when the notch width was zero and declined as the notch width increased. Although there was a significant interaction between age and notch-bandwidth, the effect was due to older subjects having higher thresholds in the widest notch condition, and probably reflects the well-known age difference for contrast sensitivity for unmasked sine wave gratings. Most importantly, in both experiments the age difference in the spatial frequency selectivity of masking was small (i.e., $\Delta\theta_{1/2} = 0.01$ and 0.06 octaves; see Table 3.2) and non-significant. Hence, Experiments 1 and 2, which used two types of static masks yielding very different masking functions, failed to find evidence for age differences in the spatial frequency selectivity of masking.

The lack of an age difference in spatial frequency selectivity of masking is surprising given recent reports of physiological changes in visual cortical neurons in senescent monkeys and cats. There is a decline in orientation and directional selectivity of V1 cells in senescent macaque monkey that is accompanied by a marked increase in spontaneous firing rates which reduces the signal-to-noise ratio (Schmolesky et al., 2000; Leventhal et al., 2003). Furthermore, the latency at which V1 cells first respond to visual stimulation is both delayed and more variable in senescent macaques (Wang et al., 2005). Although there are no published measurements of spatial frequency tuning bandwidth in senescent primate V1 neurons, Zhang et al. (2008) did report that V1 neurons in senescent macaque exhibit a decrease in their preferred spatial frequency, as well as a decrease in their spatial resolution (i.e., the highest spatial frequency to which the neurons respond). Taking the ratio of spatial resolution to preferred spatial frequency as a proxy for the tuning of these neurons, we estimate that neurons reported by Zhang et al. had a tuning width of

approximately 2.2 and 1.7 octaves in older and younger monkeys, respectively. Part of this age-related increase in frequency bandwidth may reflect the fact that the bandwidth of V1 neurons is related inversely to preferred spatial frequency (DeValois et al., 1982). Assuming that aging does not alter the relation between preferred spatial frequency and frequency bandwidth, the results of DeValois et al. (1982, see their Figure 7) suggest that approximately one-half of the 0.5 octave age difference in frequency bandwidth that we estimated from data reported by Zhang et al. could be accounted for by the age difference in peak frequency. Hence, Zhang et al.'s findings are consistent with the idea that aging is associated with a slight increase in spatial frequency bandwidth in V1 neurons. Despite these physiological changes, the current masking studies found no evidence that the frequency selectivity of masking varies with age.

There are several potential explanations for the apparent discrepancy between the physiological studies of the effects of aging on signal to noise ratio (Hua et al., 2006; Schmolesky et al., 2000) and spatial frequency coding (Zhang et al., 2008) and the psychophysical results reported here. One possibility is that the physiological age differences are due to an interaction between age and the effect of anesthesia, rather than an age-related visual processing decline. However, Wang et al. (2005) and Zhang et al. (2008), found that large variations in the level of anesthetic did not significantly alter the age differences in the physiological responses of V1 and V2 neurons, which argues against any interaction between anesthesia and age. Alternatively, it may be that the older subjects in our experiments, whose ages ranged from 62 to 77 years, simply were not old enough to exhibit effects of aging analogous to those found in the animal studies. One argument against this idea is that we did not find evidence for a significant association between masking bandwidth and age among older subjects, however it is possible that an association could be found with subjects older than 77 years of age.

Another possibility is that older subjects used top-down processes like attention to compensate for changes in visual mechanisms. Attention improves spatial resolution in Landolt-square, gap resolution, and Venier resolution tasks (Yeshurun and Carrasco, 1999), alters perceived contrast (Liu et al., 2009), and improves contrast sensitivity across a wide range of spatial frequencies Carrasco et al. (2000). Work using fMRI techniques has found that attention modulates activity in early visual cortex (Kastner et al., 1998; Serences and Boynton, 2007; Smith et al., 2006; Fischer and Whitney, 2009). The amplitude of the steady-state visually-evoked potential (ssVEP) is modulated via attention (Di Russo and Spinelli, 1999). Single cell recordings performed on macaque monkeys have found that attention alters the response properties of single neurons in many visual cortical

areas (Treue and Maunsell, 1999; McAdams and Maunsell, 1999; McAdams and Reid, 2005). Given this evidence, it is reasonable to speculate that age differences in visual attention may have compensated for differences in the frequency selectivity of low-level visual neurons.

A related hypothesis is that older and younger subjects may have used different functional networks to perform the detection task (Bennett et al., 2001; Della-Maggiore et al., 2000; McIntosh et al., 1999). Faubert (2002) has suggested that, faced with what might be widespread, diffuse neuronal loss and dysfunction, the aged brain may be able to compensate when performing simple visual tasks by engaging reserve neural resources, but that this compensation may be insufficient to maintain high levels of performance in complex tasks (Habak and Faubert, 2000; Faubert and Bellefeuille, 2002). One way of examining how compensation affected age differences in our task would be examine if using a more complex task – perhaps a dual-task procedure (Liu et al., 2009) – leads to broader spatial frequency tuning in older observers. Such a result would be consistent with previous results showing that older observers' performance on some visual and cognitive tasks suffers more under conditions of divided attention than does younger observers' (Sekuler et al., 2000; Richards et al., 2006).

The discrepancy between previously presented physiological results and the current psychophysical results also may be reconciled by considering which subset of cortical neurons contribute to behaviour. If aged observers compensate via attentional mechanisms to change the subset of cells relied up to perform our task, then further research using divided attention tasks or fMRI could reveal how the cortical networks shift with age. Zhang et al. (2008) found that, *on average*, V1 cells' spatial frequency tuning changed as age increased. Similarly, Schmolesky et al. (2000) and Hua et al. (2006) found that, on average, older cells demonstrated increased spontaneous firing rates and a decreased signal-to-noise ratio. However, in all three of these studies, some cells in older monkeys retained response properties that were similar to those found in younger animals. If psychophysical performance is determined by such a subset of cells, then one would expect no difference between age groups in the current experiments. There is evidence suggesting that performance in some psychophysical tasks may be driven by a small number of neurons (see Parker and Newsome, 1998; Gold and Shadlen, 2007). Future research is required to distinguish between the hypotheses that our tasks were merely not sensitive enough to observe the differences found in single cell recordings or that our task is tapping an alternate subset of cells. Increasing the demands of the task, measuring the response of a large population of spatial frequency-selective neurons using the steady-state visually

evoked potential (Regan and Regan, 1988), or measuring the cortical networks aged observers use with fMRI, all could be useful in providing evidence to address this apparent inconsistency between previous physiological and the present psychophysical results.

**Acknowledgements**

This research was supported by the Canada Research Chairs program, of which PJB and ABS are members, a grant from the Canadian Institutes of Health Research (CIHR) to PJB and ABS, a Natural Sciences and Engineering Research Council of Canada Postgraduate Scholarship to SWG, and the CIHR Strategic Training Grant on Communication and Social Interaction in Healthy Aging. Portions of this work were presented at the annual meeting of the Vision Sciences Society (Sarasota, FL U.S.A, May 2006) and at the McMaster Dept of Psychology Cognition/Perception Seminar, Nov 2006. Finally, thank you Donna Waxman.

# References

Andersen, G. J., Atchley, P., 1995. Age-related differences in the detection of three-dimensional surfaces from optic flow. Psychology and Aging 10 (4), 650–658.

Andersen, G. J., Ni, R., 2008. Aging and visual processing: declines in spatial not temporal integration. Vision Research 48 (1), 109–18.

Anderson, S. J., Burr, D. C., 1985. Spatial and temporal selectivity of the human motion detection system. Vision Research 25 (8), 1147–1154.

Badcock, D. R., 1988. Discrimination of spatial phase changes: contrast and position codes. Spatial Vision 3 (4), 305–322.

Bennett, P. J., Sekuler, A. B., McIntosh, A. R., Della-Maggiore, V., 2001. The effects of aging on visual memory: Evidence for functional reorganization of cortical networks. Acta Psychologica 107 (1-3), 249–273.

Bennett, P. J., Sekuler, R., Sekuler, A. B., 2007. The effects of aging on motion detection and direction identification. Vision Research 47, 799–809.

Billino, J., Bremmer, F., Gegenfurtner, K. R., May 2008. Differential aging of motion processing mechanisms: evidence against general perceptual decline. Vision Research 48 (10), 1254–61.

Brainard, D. H., 1997. The psychophysics toolbox. Spatial Vision 10, 443–446.

Carrasco, M., Penpeci-Talgar, C., Eckstein, M., 2000. Spatial covert attention increases contrast sensitivity across the csf: support for signal enhancement. Vision Research 40 (10-12), 1203–15.

Cohen, J., 1988. Statistical power analysis for the behavioral sciences, 2nd Edition. L. Erlbaum Associates, Hillsdale, N.J.

Crum, R. M., Anthony, J. C., Bassett, S. S., Folstein, M. F., 1993. Population-based norms for the mini-mental state examination by age and education level. Journal of the American Medical Association 269, 2386–2391.

Del Viva, M. M., Agostini, R., 2007. Visual spatial integration in the elderly. Investigative Ophthalmology and Vision Science 48 (6), 2940–2946.

Delahunt, P., Hardy, J., Werner, J., 2008. The effect of sensescence on orientation discrimination and mechanism tuning. Journal of Vision 8 (3), 1–9.

Della-Maggiore, V., Sekuler, A. B., Grady, C. L., Bennett, P. J., Sekuler, R., McIntosh, A. R., 2000. Corticolimbic interactions associated with performance on a short-term memory task are modified by age. Journal of Neuroscience 20, 8410–8416.

Derrington, A. M., Badcock, D. R., 1986. Detection of spatial beats: non-linearity or contrast increment detection? Vision Research 26 (2), 343–348.

DeValois, R. L., Albrecht, D. G., Thorell, L. G., 1982. Spatial frequency selectivity of cells in macaque visual cortex. Vision Research 22 (5), 545–559.

DeValois, R. L., DeValois, K. K., 1988. Spatial Vision. Oxford University Press.

Di Russo, F., Spinelli, D., 1999. Electrophysiological evidence for an early attentional mechanism in visual processing in humans. Vision Research 39 (18), 2975–85.

Faubert, J., Sep 2002. Visual perception and aging. Canadian Journal of Experimental Psychology 56 (3), 164–76.

Faubert, J., Bellefeuille, A., Feb 2002. Aging effects on intra- and inter-attribute spatial frequency information for luminance, color, and working memory. Vision Research 42 (3), 369–78.

Fischer, J., Whitney, D., 2009. Attention narrows position tuning of population responses in V1. Current Biology 19, 1356–1361.

Folstein, M. F., Folstein, S. E., McHugh, P. R., 1975. "mini-mental state." a practical method for grading the cognitive state of patients for the clinician. Journal of Psychiatric Research 12, 189–198.

Gaspar, C., Sekuler, A. B., Bennett, P. J., 2008. Spatial frequency tuning of upright and inverted face identification. Vision Research 48 (28), 2817–26.

Gold, J. I., Shadlen, M. N., 2007. The neural basis of decision making. Annual review of neuroscience 30, 535–74.

Govenlock, S. W., Taylor, C. P., Sekuler, A. B., Bennett, P. J., 2009. The effect of aging on the orientational selectivity of the human visual system. Vision Research 49, 164–172.

Habak, C., Faubert, J., 2000. Larger effect of aging on the perception of higher-order stimuli. Vision Research 40 (8), 943–50.

Habak, C., Wilkinson, F., Wilson, H. R., 2008. Aging disrupts the neural transformations that link facial identity across views. Vision Researc 48 (1), 9–15.

Henning, G. B., Hertz, B. G., Hinton, J. L., 1981. Effects of different hypothetical detection mechanisms on the shape of spatial-frequency filters inferred from masking experiments: I. Noise masks. Journal of the Optical Society of America. A, Optics, Image science, and Vision 71 (5), 574–581.

Henning, G. B., Wichmann, F. A., 2007. Some observations on the pedestal effect. Journal of Vision 7 (1), 3.

Hess, R. F., Pointer, J. S., 1987. Evidence for spatially local computations underlying discrimination of periodic patterns in fovea and periphery. Vision Research 27 (8), 1343–1360.

Hibbard, P., 2005. The orientation bandwidth of cyclopean channels. Vision Research 45 (21), 2780–2785.

Hua, T., Li, X., He, L., Zhou, Y., Wang, Y., Leventhal, A. G., 2006. Functional degradation of visual cortical cells in old cats. Neurobiology of Aging 27, 155–162.

Kastner, S., Weerd, P. D., Desimone, R., Ungerleider, L. G., 1998. Mechanisms of directed attention in the human extrastriate cortex as revealed by functional mri. Science 282 (5386), 108–11.

Kirk, R. E., 1995. Experimental design: procedures for the behavioral sciences, 3rd Edition. Brooks/Cole, Pacific Grove, Calif.

Legault, I., Allard, R., Faubert, J., 2007. Normal aging and the perception of curvature shapes. Optom Vis Sci 84 (12), 1087–1092.

Legge, G., Foley, J. M., 1980. Contrast masking in human vision. Journal of the Optical Society of America. A, Optics, Image science, and Vision 70 (12), 1458–1471.

Leventhal, A. G., Wang, Y., Pu, M., Zhou, Y., Ma, Y., 2003. GABA and its agonists improved visual cortical function in senescent monkeys. Science 300, 812–815.

Liu, T., Abrams, J., Carrasco, M., 2009. Voluntary attention enhances contrast appearance. Psychological Science 20 (3), 354.

Losada, M. A., Mullen, K. T., 1995. Color and luminance spatial tuning estimated by noise masking in the absense of off-frequency looking. Journal of the Optical Society of America. A, Optics, Image science, and Vision 12, 250–260.

Maxwell, S., Delaney, H., 2004. Designing Experiments and Analyzing Data: A Model Comparison Approach, 2nd Edition. Lawrence Erlbaum Associates, Mahwah, New Jersey.

McAdams, C. J., Maunsell, J. H. R., 1999. Effects of attention on the reliability of individual neurons in monkey visual cortex. Neuron 23, 765–773.

McAdams, C. J., Reid, R. C., 2005. Attention modulates the responses of simple cells in monkey primary visual cortex. Journal of Neuroscience 25 (47), 11023–33.

McIntosh, A. R., Sekuler, A. B., Penpeci, C., Rajah, M. N., Grady, C. L., Sekuler, R., Bennett, P. J., 1999. Recruitment of unique neural systems to support visual memory in normal aging. Current Biology 9 (21), 1275–1278.

Mullen, K. T., Losada, M. A., 1999. The spatial tuning of color and luminance peripheral vision measured with notch filtered noise masking. Vision Research 39, 721–731.

Nachmias, J., 1993. Masked detection of gratings: the standard model revisited. Vision Research 33 (10), 1359–1365.

Norman, J. F., Ross, H. E., Hawkes, L. M., Long, J. R., 2003. Aging and the perception of speed. Perception 32, 85–96.

Owsley, C., Sekuler, R., Siemsen, D., 1983. Contrast sensitivity throughout adulthood. Vision Research 23 (7), 689–699.

Parker, A. J., Newsome, W. T., 1998. Sense and the single neuron: Proving the physiology of perception. Annual Review of Neuroscience 21, 227–277.

Patterson, R. D., 1976. Auditory filter shapes derived with noise stimuli. Journal of the Acoustical Society of America 59, 640–654.

Patterson, R. D., Nimmo-Smith, I., 1980. Off-frequency listening and auditory-filter asymmetry. Journal of the Acoustical Society of America 67 (1), 229–245.

Pelli, D. G., 1997. The videotoolbox software for visual psychophysics: Transforming numbers into movies. Spatial Vision 10, 437–442.

Pilz, K. S., Bennett, P. J., Sekuler, A. B., in press. Effects of aging on biological motion discrimination. Vision Research.

R Development Core Team, 2007. R: A Language and Environment for Statistical Computing. R Foundation for Statistical Computing, Vienna, Austria.

Regan, D., Regan, M. P., 1988. Objective evidence for phase-independent spatial frequency analysis in the human visual pathway. Vision Research 28, 187–191.

Richards, E., Bennett, P. J., Sekuler, A. B., Nov 2006. Age related differences in learning with the useful field of view. Vision Res 46 (25), 4217–31.

Roudaia, E., Bennett, P., Sekuler, A., 2008. The effect of aging on contour integration. Vision Research 48, 2767–2774.

Schmolesky, M. T., Wang, Y., Pu, M., Leventhal, A. G., 2000. Degradation of stimulus selectivity of visual cortical cells in senescent rhesus monkeys. Nature Neuroscience 3, 384–390.

Sekuler, A. B., Bennett, P. J., Mamelak, M., 2000. Effects of aging on the useful field of view. Experimental Aging Research 26 (2), 103–20.

Serences, J. T., Boynton, G. M., Jul 2007. Feature-based attentional modulations in the absence of direct visual stimulation. Neuron 55 (2), 301–12.

Smith, A., Cotillon-Williams, N., Williams, A., 2006. Attentional modulation in the human striate cortex: The time-course of the bold response and its implications. Neuroimage 29, 328–334.

Solomon, J. A., Pelli, D. G., 1994. The visual filter mediating letter identification. Nature 369 (6479), 395–397.

Stromeyer, C. F., III, Julesz, B., 1972. Spatial-frequency masking in vision: critical bands and spread of masking. Journal of the Optical Society of America. A, Optics, Image science, and Vision 62, 1221–1232.

Stromeyer, C. F., III, Klein, S., 1974. Spatial frequency channels in human vision as asymmetric (edge) mechanisms. Vision Research 14, 1409–1420.

Thomas, J. P., 1985. Effect of static-noise and grating masks on detection and identification of grating targets. Journal of the Optical Society of America A 2 (9), 1586–1592.

Treue, S., Maunsell, J. H., Sep 1999. Effects of attention on the processing of motion in macaque middle temporal and medial superior temporal visual cortical areas. Journal of Neuroscience 19 (17), 7591–602.

Tyler, C., Chan, H., Liu, L., McBride, B., Kontsevich, L., 1992. Bit-stealing: How to get 1786 or more grey levels from an 8-bit color monitor. In: Rogowitz, B. (Ed.), SPIE Proceedings: Human vision, visual processing, and digital display III. Vol. 1666. pp. 351–364.

Wang, Y., Zhou, Y., Ma, Y., Leventhal, A., 2005. Degradation of signal timing in cortical areas V1 and V2 of senescent monkeys. Cerebral Cortex 15 (15), 403–408.

Watson, A. B., Pelli, D. G., 1983. Quest: A bayesian adaptive psychophysical method. Perception & Psychophysics 33, 113–120.

Yeshurun, Y., Carrasco, M., Jan 1999. Spatial attention improves performance in spatial resolution tasks. Vision Research 39 (2), 293–306.

Zhang, J., Wang, X., Wang, Y., Fu, Y., Liang, Z., Ma, Y., Leventhal, A. G., 2008. Spatial and temporal sensitivity degradation of primary visual cortical cells in senescent rhesus monkeys. European Journal of Neuroscience 28, 201–207.

# Chapter 4

# Orientation tuning in human visual cortex in normal aging

**Abstract**

Otherwise healthy, older humans exhibit a variety of visual deficits that cannot be fully explained by pre-cortical factors. Primate models suggest that, in senescence, orientation-selective V1 neurons become markedly detuned on average, possibly due to a decline in GABAergic inhibitory activity (Leventhal et al., 2003). However, recent psychophysical studies (e.g., Govenlock et al., 2009) do not find evidence of this decline in older humans. In the current study, we measured the average tuning of orientation-selective visual cortical neurons in older humans using a two-grating, steady-state visually evoked potential (ssVEP) method suggested by Regan and Regan (1987). We found this measure of average neuronal tuning to be preserved in older age. This result suggests that V1 orientation tuning does not change in older human aging, or that tuning does change, but that the aged brain is able to adaptively tune these neurons in an on-line, ad hoc fashion by virtue of focused attention or consciousness — faculties that were denied the primates in the aforementioned single-cell studies — in order to maintain psychophysical tuning.

## 4.1 Introduction

A large body of evidence, both behavioural and physiological, suggests that low-level vision consists of a bank of quasi-linear spatial filters or channels that are selective for orientation, spatial frequency, and direction of motion (see DeValois and DeValois, 1988, for a review). Given internal noise, channel bandwidths along these dimensions determine the fidelity with which the visual scene is encoded: a narrower bandwidth enables these filters to convey information more precisely. Thus, the bandwidth of these filters constrains the ability of higher-level mechanisms to detect and discriminate complex, everyday visual forms such as faces and words.

There is reason to suspect, however, that the bandwidth of these mechanisms may deteriorate with normal, healthy aging. Specifically regarding orientation, using single-cell techniques, Schmolesky et al. (2000) found that V1 neurons in senescent macaques demonstrate markedly broader tuning than those measured in younger adult conspecifics. Leventhal et al. (2003) replicated that finding and implicated an age-related GABAergic inhibitory deficit as the cause. Also in senescent macaques, Yu et al. (2006) found broadening of orientation tuning in area V2 neurons, above and beyond that which would be expected from those neurons' detuned V1 input. Should this cortical detuning be occurring in older humans, it could explain reports of a declining ability of older humans to perceive complex visual forms (e.g., Stanford and Pollack, 1984; Herbert et al., 2002; Boutet and Faubert, 2006; Del Viva and Agostini, 2007; Habak et al., 2008; Roudaia et al., 2008).

In disagreement with these physiological reports, however, two recent psychophysical masking studies found no evidence for any age-related broadening of orientation tuning (Govenlock et al. 2009; Delahunt et al. 2008). One hypothesis for this discrepancy is that perception for such low-level visual properties in older age may rely on a subset of neurons, rather than an indiscriminate pooling across a population of neurons. In the aforementioned single-cell studies, although senescent neurons demonstrated detuning on average, some outliers did retain fine, young-like tuning. Thus, although older humans' neurons may be detuned on average, older humans' psychophysical tuning may be unaffected because it relies on a subset of neurons that retain fine tuning into older age. Indeed, there is evidence that some percepts seem to be driven by the most sensitive neurons in a given population (for a review, see Parker and Newsome, 1998; Gold and Shadlen, 2007). A second hypothesis is the possibility that older humans' perception

does rely on something like the population-average tuning, and that orientation-selective neurons are detuned when in a resting or unattended state in older age, but that these neurons are then tuned in an on-line, ad hoc fashion by the compensatory action of attention or consciousness—the senescent monkeys in the physiology studies would have been denied such compensation because they were globally anesthetized.

To distinguish these two hypotheses, we employed an EEG technique that enabled us to measure the tuning of orientation-selective neurons in human visual cortex, *en masse* (i.e., a measure of the population response). The steady-state visually-evoked potential (ssVEP) is the electrophysiological response to one or more visual stimuli whose luminance or contrast is temporally oscillating in some fashion. Due to response non-linearities in visual neurons, to the extent that two flickering, spatially-superimposed stimuli fall within the passband of the same neurons, energy at the sum of the two flicker frequencies, as well as other frequencies, will be recordable at scalp electrodes. By varying the orientation difference between two such stimuli and observing the amplitude of this summative frequency term, one can measure the orientation bandwidth of the neural mechanisms producing these distortion products (see Methods section for more details). The ssVEP has been used in this way to investigate orientation tuning in younger adults (Regan and Regan, 1987) and infants (Candy et al., 2001), but not in older adults. In the current study, we found no difference in average neuronal orientation tuning in older aging, supporting the hypothesis that the conscious, attending aged brain is able to tune what would otherwise be detuned orientation-selective visual cortex neurons. These results are also consistent with the ideas that the orientation tuning of V1 neurons does not change in older age in humans, and that the aforementioned senescent primate results are either particular to primates, that the human subjects in the current study had not achieved the same degree of senescence as the senescent primates, or that there was an interaction between anesthesia and senescence in the primate studies.

## 4.2 Materials and Methods

**Participants** The research protocol was approved by the McMaster University Research Ethics Board. Written, informed consent was obtained from each subject prior to the start of the experiment. Twelve younger (mean age = 23.2 years; SD = 2.6; 9 females) and 12 older (mean age = 69.6; SD = 4.0; 10 females) were paid $10 for their participation in this experiment, with the exception of 4 younger subjects who were lab members at the time,

including co-author SWG. By self-report, all subjects were healthy and free of any history of cardiovascular, neurological, or visual pathology such as strokes, cataracts, or macular degeneration. Wearing their optical correction, if necessary, subjects yielded age-normal near and far decimal logMAR acuities (CSV-100EDTRS eye charts, Precision Vision, LaSalle, Illinois, USA) and Pelli-Robson contrast sensitivity (Pelli et al., 1988; Mantyjarvi and Laitinen, 2001). Older subjects were free of age-related dementia as evidenced by their scores in the normal range on the Mini-Mental State Examination, corrected for age and education (Crum et al., 1993).

**Apparatus.** The experiment was programmed in MatLab v5.2.1 (The Mathworks) using the Psychophysics and Video Toolboxes (Brainard, 1997; Pelli, 1997) on an Apple Dual-G4 PowerMac computer with an NVIDIA GeForce Ti 4600 graphics card. Stimuli were displayed on a 20-inch Sony Trinitron GDM-F520 monitor with a frame rate of 120 Hz and resolution of 800 $\times$ 600 pixels, which subtended 17 $\times$ 15 deg at a viewing distance of 114 cm. The display was covered by a circular aperture (diameter = 14 deg). Mean luminance, which was held constant throughout the experiment, was $32 cd/m^2$.

**ssVEP tuning paradigm.** The human electrophysiological response – measured via EEG – to two superimposed, independently temporally-modulated visual patterns can contain energy at intermodulation frequencies, which are frequencies that are not present in the input stimuli (i.e., this is a nonlinear phenomenon). Specifically, Regan and Regan (1987) established that the steady state response elicited by two superimposed sine-wave gratings flickering at frequencies `F1` and `F2` typically contains energy at intermodulation frequencies `nF1` $\pm$ `mF2`, where `n` and `m` are small, non-negative integers. Candy et al. (2001) noted that activity at these intermodulation frequencies would be produced by a mechanism that summed, and then squared the two sinusoidal inputs. Further, they suggested that this squaring operation could be instantiated, physiologically, by the full-wave rectification performed by the phase-insensitive complex cells in V1, along with the effective full-wave rectification resulting from any pair of half-wave rectifying simple—phase *sensitive*—cells, one cell responding spatially anti-phase to the other.

Regan and Regan (1987) noted that the non-linearities in the steady state response could be exploited to measure population tuning profiles of visual cortical neurons. As the difference between two superimposed, flickering stimuli is increased along some dimension (e.g., orientation or spatial frequency), the extent to which the two stimuli are summed

by the mechanisms that produce the non-linearity should decrease if those mechanisms are selective along that dimension. This stimulus-dependent decrease in intermodulation activity can be used as an estimate of the tuning of the neural population response along that dimension. Candy et al. (2001), for example, used the amplitude of the F1+F2 component to measure orientation tuning during infant development. In the present investigation, we varied the orientation offset between two independently counterphase-flickering Gabor patterns and recorded F1+F2 activity to estimate population orientation tuning in a group of younger and older adults.

**Stimuli.** The stimuli consisted of two greyscale, counterphase-flickering, 1 c/deg gaussian-damped ($\sigma$ = 1.7 deg) sinewave gratings that were superimposed in both space and time. Both gratings were 40% Michelson contrast and were in cosine phase with respect to the center of the screen. One grating was always horizontally-oriented and was temporally square-wave counterphase modulated at F1 (nominally 6.67 Hz). In different experimental conditions, the other grating was oriented at either 0, 2, 5, 10, 20, 30, 40, 60, 80, or 90 deg counterclockwise, where 0 is horizontal. This variably-oriented Gabor was square-wave counterphase modulated at F2 (nominally 8.57 Hz).

**Procedure** Subjects were seated comfortably in an electrically and acoustically-shielded room in which the only source of light was the stimulus monitor. A chin rest ensured constant viewing distance. After 30 s of initial dark adaptation, subjects initiated each trial by pressing the space bar on a keyboard. Subjects engaged each of the 10 trial types (i.e., grating orientation offsets) twice for a total of 20 trials. Each trial was 54.6 s in duration. During each trial, subjects passively viewed the dynamic visual pattern while fixating a small, static, centrally-located black dot (diameter = 10 pixels). Subjects were encouraged to minimize blinking and other muscle movement as much as possible, and to relax and maintain fixation. Subjects began the experiment alert and focused, and all indications suggested that they remained so throughout the relatively brief 20 minute experiment.

**EEG recording** Subjects' EEG was acquired with a 256-channel Geodesic Sensor Net (Electrical Geodesics Inc., Eugene, Oregon). The analog signal was digitized at 500Hz and bandpass filtered between 0.1 and 200 Hz. Impedances for all relevant electrodes were kept below 50 $k\Omega$, which is adequate for EGI's high-impedance acquisition method.

**Data Analysis - Measuring F1+F2 Activity** Data were initially referenced to electrode Cz, and then were then re-referenced off-line to the mean of all the electrodes. The first 4.2 s of each trial was discarded to avoid transient VEPs due to stimulus onset. The remaining 50.4 s of data were then Fourier-transformed using the `fft` function in R (R Development Core Team, 2009). For each subject, the amplitude spectra for both trials in each condition were averaged. Sampling at 500 Hz for 50.4s yielded frequency bins that were approximately 0.02 Hz wide. As can be seen in Figures 4.2 and 4.3, the energy due to the intermodulation frequency (`F1+F2`) fell within the bin encompassing 15.24 Hz, and there was little spillover into nearby bins. Next, for each subject, we characterized the signal-to-noise ratio (SNR) of the `F1+F2` response in each condition by dividing the response in the 15.24 Hz bin ("signal") by the mean response in two flanking 10-bin regions ("noise"), with a one bin buffer between the signal and noise to avoid spillover energy. In other words, the signal was the 15.24 Hz bin and the noise was all bins in the 15.0-15.48 Hz range except for the 3 bins centered on the signal.

Previous work suggests the ssVEP originates mainly from areas V1 and V5/MT (Di Russo et al., 2007), and is concentrated, on the scalp, over the occipital pole (e.g., Clementz et al., 2008, Figure 2). Oz is the nearest electrode to the occipital pole for most subjects. To verify that electrode Oz was approximately the site of maximal `F1+F2` activity, we calculated `F1+F2` amplitude at each electrode for the 0 deg offset condition for each subject. We then took the mean of that activity across subjects in each age group, normalized that activity by the electrode with the maximal activity in each age group, and employed EEGLAB's `headplot` function, which uses spherical splines, to generate the images seen in Figure 4.1. On average, both age groups showed maximal `F1+F2` activity near the occipital pole with comparable amounts of spread to nearby occipital scalp. Accordingly, only the results for Oz are reported here. Note, however, that other schemes for functionally or anatomically selecting electrodes on a subject-by-subject basis were employed as well, and did not qualitatively alter the current results.

## 4.3 Results

All analyses, other than the aforementioned scalp topographics, were performed with R (R Development Core Team, 2009). *t*-tests used the Welch-correction for violations of the homogeneity of variance assumption and ANOVAs used the Huynh-Feldt method to correct for violations of the sphericity assumption for within-subject variables (Maxwell

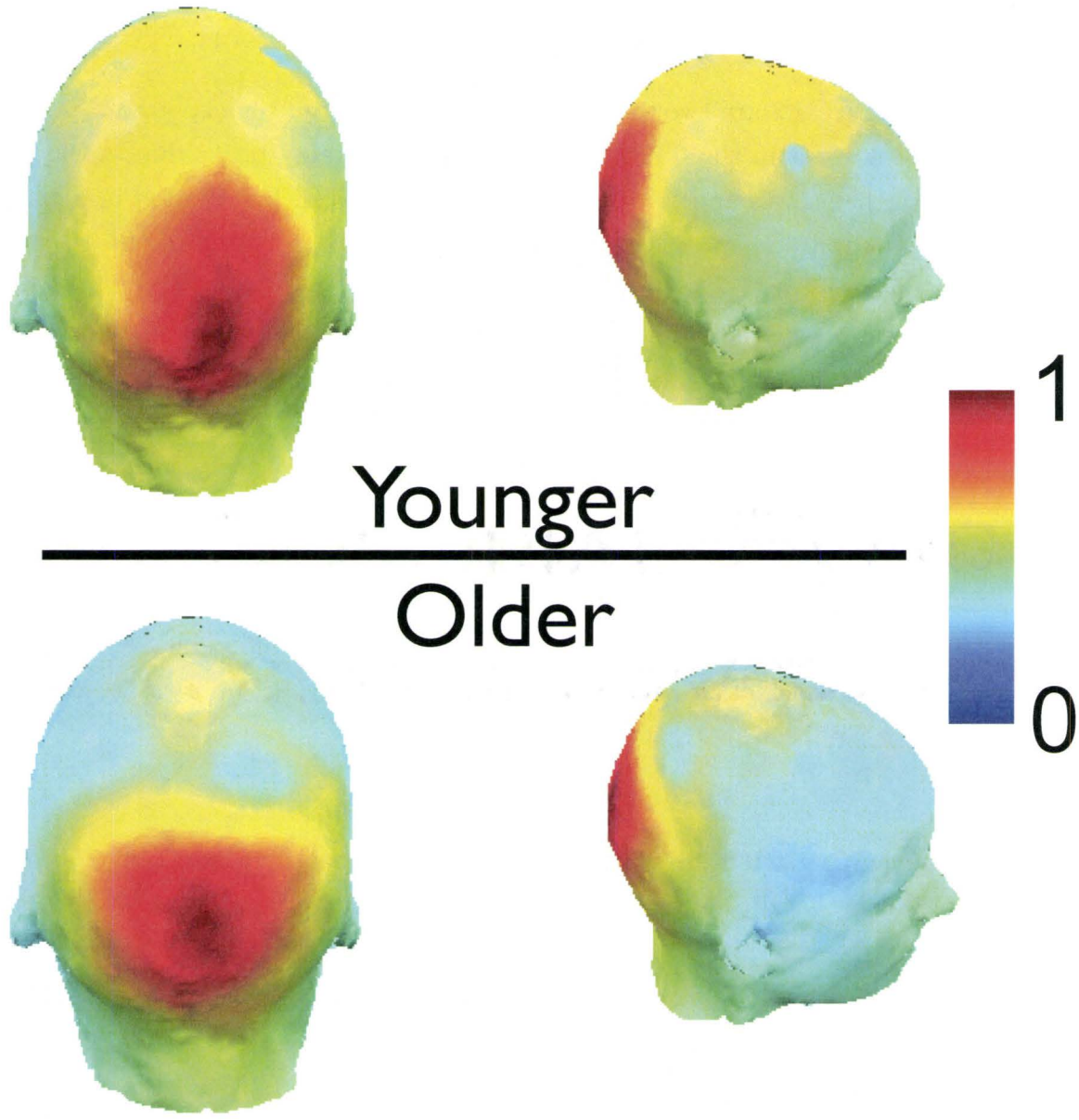


Figure 4.1: Group averaged topographic F1+F2 SNR for the 0 degree test-mask offset condition normalized by the maximal SNR site in each group. The location of central tendency and the spread of the activity appears comparable across age groups.

and Delaney, 2004); p-values reported below are the corrected p-values. One younger and two older subjects yielded results that, when subjected to curve-fitting (see below), yielded fit parameters that were more than two standard deviations away from their respective group means. These three subjects were declared outliers and their data are excluded from the present analyses and figures (including Figure 4.1).

Shown in Figure 4.2 are two views of the frequency amplitude spectrum produced by one typical subject in the 0 deg condition: several energy peaks due to the visual stimulus make themselves apparent, including F1+F2 at 15.24 Hz. Plotted in Figure 4.3 is the average amplitude spectra from 15.0 Hz to 15.5 Hz for each of the 10 grating orientation-offsets for each age group. These plots show that F1+F2 activity is clearly tuned for the test-mask orientation offset, with activity being highest at small orientation offsets. The degree of tuning (i.e., the rate of drop-off) appears to be equivalent across age groups in these plots. Younger subjects appear to exhibit stronger signals – at least at small orientation offsets – and less noise than older subjects. These two effects conspire to slightly decrease the SNR of F1+F2 activity in older subjects at smaller offsets. SNR is plotted in Figure 4.4. A 2 (age) by 10 (orientation offset) ANOVA on these F1+F2 SNR results found a significant effect of orientation offset [$F(9,171) = 13.46$, $p < 0.001$], but no effect of age [$F(1,19) = 1.13$, $p = 0.30$] and no age $\times$ condition interaction [$F(9,171) = 1.00$, $p = 0.41$]. The lack of an interaction suggests that the effect of orientation offset on F1+F2 SNR was similar in both age groups.

**Quantifying tuning with curve-fitting** To further quantify F1+F2 tuning as a function of age, we employed the following decaying exponential function:

$$SNR(x) = k + a \cdot \exp\left(-\frac{x}{b}\right) \tag{4.1}$$

where $x$ is orientation offset, $k$ is the lower asymptote, $a$ is the difference between the maximum (i.e., y-intercept) and the lower asymptote, and $b$ governs the rate of decline from the maximum SNR, $(k + a)$, to the minimum SNR, $k$. Equation 4.1 was first fit to the average SNR in each age group, and the resulting parameters were used to draw the smooth curves in Figure 4.4; as can be seen, Equation 4.1 provided reasonably good fits to the data in both age groups. Next, Equation 4.1 was fit to the data from each subject in each age group. The means and standard errors of the best-fitting parameters are listed in Table 5.1. Separate $t$-tests found that none of the parameters differed between

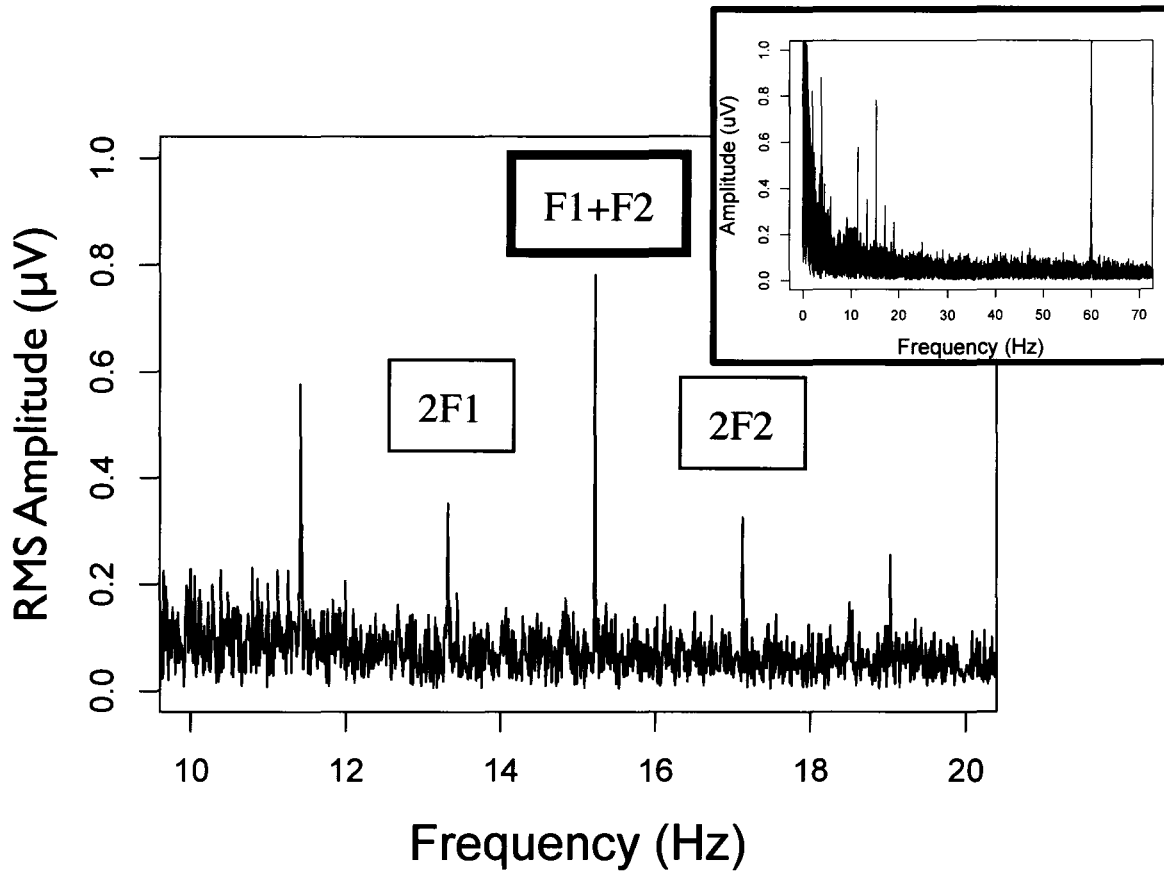


Figure 4.2: Frequency spectrum results from an example subject in the 0 degree grating-offset condition. Between 10 and 20 Hz, harmonics of the individual stimulus components (`2F1` = 13.34 Hz; `2F2` = 17.14 Hz) and the intermodulation term of interest (`F1+F2` = 6.67 + 8.57 = 15.24 Hz) make themselves apparent. The peaks not labeled are `3F1-F2` (11.44 Hz) and `3F2-F1` (19.04 Hz). A more global view (inset) features energy at 60 Hz due to AC electricity, and the $1/f$ profile and alpha concentration (relatively strong activity at approximately 10 Hz) characteristic of human EEG (Barlow, 1993).

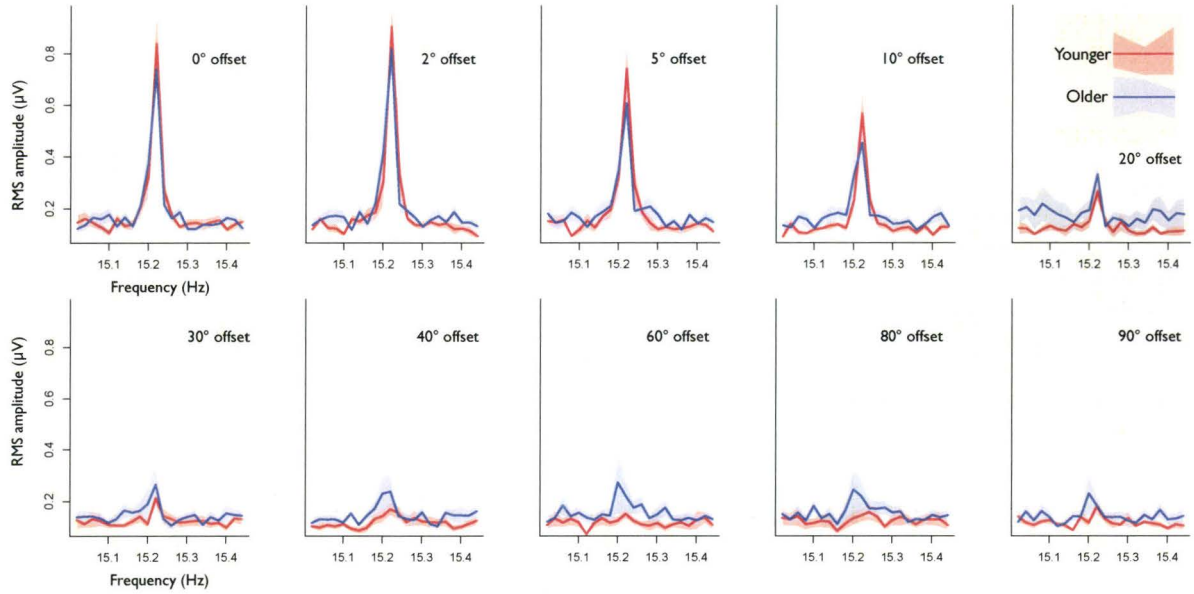


Figure 4.3: Mean frequency amplitude spectra by age group and offset condition in the region around F1+F2. At each of the 10 grating orientation offsets, the thick red and blue lines show the mean activity for the younger and older subjects, respectively. The lighter red and blue bands plot the respective standard errors for those means. F1+F2 energy is tuned for the orientation offset, with energy being highest at small offsets. Younger subjects appear to exhibit stronger signals at small offsets, and less noise (i.e., energy in the flanking regions) at all offsets. However, both age groups' F1+F2 activity exhibit comparable rates of drop-off, or tuning.

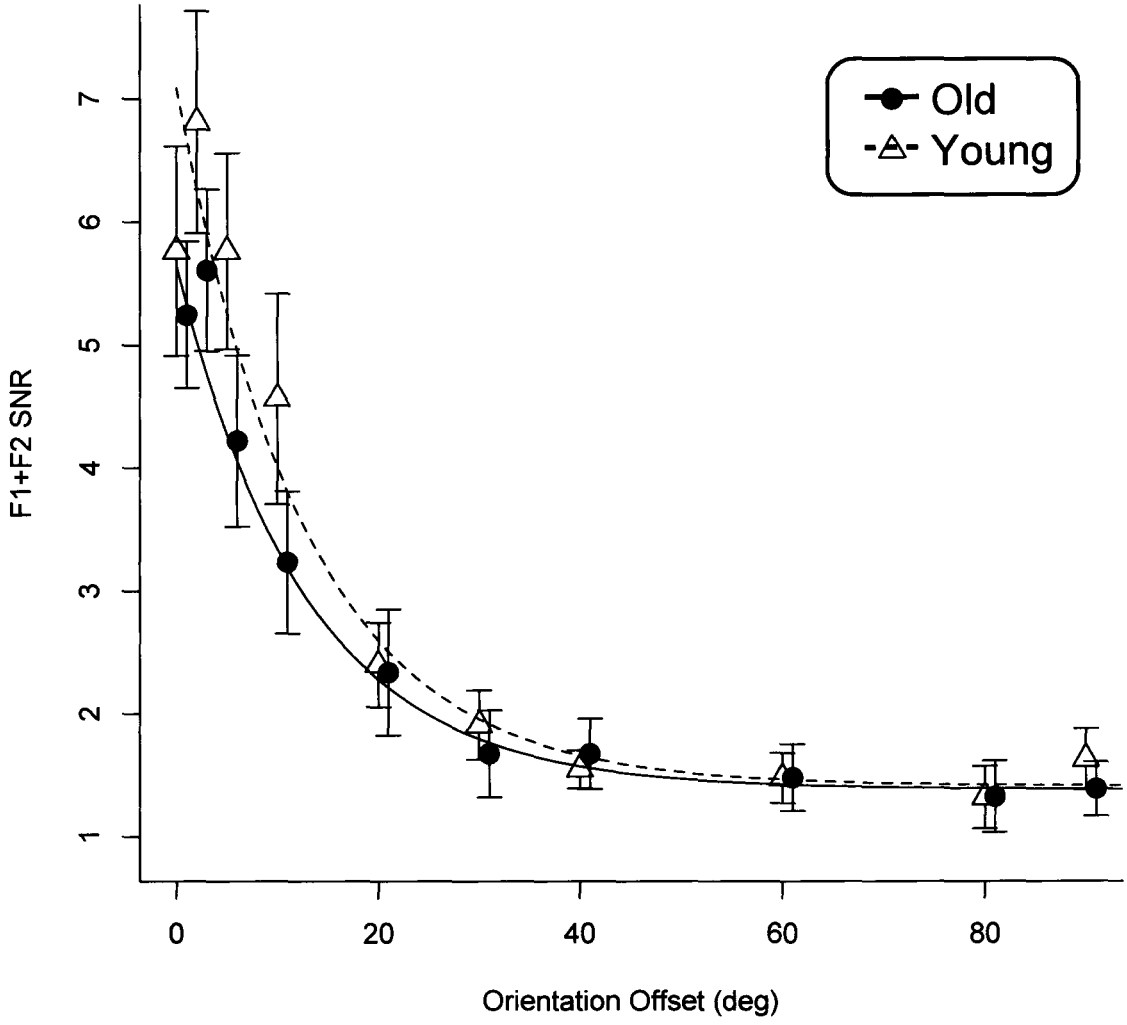


Figure 4.4: F1+F2 tuning. Mean F1+F2 SNRs for older and younger subjects are plotted as a function of grating orientation offset condition. Error bars represent the standard errors of the means. Equation 4.1 was fit to the average SNRs for each age group; the solid and dashed curves represent the best-fitting result for older and younger subjects, respectively. Older subjects' data points, but not their best-fitting curve, have been offset by 1 degree along the x-axis for graphical visibility purposes only.

age groups ($p > 0.4$).

| | younger subjects $\hat{\mu} \pm \hat{\sigma}_\mu$ | older subjects $\hat{\mu} \pm \hat{\sigma}_\mu$ |
|---|---|---|
| $k$ | $1.31 \pm 0.18$ | $1.19 \pm 0.16$ |
| $a$ | $5.91 \pm 0.97$ | $4.88 \pm 0.59$ |
| $b$ | $14.87 \pm 2.48$ | $12.82 \pm 2.37$ |
| $\theta_{1/2}$ | $16.04 \pm 3.09$ | $15.21 \pm 4.01$ |

Table 4.1: Parameters $k$, $a$, $b$, and $\theta_{1/2}$ (half-height half-width) estimated from the F1+F2 tuning results.

Estimates of both physiological and psychophysical orientation tuning are often expressed in terms of half-width at half-height, $\theta_{1/2}$, which in the current context corresponds to the orientation at which the response variable – here, SNR – drops to one-half of its peak value. Thus, Equation 4.1 was set to one-half of its maximum and rearranged for $x$ to estimate $\theta_{1/2}$ for each subject. The means of $\theta_{1/2}$ for younger and older subjects were 16.04 and 15.21 deg, respectively. The difference between these group means, listed in Table 5.1, was not statistically significant, $t(19) = 0.1522$, $p = 0.88$.

## 4.4 Discussion

**Cortical orientation tuning is preserved with age** Single-cell recordings of visual neurons show that orientation selectivity is reduced in senescence (e.g., Schmolesky et al., 2000). However, recent psychophysical studies have found that orientation tuning remains intact in older age (Delahunt et al., 2008; Govenlock et al., 2009). One explanation for the apparent contradiction between the physiological and psychophysical studies is that older human subjects base their psychophysical judgements on the responses of a relatively small number of cortical cells (Parker and Newsome, 1998; Gold and Shadlen, 2007) that have orientation selectivity that is comparable to that found in cells in younger brains. To test this idea, the current study measured the orientation selectivity of a non-linear component in the ssVEP. Presumably, the orientation selectivity of this component represents something like the average selectivity of a large population of cells that contribute to the steady-state response. If this assumption is correct, and if

psychophysical performance is based on a small subset of the cells contributing to the ssVEP, then the population response might be more sensitive to age-related changes in orientation selectivity of cortical neurons. Our results were inconsistent with this prediction. Although, like Candy et al. (2001), we found that the F1+F2 steady-state VEP intermodulation term was tuned for the orientation offset between two flickering, superimposed gratings, there was no evidence to support the idea that the orientation tuning of that response differed in younger and older subjects.

There is a stark difference between the marked detuning of V1 (Schmolesky et al., 2000; Leventhal et al., 2003) and V2 (Yu et al., 2006) neurons found in senescent primate models, and the preservation of visual cortex tuning in older age found in the current human study. One possible explanation is that the primates under examination in the single-cell studies were globally anesthetized, and there may be an interaction between age and the anesthetic that led to the very broadly-tuned responses of the senescent neurons. Evidence against this possibility comes from the fact that Wang et al. (2005) manipulated the level of anesthetic used and found that it has no observable effect on the tuning of the neurons under investigation in either old or young macaques. (See Discussion section of Chapter 5 for more details on this matter.)

A second explanation for the difference between the single-cell studies and the current EEG result is that older observers may utilize focussed attention, or more generally, consciousness – faculties denied the anesthetized macaques – to tune what are otherwise detuned neurons. Although attention has not been shown to significantly affect the tuning bandwidth of neurons in early visual cortical areas in young adult primates (McAdams and Maunsell, 1999), the effects that attention and consciousness have on physiology and perception during normal aging remains largely unexplored. Regardless, attention has been shown to affect the responsiveness of early visual neurons in at least some ways: attention causes increases in those neurons' gain in young primate single-cell studies (McAdams and Maunsell, 1999; McAdams and Reid, 2005); attention has been shown to increase the amplitude of the ssVEP for simple, one-component stimuli in young human adults (Hillyard et al., 1997; Di Russo and Spinelli, 1999), akin to either 2F1 or 2F2 in the current study; and attention sharpens the tuning of V1 BOLD response to stimulus position (Fischer and Whitney, 2009). To test this explanation, older humans' attention could be diverted away from the steady-state stimulus in the current experiment with some other behavioural task; if older humans are using attention to tune early visual neurons, then such a manipulation should result in detuning of the F1+F2 response.

A third explanation for the difference between the single-cell studies and the current EEG result is that the human brain may undergo compensatory reorganization in older age that acts to preserve orientation tuning in visual cortex neurons. A series of studies have shown that, in the presence of equivalent behavioural performance on a simple visual task, underlying patterns of brain activity substantially differ between younger and older adults (McIntosh et al., 1999; Della-Maggiore et al., 2000; Bennett et al., 2001). In those studies, older adults enlisted medial temporal and frontal areas that younger adults did not, and also demonstrated different patterns of functional connectivity between those areas and visual cortex. These different patterns of brain activity may reflect age-related reorganization whereby higher brain regions are used to compensate for degraded primary sensory cortex function. In opposition to this idea, there is little indication in Figure 4.1 that the current patterns of electrical activity recorded at the scalp differed between age groups. By extension, this lack of a difference in scalp-activity provides no reason to suspect that the location of the underlying neural generators of this activity differed between age groups. However, these scalp topographies are not indicative of the functional connectivities (i.e., spatial and temporal dependencies) that exist between brain regions, which, as mentioned, was a key feature that distinguished older from younger brain activity in the aforementioned studies of cortical reorganization in older age (e.g., McIntosh et al., 1999).

**Comparison to previous orientation-tuning literature** The orientation tuning bandwidth measured in the current study is similar to that found by a variety of previous psychophysical and physiological investigations (see Table 4.2). Behavioural sensitivity for a sine-wave grating, such as that employed in the current study, is differentially affected by a superimposed masking grating depending on the relative orientation between the two gratings. This phenomenon has been measured by several researchers to quantify behavioural orientation tuning in younger (Campbell and Kulikowski, 1966; Phillips and Wilson, 1984; Anderson et al., 1991) and older (Delahunt et al., 2008; Govenlock et al., 2009) adults. Half-width half-height (i.e., $\theta_{1/2}$) in these studies was typically found to be in the range of 10-15 deg. Using the current two-grating ssVEP method to investigate orientation tuning during infant development, Candy et al. (2001) found $\theta_{1/2}$ to be approximately 10 deg (visually estimated from Figure 7 of Candy et al.) for five control adult subjects. Using the 2F1+2F2 intermodulation term of the ssVEP, Regan and Regan (1987) found orientation bandwidth to be about 6 deg (visually estimated from Figure 1 Regan & Regan). Single-cell studies in primates (Geisler and Albrecht,

1997) and DeValois et al. (1982) have found mean orientation bandwidth to be about 20 deg. Averaged across age groups, the current study found orientation bandwidth, $\theta_{1/2}$, to be 15.64 deg, which is similar to the estimates obtained in previous psychophysical and physiological studies.

Table 4.2: Past and present orientation tuning bandwidth measurements.

| Study | Method | $\theta_{1/2}$ (deg) |
|---|---|---|
| Campbell and Kulikowski (1966) | Psychophysical (grating masking) | 12 |
| Phillips and Wilson (1984) | Psychophysical (grating masking) | 15.5 |
| Anderson et al. (1991) | Psychophysical (grating masking) | 15.2 |
| Govenlock et al. (2009) | Psychophysical (grating masking) | |
| | younger (age 18–30) | 14.41 |
| | older (age 64 – 77) | 14.33 |
| Delahunt et al. (2008) | Psychophysical (grating masking) | |
| | younger (age 20–33) | 11.11 |
| | older (age 65 – 85) | 11.58 |
| DeValois et al. (1982) | Single-cell physiology | ≈20 |
| Geisler and Albrecht (1997) | Single-cell physiology | ≈20 |
| Candy et al. (2001) | ssVEP (human EEG) | ≈10 |
| Regan and Regan (1987) | ssVEP (human EEG) | ≈6 |
| **current study** | **ssVEP (human EEG)** | |
| | younger (age 18–28) | 16.04 |
| | older (age 62–74) | 15.21 |

**A luminance or contrast-selective mechanism as an alternative explanation for F1+F2 activity** Regan and Regan (1988) pointed out that a mechanism that responds to the time-varying maximum luminance of the stimulus employed in the current study, as opposed to its orientation content, would also produce energy at intermodulation frequencies, including F1+F2. If the two gratings are, at the outset of a trial, in 0 deg relative spatial phase, for small orientation offsets the four unique states that the flickering compound pattern can take have very different maximum luminances (and contrast energies). At larger orientation offsets (e.g., when the gratings are perpendicular to one

another) the four unique states all have the same maximum luminance (and contrast energy). A mechanism that responds to changes in maximum luminance and/or contrast energy in the time-varying signal will produce a response at many intermodulation frequencies, including F1+F2, for small, but not large, orientation offsets. Therefore, activity that is tuned to the relative orientation of the two flickering gratings is not necessarily due to an orientation-selective mechanism.

Candy et al. (2001) acknowledged this possible confound (p. 4535), but concluded that a luminance- or contrast energy-selective mechanism would produce orientation tuning that was significantly narrower than their observed results. Similarly, we have modelled the response of a luminance or contrast energy selective mechanism, and determined that the orientation bandwidth ($\theta_{1/2}$) of its response would be slightly less than 8 deg. Across all subjects included in our analyses, the average bandwidth was 15.64 degrees, which was significantly greater than 8 deg $t(20) = 2.92$, $p < 0.01$. Further, our modelling shows that a luminance or contrast energy selective mechanism would produce no F1+F2 activity beyond $\approx 23$ deg. As seen in Figure 4.4, the SNR of F1+F2 is greater than the lower asymptotic value even at an orientation offsets near 20 deg. Finally, as discussed above, the current estimates of orientation bandwidth are similar to previously-reported values. For these reasons, we suggest that the current findings reflect the responses of orientation-selective mechanisms, as opposed to luminance- or contrast energy-selective mechanisms.

**Conclusion** Although there are several reports of orientation detuning in senescent primate visual cortex neurons, older age does not affect human psychophysical orientation tuning, nor does it affect average neural orientation tuning as measured with the ssVEP in the current study. The current result suggests that older humans do not compensate for detuned neurons by monitoring a subset that retain fine, young-like tuning. Instead, older humans can rely on something like the population average tuning to determine their perception. Given the senescent primate physiology, however, further experimentation should explore the extent to which older humans may be using attention and/or functional reorganization to compensate for, and tune, what may otherwise be detuned neurons.

**Acknowledgements**

This research was supported by the Canada Research Chairs program, of which PJB and ABS are members, a grant from the Canadian Institutes of Health Research (CIHR) to PJB and ABS, a Natural Sciences and Engineering Research Council of Canada Postgraduate Scholarship to SWG, and the CIHR Strategic Training Grant on Communication and Social Interaction in Healthy Aging. Portions of this work were presented at the annual meeting of the Vision Sciences Society (Sarasota, FL U.S.A, May 2008).

# References

Anderson, S. J., Burr, D. C., Morrone, M. C., 1991. Two-dimensional spatial and spatial-frequency selectivity of motion-sensitive mechanisms in human vision. Journal of the Optical Society of America. A, Optics, Image science, and Vision 8 (8), 1340–1351.

Barlow, J. S., 1993. The electroencephalogram: Its patterns and origins. MIT Press: Cambridge MA.

Bennett, P. J., Sekuler, A. B., McIntosh, A. R., Della-Maggiore, V., 2001. The effects of aging on visual memory: Evidence for functional reorganization of cortical networks. Acta Psychologica 107 (1-3), 249–273.

Boutet, I., Faubert, J., 2006. Recognition of faces and complex objects in younger and older adults. Memory and Cognition 34 (4), 854–864.

Brainard, D. H., 1997. The psychophysics toolbox. Spatial Vision 10 (4), 433–436.

Campbell, F. W., Kulikowski, J. J., 1966. Orientational selectivity of the human visual system. Journal of Physiology 187, 437–445.

Candy, T. R., Skoczenski, A. M., Norcia, A. M., Jun 2001. Normalization models applied to orientation masking in the human infant. Journal of Neuroscience 21 (12), 4530–41.

Clementz, B. A., Wang, J., Keil, A., 2008. Normal electrocortical facilitation but abnormal target identification during visual sustained attention in schizophrenia. Journal of Neuroscience 28 (50), 13411–8.

Crum, R. M., Anthony, J. C., Bassett, S. S., Folstein, M. F., 1993. Population-based norms for the mini-mental state examination by age and education level. Journal of the American Medical Association 269, 2386–2391.

Del Viva, M. M., Agostini, R., 2007. Visual spatial integration in the elderly. Investigative Ophthalmology and Vision Science 48 (6), 2940–2946.

Delahunt, P., Hardy, J., Werner, J., 2008. The effect of sensescence on orientation discrimination and mechanism tuning. Journal of Vision 8 (3), 1–9.

Della-Maggiore, V., Sekuler, A. B., Grady, C. L., Bennett, P. J., Sekuler, R., McIntosh, A. R., 2000. Corticolimbic interactions associated with performance on a short-term memory task are modified by age. Journal of Neuroscience 20, 8410–8416.

DeValois, R. L., DeValois, K. K., 1988. Spatial Vision. Oxford University Press.

DeValois, R. L., Yund, W., Hepler, N., 1982. The orientation and direction selectivity of cells in macaque visual cortex. Vision Research 22 (5), 531–544.

Di Russo, F., Pitzalis, S., Aprile, T., Spitoni, G., Patria, F., Stella, A., Spinelli, D., Hillyard, S. A., 2007. Spatiotemporal analysis of the cortical sources of the steady-state visual evoked potential. Human Brain Mapping 28, 323–334.

Di Russo, F., Spinelli, D., Sep 1999. Electrophysiological evidence for an early attentional mechanism in visual processing in humans. Vision Res 39 (18), 2975–85.

Fischer, J., Whitney, D., 2009. Attention narrows position tuning of population responses in v1. Current Biology 19, 1356–1361.

Geisler, W. S., Albrecht, D. G., 1997. Visual cortex neurons in monkeys and cats: detection, discrimination, and identification. Visual Neuroscience 14 (5), 897–919.

Gold, J. I., Shadlen, M. N., 2007. The neural basis of decision making. Annual Review of Neuroscience 30, 535–74.

Govenlock, S. W., Taylor, C. P., Sekuler, A. B., Bennett, P. J., 2009. The effect of aging on the orientational selectivity of the human visual system. Vision Research 49, 164–172.

Habak, C., Wilkinson, F., Wilson, H. R., 2008. Aging disrupts the neural transformations that link facial identity across views. Vision Res 48 (1), 9–15.

Herbert, A. M., Overbury, O., Singh, J., Faubert, J., 2002. Aging and bilateral symmetry detection. Journal of Gerontology Series B: Psychological Science and Social Sciences 57, P241–P245.

Hillyard, S., Hinrichs, H., Tempelmann, C., Morgan, S., Hansen, J., Scheich, H., Heinze, H., 1997. Combining steady-state visual evoked potentials and fmri to localize brain activity during selective attention. Human Brain Mapping 5 (4), 287–292.

Leventhal, A. G., Wang, Y., Pu, M., Zhou, Y., Ma, Y., 2003. GABA and its agonists improved visual cortical function in senescent monkeys. Science 300, 812–815.

Mantyjarvi, M., Laitinen, T., 2001. Normal values for the pelli-robson contrast sensitivity test. Journal of Cataract and Refractive Surgery 27 (2), 261–266.

Maxwell, S., Delaney, H., 2004. Designing Experiments and Analyzing Data: A Model Comparison Approach, 2nd Edition. Lawrence Erlbaum Associates, Mahwah, New Jersey.

McAdams, C. J., Maunsell, J. H. R., 1999. Effects of attention on the reliability of individual neurons in monkey visual cortex. Neuron 23, 765–773.

McAdams, C. J., Reid, R. C., 2005. Attention modulates the responses of simple cells in monkey primary visual cortex. J Neurosci 25 (47), 11023–33.

McIntosh, A. R., Sekuler, A. B., Penpeci, C., Rajah, M. N., Grady, C. L., Sekuler, R., Bennett, P. J., 1999. Recruitment of unique neural systems to support visual memory in normal aging. Current Biology 9, 1275–1278.

Parker, A. J., Newsome, W. T., 1998. Sense and the single neuron: Probing the physiology of perception. Annual Review of Neuroscience 21, 227–277.

Pelli, D., Robson, J., Wilkins, A., 1988. The design of a new chart for measuring contrast sensitivity. Clinical Vision Sciences 2 (3), 187–199.

Pelli, D. G., 1997. The videotoolbox software for visual psychophysics: Transforming numbers into movies. Spatial Vision 10, 437–442.

Phillips, G., Wilson, H., 1984. Orientation bandwidths of spatial mechanisms measured by masking. Journal of the Optical Society of America. A, Optics, Image science, and Vision 1 (2), 226–232.

R Development Core Team, 2009. R: A Language and Environment for Statistical Computing. R Foundation for Statistical Computing, Vienna, Austria.
URL http://www.R-project.org

Regan, D., Regan, M., 1988. Objective evidence for phase-independent spatial frequency analysis in the human visual pathway. Vision Rsearch 28 (1), 187–191.

Regan, D., Regan, M. P., 1987. Nonlinearity in human visual resonses to two-dimensional patterns, and a limitation of fourier methods. Vision Rsearch 27 (12), 2181–2183.

Roudaia, E., Bennett, P., Sekuler, A., 2008. The effect of aging on contour integration. Vision Research 48, 2767–2774.

Schmolesky, M. T., Wang, Y., Pu, M., Leventhal, A. G., 2000. Degradation of stimulus selectivity of visual cortical cells in senescent rhesus monkeys. Nature Neuroscience 3, 384–390.

Stanford, T., Pollack, R. H., 1984. Configuration color vision tests: the interaction between aging and the complexity of figure-ground segregation. Journal of Gerontology 39 (5), 568–571.

Wang, Y., Zhou, Y., Ma, Y., Leventhal, A., 2005. Degradation of signal timing in cortical areas V1 and V2 of senescent monkeys. Cerebral Cortex 15 (15), 403–408.

Yu, S., Wang, Y., Li, X., Zhou, Y., Leventhal, A. G., 2006. Functional degradation of extrastriate visual cortex in senescent rhesus monkeys. Neuroscience 140, 1023–1029.

# Chapter 5

# Spatial frequency tuning in human visual cortex in normal aging

**Abstract**

Physiological studies suggest that the spatial frequency (SF) bandwidth of visual cortical neurons may become more broadly tuned in old age (Zhang et al., Eur J Nsc, 2008, 28, 201–07). However, behavioural measures of frequency selectivity in humans do not find evidence for broader tuning in old age (Govenlock et al. 2010; Chapter 3). This disagreement between primate physiology and human behaviour may arise if the performance of older subjects in psychophysical tasks relies on a subset of neurons that retain a high degree of frequency selectivity even in old age. To test this hypothesis, in the current study we recorded the steady-state visually-evoked potential (ssVEP) to estimate the frequency selectivity of cortical neurons, *en masse* (Regan and Regan, 1988). Specifically, we measured the ssVEP elicited by overlapping sine wave gratings that flickered at different rates (e.g., `F1` and `F2` Hz), and examined how the amplitude at two intermodulations frequencies, `F1+F2` and `2F1+2F2`, varied as a function of the spatial frequency difference between the two gratings. Consistent with previous results, we found that ssVEP amplitude at some intermodulation frequencies was selective for spatial frequency, but we found no evidence that frequency selectivity differed between younger and older subjects. Our results are consistent with the hypothesis that average spatial frequency tuning of visual cortical neurons is preserved in old age.

## 5.1 Introduction

Much evidence suggests that the early visual system registers the visual scene with a bank of quasi-linear, quasi-independent spatial frequency channels, each preferring luminance changes at a particular spatial scale or frequency, and each having some degree of tuning or selectivity about its preference. Given internal noise, the tuning of these mechanisms is positively related to the amount of information that they pass on to higher visual processes, which give rise to complex percepts of textures, curvature, objects, and faces, for example. Because the perception of complex visual forms declines in older age (e.g., Stanford and Pollack, 1984; Herbert et al., 2002; Boutet and Faubert, 2006; Del Viva and Agostini, 2007; Habak et al., 2008; Roudaia et al., 2008), there is reason to suspect that the tuning of these low-level mechanisms broadens, and/or that the ability to integrate the output of these low-level mechanisms to form complex percepts declines with age. Therefore, studies finding an age-related decline for any complex visual form that requires the integration of output from lower-level mechanisms cannot specifically implicate a decline of integrative mechanisms until it is shown that the tuning of lower-level spatial frequency-selective mechanisms does not broaden in older age. The current study is the first assessment of the tuning of these mechanisms in normal, older aging.

Mammalian spatial frequency tuning first arises in the center-surround receptive fields of retinal ganglion (Kuffler, 1953; Rodieck and Stone, 1965) and LGN (So and Shapley, 1981) neurons. This tuning becomes sharper and is coupled with orientation selectivity in V1 neurons (Campbell et al., 1969; Maffei and Fiorentini, 1973; De Valois et al., 1982). Although there are no published reports that directly measure physiological spatial frequency tuning in senescence, Zhang et al. (2008) did find that the difference, in octaves, between a V1 neuron's preferred spatial frequency and its spatial resolution (i.e., the highest spatial frequency to which it responded) was greater in senescent monkeys. This result is consistent with the claim that aging diminishes the spatial frequency selectivity of V1 neurons. Further, other single-cell studies have found that tuning for orientation is significantly broader as a function of senescence in macaques (Schmolesky et al., 2000; Leventhal et al., 2003; Yu et al., 2006); this broadening of tuning is thought to be due to a deficit in GABAerigic lateral inhibitory activity, which many researchers suggest, in conjunction with the spatial arrangement of their geniculate inputs, is responsible for the degree of orientation and spatial frequency tuning seen in V1 neurons (e.g., Ringach et al., 2002; Zhu et al., 2010) (but cf., Ferster and Miller, 2000). Together, these results suggest

that spatial frequency tuning may become broader in senescent visual cortical neurons.

Nevertheless, psychophysical masking studies have found no evidence for broader orientation (Delahunt et al., 2008; Govenlock et al., 2009) or spatial frequency (Govenlock et al., 2010) tuning in normal, older adult humans. One possible explanation of the apparent discrepancy between the two sets of findings is based on the idea that psychophysical results may reflect the properties of a small subset of visual neurons. Some percepts may be determined by a surprisingly small number of neurons (for a review, see Parker and Newsome, 1998; Gold and Shadlen, 2007). Thus, although older humans may have detuned neurons on average, their psychophysical performance may rely on a subset of neurons that remain selective into older age. In other words, most visual neurons in senescent cortex may be de-tuned – as the physiology suggests – but psychophysical performance may depend most strongly on the minority of cells that retain a high degree of orientation and frequency selectivity. If this hypothesis is correct, then EEG-based estimates of frequency selectivity (Regan and Regan, 1988), which reflect the activity of large populations of neurons, may be more sensitive to age-related changes in frequency selectivity than psychophysical measures. In the current study, we measured aspects of the steady-state visually-evoked potential (ssVEP) to infer the population-average tuning of visual cortex neurons. The ssVEP is the corresponding EEG response to visual stimuli whose attributes are temporally oscillating in some fashion (e.g., flickering). The ssVEP has been used to investigate many aspects of visual function, including spatial- and object-based models of visual attention in both normal (e.g., Hillyard et al., 1997; Di Russo and Spinelli, 1999; Müller and Hillyard, 2000; Müller and Hübner, 2002; Müller et al., 2003; Ding et al., 2006) and clinical (Clementz et al., 2008) populations, perceptual binding (e.g., Sutoyo and Srinivasan, 2009), figure-ground interactions (Appelbaum et al., 2008), and the early detection of glaucoma (Vaegan et al., 2008). The ssVEP is also emerging as a widely-used phenomenon for brain-computer interfaces (e.g., Wang et al., 2006).

The current experiment takes advantage of nonlinear response properties of visual neurons. Consider the case where a visual neuron is stimulated by two overlapping sine wave gratings that are flickering at `F1` and `F2` Hz. If the neuron was linear, then its response would be the sum of its responses to the individual components. If the neuron responded to the two gratings presented individually, then a spectral analysis of its time-varying response to the compound would reveal non-zero components at `F1` and `F2` Hz. Neurons, however, typically are not linear, and therefore their temporal response to the flickering compound stimulus will have non-zero components at so-called intermodulation frequencies, `mF1`

± nF2, where m and n are small, positive integers. Critically, a non-zero response at an intermodulation frequency implies that *both* flickering components stimulated the neuron, and therefore the response amplitude at these frequencies potentially can be used to study the tuning properties of a neuron. For example, the response amplitude at F1 + F2 Hz may be large when the two gratings have similar spatial frequencies and gradually diminish as the spatial frequency difference increases: the function relating response amplitude to the frequency difference would be one way of characterizing the spatial frequency selectivity of that neuron. As one might expect from the non-linear response properties of visual neurons, the ssVEP produced by overlapping flickering gratings also contains non-zero responses at intermodulation frequencies. Moreover, the amplitudes of these ssVEP frequencies depend on the difference between the orientations (Regan and Regan, 1987; Candy et al., 2001; Govenlock et al., in preparation) and spatial frequencies (Regan and Regan, 1988) of the two flickering gratings, and the frequency and orientation tuning curves derived from these EEG data are qualitatively similar to ones derived by psychophysical methods.

In the current experiment, following Regan and Regan (1988), we fixed the spatial frequency of one counter-phase flickering sine wave grating and varied the spatial frequency of a second, spatially- and temporally-overlapping grating that was flickering at a slightly different rate. Taking the dependent amount of either F1+F2 or 2F1+2F2 intermodulation activity recorded in the EEG activity of a group of younger and older adults as a proxy for the average spatial frequency tuning of visual cortex neurons, we found no effect of age on spatial frequency tuning in visual cortex. This finding supports the hypothesis that, although senescent neurons may be otherwise detuned, the awake and attending older brain is able to compensate and tune those neurons in an on-line fashion. Further experiments are needed to delineate the effects of attention from those of consciousness, *per se*.

## 5.2 Materials and Methods

**Participants** The research protocol was approved by the McMaster University Research Ethics Board; written, informed consent was obtained from each subject prior to the start of the experiment. Twelve younger (mean age = 21.9 years; SD = 2.0; 3 females) and 12 older (mean age = 68.9; SD = 4.3; 4 females) were paid $10 for their participation in this experiment, with the exception of five younger subjects who were lab members at

the time, including co-author SWG. By self-report, all subjects were healthy and free of any history of cardiovascular, neurological, or visual pathology such as strokes, cataracts, or macular degeneration. Wearing their optical correction, if necessary, subjects yielded normal near and far decimal logMAR acuities (CSV-100EDTRS eye charts, Precision Vision, LaSalle, Illinois, USA) and Pelli-Robson contrast sensitivity (Pelli et al., 1988; Mantyjarvi and Laitinen, 2001). Older subjects were free of age-related dementia as evidenced by their scores in the normal range on the Mini-Mental State Examination, corrected for age and education (Crum et al., 1993).

**Apparatus** The experiment was programmed in MatLab v5.2.1 (The Mathworks) using the Psychophysics and Video Toolboxes (Brainard, 1997; Pelli, 1997) on an Apple Dual-G4 PowerMac computer with an NVIDIA GeForce Ti 4600 graphics card. Stimuli were displayed on a 20-inch Sony Trinitron GDM-F520 monitor with a frame rate of 120 Hz and resolution of 800 × 600 pixels, which subtended 17 × 15 deg at a viewing distance of 114 cm. The screen was fit with a circular aperture with a diameter of 14 deg. Mean luminance was $32 cd/m^2$.

**Stimuli** The stimuli consisted of two greyscale, counterphase-flickering Gabor patterns (i.e., Gaussian-damped sinewave gratings; $\sigma$ = 1.7deg) that were superimposed in both space and time. Both Gabors had a Michelson contrast of 40%; both gratings were in $\pm$ cosine phase relative to the peak of the Gaussian envelope. One Gabor, which we shall arbitrarily refer to as the "target," was fixed at 1 cyc/deg and was counterphase-flickered at a frequency of `F1` (nominally 6.67 Hz). In seven different experimental conditions, the other Gabor, referred to as the "mask," had a spatial frequency that was offset from that of the target by either -0.66, -0.33, -0.17, 0, +0.17, +0.33, or +0.66 octaves. The mask was counterphase-flickered at a frequency of `F2` (nominally 8.57 Hz). These modulation rates were constrained by the monitor refresh rate and the need to keep the intermodulation terms isolatable, in frequency space, from the individual Gabors' harmonics. The target Gabor was horizontally oriented, and the mask Gabor was oriented 7 deg counter-clockwise from horizontal.

**Procedure** Subjects were seated comfortably in an electrically and acoustically shielded room in which the only source of light was the stimulus monitor. A chin rest ensured constant viewing distance. After 30 s of light adaptation, subjects initiated each trial

by pressing the spacebar on a keyboard. The first 12 subjects (of which six were older) engaged each of the seven trial types (i.e., mask orientation offsets) twice for a total of 14 trials; the last 12 subjects engaged each trial type thrice for a total of 21 trials. Each trial was 54.6 s in duration. During each trial, subjects passively viewed the dynamic visual pattern while fixating a small, centrally-located black dot (diameter = 10 pixels). Subjects were encouraged to minimize excessive blinking and other muscle movement as much as possible, and to relax and maintain fixation. The entire testing session lasted 14-21 minutes.

**EEG recording** Subjects' EEG was acquired with a 256-channel Geodesic Sensor Net (Electrical Geodesics Inc., Eugene, Oregon). The analog signal was digitized at 500 Hz and bandpass filtered between 0.1 and 200 Hz. Impedances for all relevant electrodes were kept below 50 $k\Omega$.

**Data Analysis - Isolating/Characterizing F1+F2 Activity** Data from each electrode were initially referenced to electrode Cz, and then were then re-referenced off-line to the mean of all the electrodes. The first 4.2 seconds of each trial was trimmed from the data to avoid transients due to stimulus onset. The remaining 50.4 s of data were then Fourier transformed. The frequency amplitude spectra for each of the subjects' two or three (see above) runs in each condition were averaged together to yield more stable estimates of their frequency amplitude responses. Sampling at 500 Hz for 50.4 s yielded frequency bins that were approximately 0.02 Hz wide. As seen in Figures 5.1 and 5.2, the energy due to the intermodulation term of interest (`F1+F2`) localized well to the bin encompassing 15.24 Hz with little spillover into nearby bins. Next, for each subject, we characterized the strength of the `F1+F2` response in each target-mask offset condition by dividing the response in the 15.24 Hz bin ("signal") by the mean response in two flanking 10 bin regions ("noise"), with a one bin buffer between the signal and noise to avoid spillover energy. In other words, the signal was the 15.24 Hz bin and the noise was all the bins from 15.0 to 15.48 Hz except for the 3 bins centered on the signal.

Previous literature suggests the ssVEP originates mainly from areas V1 and V5 (Di Russo et al., 2007), and is concentrated, on the scalp, over the occipital pole (e.g., Clementz et al., 2008, figure 2). Oz is the nearest electrode to the occipital pole for most subjects. However, to allow for inter-subject variability in cortical and electrode positioning, we determined an "electrode-of-interest" for each subject, defined as the

electrode at which F1+F2 activity was the greatest in the 0 octave offset condition. For 8 of 24 subjects, this was electrode Oz; in the other subjects the electrode-of-interest was up to three electrodes away from Oz, reflecting inter-subject variability in how the electrode cap fit, and, presumably, how visual cortex was folded and positioned.

## 5.3 Results

All analyses were performed with R (R Development Core Team, 2009). $t$-tests were Welch-corrected for violations of the homogeneity of variance assumption, and ANOVA's used the Huynh-Feldt (HF) method to correct for violations of the sphericity assumption for within-subject variables (Maxwell and Delaney, 2004); reported p-values are the corrected p-values. One younger and three older subjects yielded results that were not amenable to our curve-fitting analysis, and were therefore declared outliers; their data are excluded from all statistical analyses, and their data are included only in Figures 5.4 and 5.5 (see below for further justification).

Figure 5.1 shows the relevant section of the frequency amplitude spectrum from a typical subject in the 0 octave condition. Several energy peaks due to the visual stimulus make themselves apparent, including F1+F2 at 15.24 Hz. Plotted in Figure 5.2 is the average amplitude spectra from 15.0 to 15.5 Hz for each of the 7 spatial frequency offsets for each age group. These plots show that F1+F2 activity is clearly tuned for the spatial frequency offset, with activity being highest when the two gratings have the same frequency. Younger subjects appear to exhibit stronger signals overall. However, the degree of tuning (i.e., the rate of drop-off) appears to be similar across age groups.

SNR measured at the frequency F1 + F2 is plotted as a function of the spatial frequency offset in Figure 5.3. A 2 (age) by 7 (offset condition) ANOVA on these F1+F2 SNR results found a significant effect of offset condition [$F(6,108) = 42.01$, $p < 0.001$], but no effect of age [$F(1,18) = 3.80$, $p = 0.067$] and no age $\times$ condition interaction [$F(6,108) = 2.19$, $p = 0.071$]. The failure to find an interaction suggests that F1+F2 SNR was affected similarly by spatial frequency offset in both age groups.

**Quantifying tuning with curve-fitting** To better quantify F1+F2 tuning as a function of age, we employed the following Gaussian function

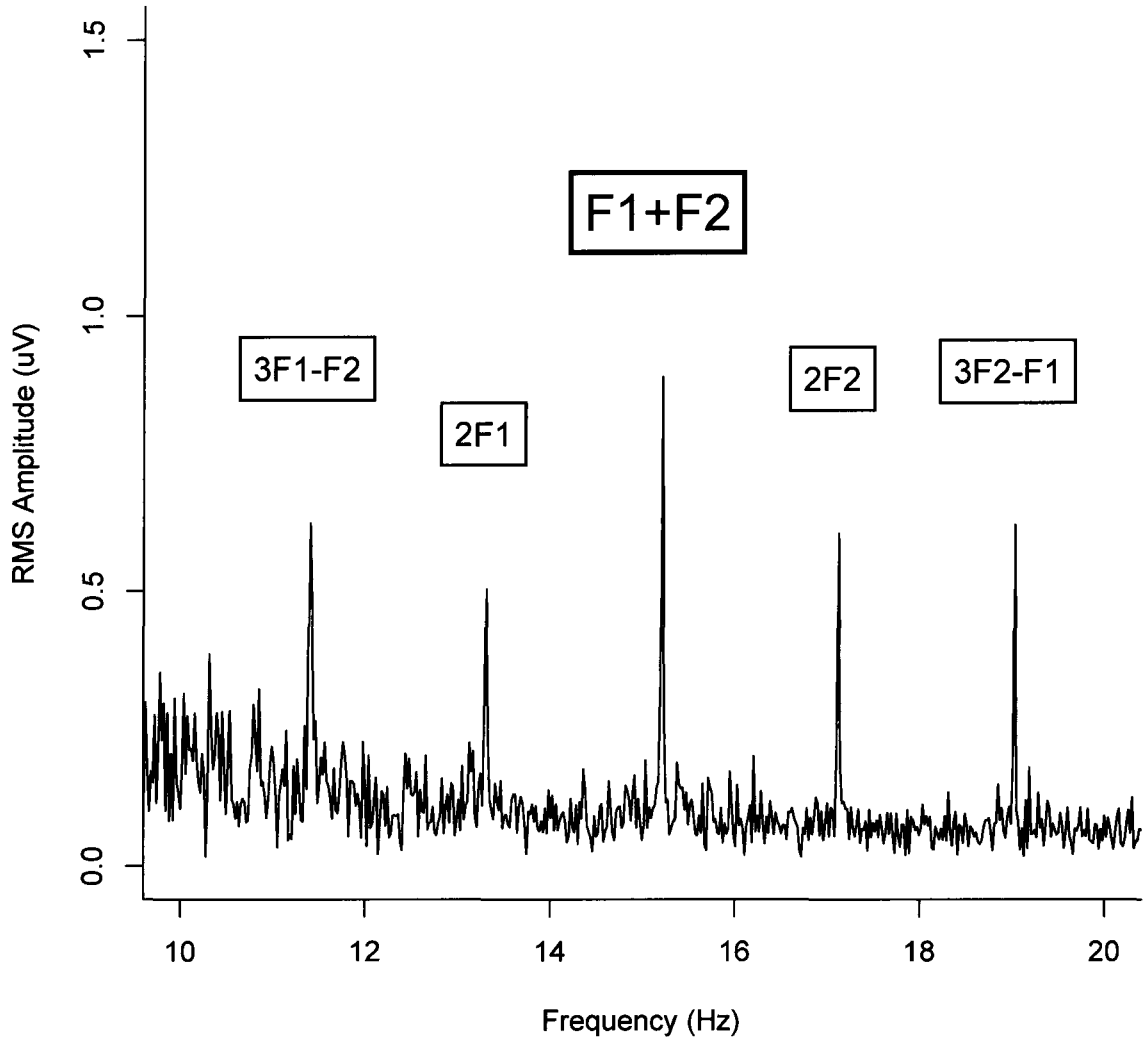


Figure 5.1: Frequency spectrum results from a typical subject in the condition in which the spatial frequencies of the target and mask differed by 0 octaves (i.e., the frequencies were the same). The second harmonics (`2F1` = 13.34 Hz; `2F2` = 17.14 Hz) of the two flicker frequencies, and several intermodulation terms (`3F1-F2` = 11.44 Hz; `3F2-F1` = 19.04 Hz; `F1+F2` = 6.67 + 8.57 = 15.24 Hz) are apparent.

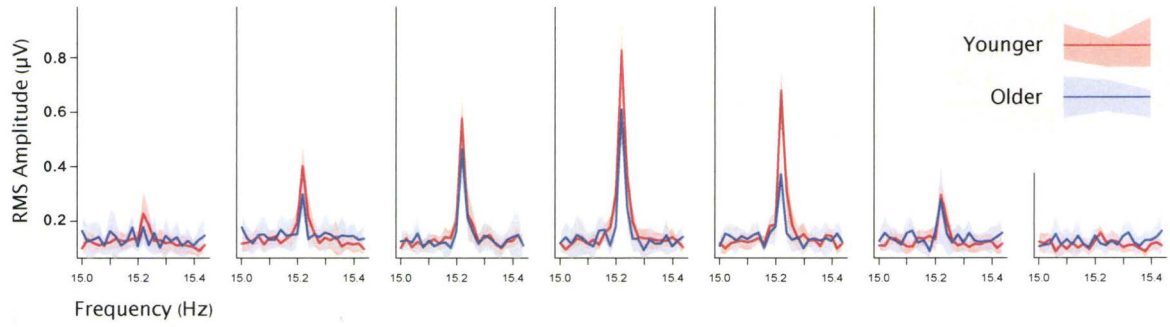


Figure 5.2: Spectral activity by age group and condition in the frequency region around F1+F2 Hz. At each of the 7 target-mask spatial frequency offsets (-0.66, -0.33, -0.17, 0, +0.17, +0.33, and +0.66 octaves), the thick red and blue lines show the mean activity for the younger and older subjects, respectively. The lighter red and blue bands plot the respective 95% confidence intervals for those means.

$$SNR(x) = k + a \cdot \exp\left(-\frac{x^2}{2b^2}\right) \tag{5.1}$$

where $x$ is the spatial frequency offset, $k$ is the lower asymptote, $a$ is the difference between the maximum and the lower asymptote, and $b$ governs the rate of decline from the maximum SNR, $(k + a)$, to the minimum SNR, $k$. During fitting, all parameters were restricted to positive numbers only. Equation 5.1 was first fit to the average thresholds in each age group, and the resulting parameters were used to draw the smooth curves in Figure 5.3, which provided reasonably good fits to the mean data in both age groups. Next, to make group-wise comparisons, Equation 5.1 was fit to the data from each subject in each age group. The means and standard errors of the best-fitting parameters are listed in Table 5.1. Separate t-tests found no effect of age for any of these fit parameters ($p \geq 0.16$). The best-fitting curve for each subject is overlain on their F1+F2 SNRs in Figures 5.4 and 5.5.

Previous estimates of both physiological and psychophysical spatial frequency tuning have often been expressed in terms of half-amplitude half-bandwidth, $\theta_{1/2}$, defined as the spatial frequency at which the response variable – here, SNR – drops to one-half of its peak value. Thus, Equation 5.1 was set to one half of its maximum and rearranged for $x$ to estimate $\theta_{1/2}$ for each subject. The mean of $\theta_{1/2}$ was 0.33 octaves for younger subjects, and 0.28 octaves for older subjects (Table 5.1). The difference between the group means was not statistically significant, $t(18) = 1.08$, $p = 0.29$.

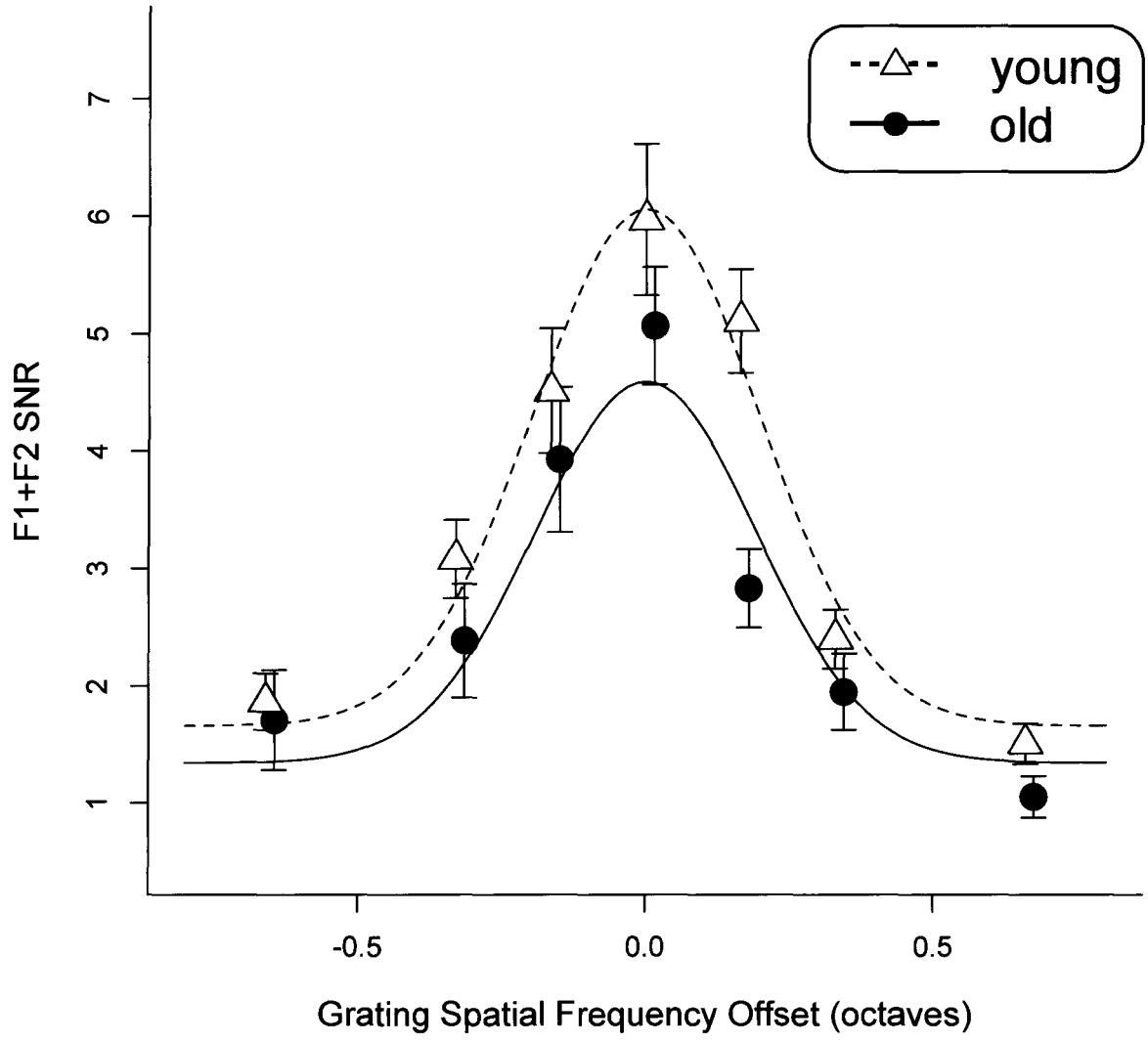


Figure 5.3: Mean F1+F2 SNRs for older and younger subjects are plotted as a function of target-mask spatial frequency offset. Error bars represent the ± one standard error of the mean. Equation 5.1 was fit to the average SNRs for each age group: the solid and dashed lines represent the best-fitting result for older and younger subjects, respectively. Older subjects' data, but not the curve, has been offset by 0.015 octaves along the x-axis for graphing visibility.

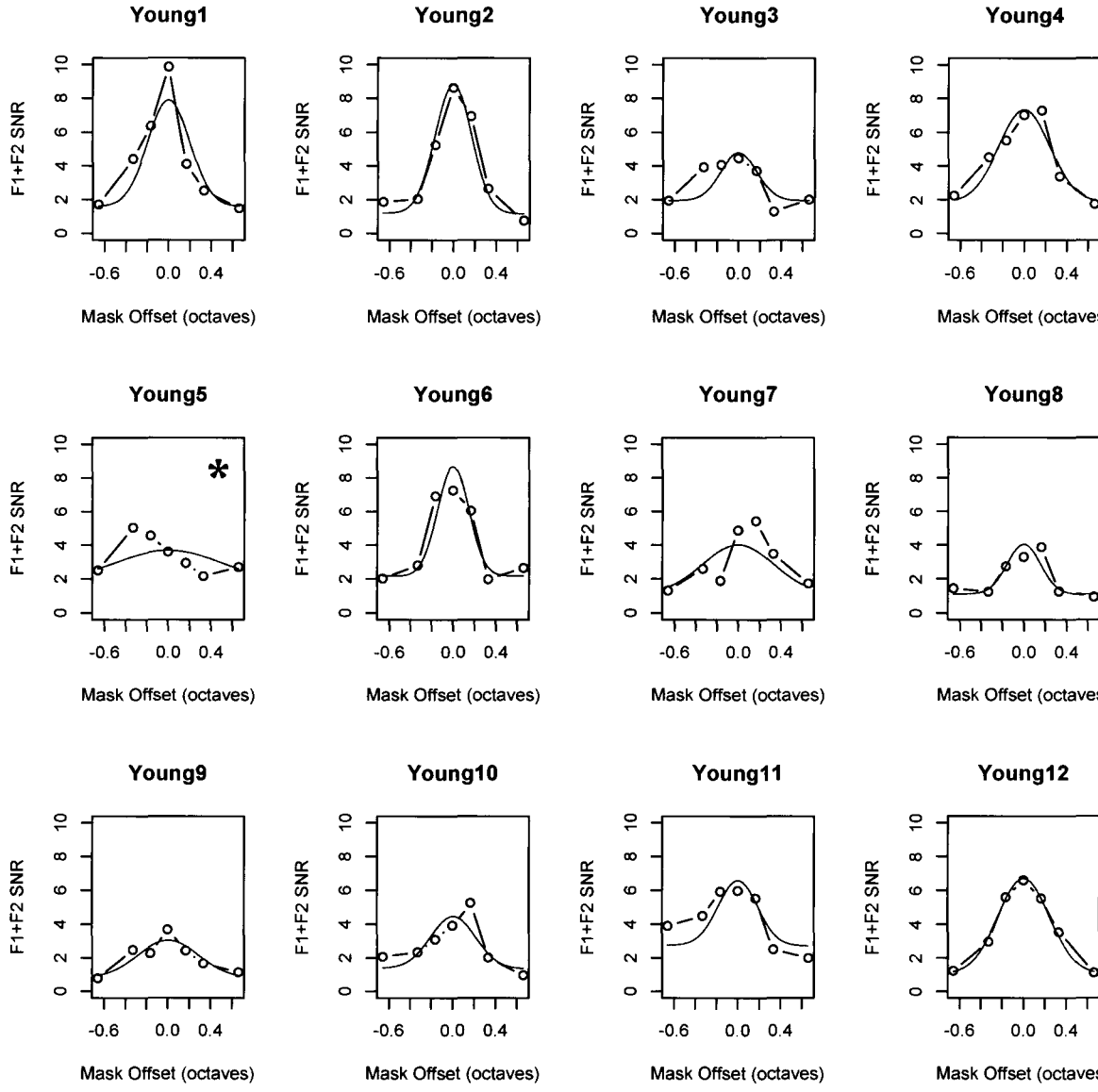


Figure 5.4: Individual results and curve-fits for all younger subjects. F1+F2 SNR is presented as a function grating SF-offset for each subject separately. The best-fit of Equation 5.1 is also plotted for each subject. Young subject number 5 was declared an outlier and is highlighted with an asterisk.

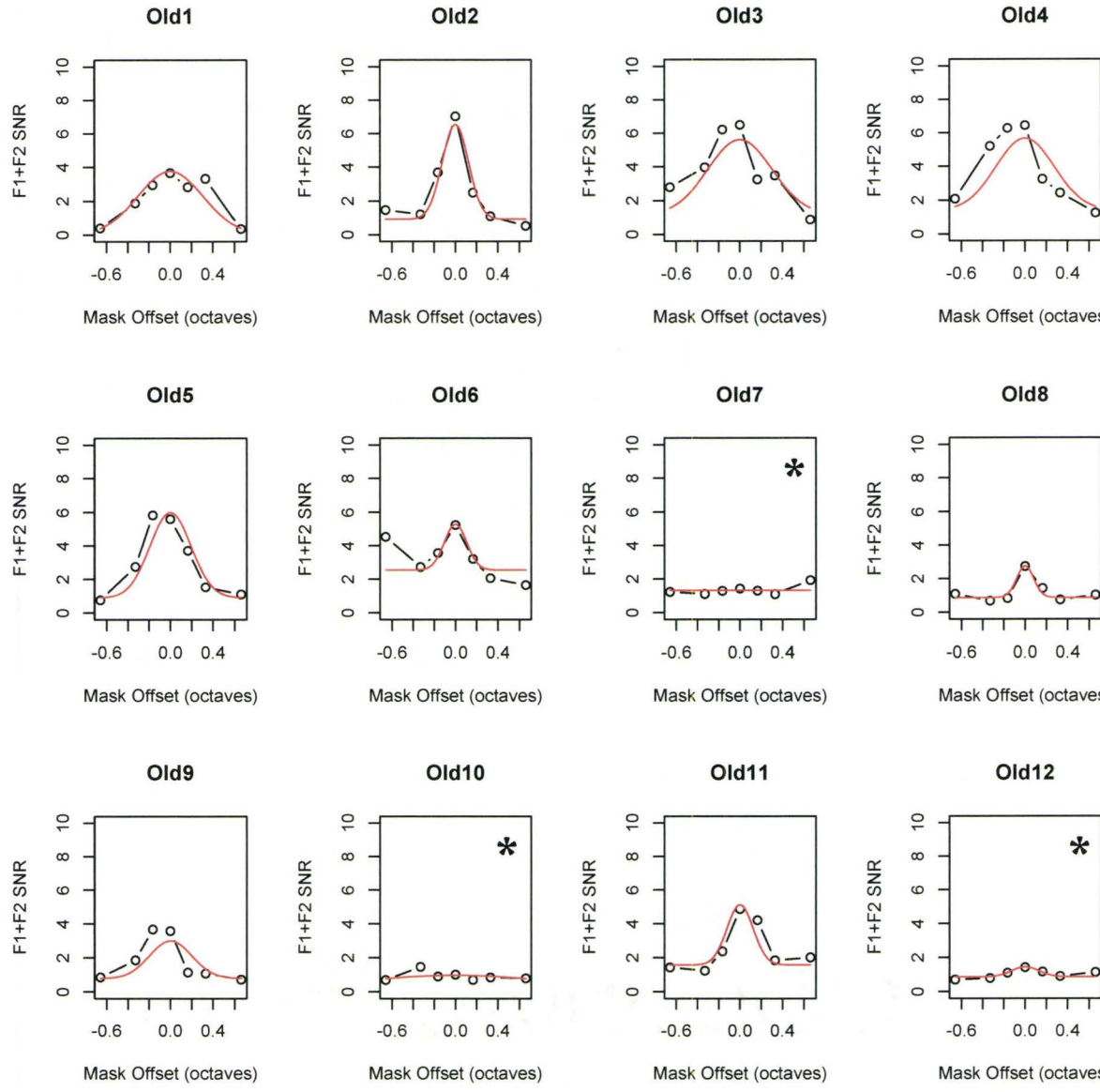


Figure 5.5: As in Figure 5.4, individual results and curve-fits for all older subjects. The three older subjects that were deemed outliers are highlighted with asterisks.

Table 5.1: Parameters $k$, $a$, $b$, and $\theta_{1/2}$ estimated from the F1+F2 tuning results.

| | younger subjects $\hat{\mu} \pm \hat{\sigma}_{\mu}$ | older subjects $\hat{\mu} \pm \hat{\sigma}_{\mu}$ | $p$-value |
|---|---|---|---|
| $k$ | $1.54 \pm 0.18$ | $1.12 \pm 0.23$ | 0.16 |
| $a$ | $4.49 \pm 0.56$ | $3.72 \pm 0.43$ | 0.29 |
| $b$ | $0.211 \pm 0.017$ | $0.190 \pm 0.029$ | 0.54 |
| $\theta_{1/2}$ | $\mathbf{0.326 \pm 0.0268}$ | $\mathbf{0.279 \pm 0.0348}$ | **0.29** |

**Outlier rejection** As numbered in Figures 5.5 and 5.4, older subject number 10 yielded a value of $\theta_{1/2}$ that was 2.68 SD's from their respective group mean. Young subject 5 and older subjects 7 and 12 yielded results such that there was no half-height half-width (i.e., $\theta_{1/2}$) solution for their best-fit curve; this is because their fit-curves are low and broad, and asymptote before dropping to half of their maximum. These four subjects were declared outliers and were excluded from all of the current analyses and figures (except, of course, for Figures 5.5 and 5.4). One could argue that rejection on the grounds that their curves were too flat to yield a value for $\theta_{1/2}$ is discarding what is actually a detuned response, perhaps related to the senescent single-cell detuning discussed, in part, to motivate the current study. However, these subjects did not yield a noticeable F1+F2 response, detuned or otherwise. Therefore, we rejected them on the grounds that, for whatever reason, we were unable to recover any significant signal from their EEG.

**Comparison to previous spatial frequency-tuning literature** The estimates of spatial frequency bandwidth from the current study are somewhat smaller than previous psychophysical and physiological estimates. Previous psychophysical studies (e.g., Stromeyer and Julesz, 1972; Stromeyer and Klein, 1974; Legge and Foley, 1980; Anderson and Burr, 1985; Govenlock et al., 2010) in which the target was a sine-wave grating and the high-contrast mask was either another grating or filtered noise, whose spatial frequency (content) was experimentally varied, have reported half-height half-widths in the range of 0.5 and 1.0 octaves (see discussion of Table 3.3 in Chapter 3). In two extensive single-cell surveys of V1 neurons in primates, researchers found median half-height half-width to be about 0.7 octaves (De Valois et al., 1982; Geisler and Albrecht, 1997). In the only previous use of the current two-grating ssVEP method to measure tuning, Regan and Regan (1988)

found half-height half-width to be about 0.5 octaves (estimated by visual inspection of Figure 3 of Regan & Regan). Averaged across age groups, in the current study we found half-height half-width to be 0.30 octaves as measured with F1+F2 intermodulation activity.

Because Regan and Regan (1988) reported tuning results for only one subject, it is difficult to say whether the current results are different from theirs, but it could be relevant that Regan and Regan (1988) used the 2F1+2F2 intermodulation term as the tuning response variable, instead of F1+F2. Regarding the difference between the current results and single-cell physiological results (e.g., Geisler and Albrecht, 1997), it could be that the F1+F2 ssVEP response is dominated by a more finely-tuned subset of the population of spatial frequency-selective visual cortex neurons. There is some suggestion that more finely-tuned spatial frequency-selective cells demonstrate heightened contrast sensitivity (see p552, De Valois et al., 1982), and thus may respond more vigorously to the current, 40% contrast stimulus component gratings, thereby dominating the ssVEP recorded at the scalp, than more broadly-tuned cells. That the current results find smaller bandwidths than previous psychophysical results may also be related to this idea: if psychophysical tuning is closer to the neuronal population average tuning, but the ssVEP is dominated by the most finely tuned neurons, then one would expect the currently observed ssVEP tuning to be sharper than that observed psychophysically.

**On the suitability of F1+F2 as a proxy for spatial frequency tuning** Due to its robust SNR and tuning-like response to the relative spatial frequencies of the flickering stimulus components, F1+F2 activity is an appealing signal to use as a proxy for average SF-tuning of visual cortex neurons. However, if the relative spatial phase of the two flickering components is set to 0 deg, as it was in the current study, the spatial frequency-offset is confounded with another property of the complex stimulus: maximum luminance or contrast energy. If the stimulus components are discretely, counter-phase flickered — as they were in the present study — there are four different states that the complex stimulus can take over the course of a trial: both components can be in their initial phase, both can be in their anti-phase, one can be in its initial phase and the other in its anti-phase, and vice versa. At small spatial frequency offsets, the maximum luminance and the contrast energy of these four states varies significantly, and therefore there is a time-varying luminance (and contrast energy) signal. A mechanism that responds to this signal would produce all of the harmonic and intermodulation frequencies observed in the current data. At large spatial frequency offsets, the amplitude of the luminance (and contrast energy) signal is very small, and therefore a mechanism responding to luminance

or contrast energy would produce little harmonic or intermodulation activity at large spatial frequency offsets. In other words, mechanisms sensitive to luminance or contrast energy could produce responses that were selective for spatial frequency, even though the mechanisms themselves lacked spatial frequency tuning. This means that F1+F2 activity may not be due to spatial frequency-selective mechanisms, which would confound its use in the current investigation of spatial frequency tuning.

In favour of a spatial frequency-selective model for the current F1+F2 results is the fact that the current bandwidths are somewhat comparable to those observed in previous physiological and psychophysical work (see *Comparison to previous spatial frequency-tuning literature*, above). However, to further determine if the data in Figure 5.3 were produced by a mechanism sensitive only to time-varying changes in maximum luminance and/or contrast, we calculated the amplitude of the luminance and contrast energy signals produced by our stimuli at a frequency of F1 + F2 Hz as a function of the spatial frequency offset between the mask and target gratings. Using maximum luminance or contrast energy yielded very similar results, so only the results based on the maximum luminance signal are reported. The amplitude of the time-varying luminance signal is greatest in the 0-octave offset condition, and declines as the spatial frequency of the mask is increased or decreased relative to the frequency of the target. The decrease in amplitude is slightly asymmetric: the half-height half-width (i.e., $\theta_{1/2}$) was $\approx 0.18$ and $\approx 0.23$ octaves for increases and decreases in the mask spatial frequency, respectively. The average of these two bandwidth estimates, 0.205 octaves, was smaller than the the average spatial frequency bandwidth measured on all subjects in our experiment ($M = 0.305$ octaves; $t(19) = 4.62$, $p < 0.001$). This result means that the current bandwidths observed for F1+F2 activity are broader than would be expected if F1+F2 activity were produced exclusively by a luminance-selective mechanism. Plotted in Figure 5.6 is F1+F2 SNR averaged across all subjects in both age groups. The normalized amplitude of the luminance signal, as well as the best-fitting Gaussian, are overlaid with the data.

Another way to determine the causal mechanism for the current F1+F2 results is to consider the activity produced at large SF-offsets. A luminance-selective model would produce less than 1/100th of its maximal activity at mask SF-offsets of -0.64 and +0.43 octaves (i.e., it asymptotes toward producing no energy whatsoever at approximately those offsets). As seen in Figure 5.3, except for older subjects in the +0.66 octave offset condition, the currently observed F1+F2 activity is significantly greater than an SNR of 1 (i.e., no activity) at all SF-offsets, suggesting that F1+F2 activity is produced at some low level by broadly-tuned SF-selective mechanisms at large offsets.

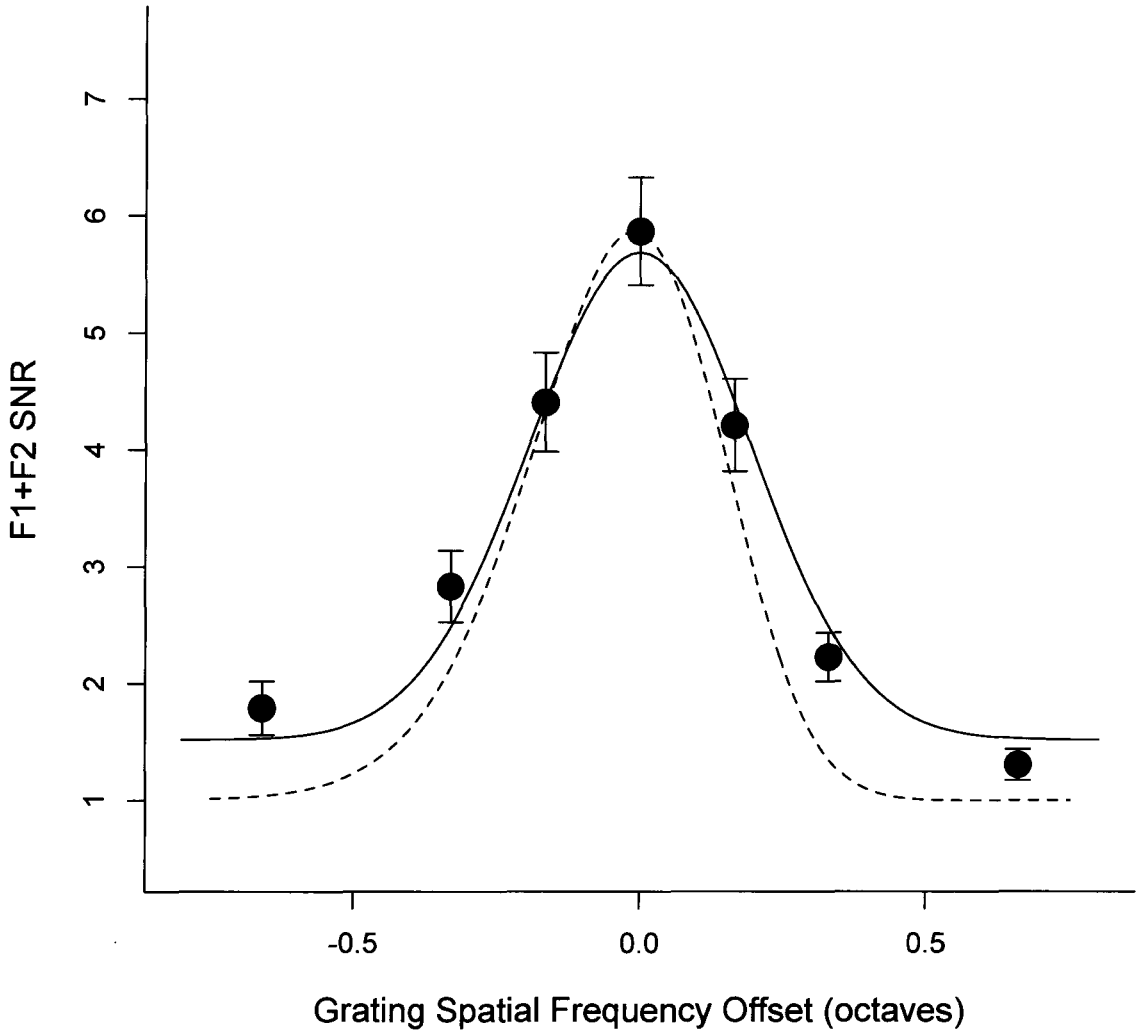


Figure 5.6: Model comparison of F1+F2 SNR. The data points and error bars represent the mean and ± one standard error of F1+F2 SNR for all subjects (i.e., the same data as in Figure 5.3, but collapsed across age group). The DASHED line shows the amplitude of the time-varying maximum luminance signal at F1+F2, normalized by the observed SNR in the 0 octave condition. The SOLID line represents the best-fitting Gaussian (i.e., Equation 5.1), which represents a model that is selective for spatial frequency, *perse*.

In sum, the currently observed F1+F2 results are not well-modelled exclusively by a luminance-selective mechanism, and are somewhat comparable to previous spatial frequency tuning results. It seems plausible, however, that the current results are due to some combination of luminance-selective and spatial frequency-selective mechanisms. Further experimentation and modelling will be required to more clearly delineate the contributions of each type of mechanism.

**2F1+2F2 results** Setting the relative spatial phase of the two flickering gratings to 90 deg eliminates the time-varying luminance and contrast energy signals at all temporal frequencies because, for all spatial frequency offsets, the maximum luminance and contrast energy are constant across all four possible states of the complex pattern. Regan and Regan (1988) manipulated the relative spatial phase of the two flickering gratings and found that F1+F2 activity was significantly reduced at 90 deg relative spatial phase, which is consistent with the hypothesis that luminance and/or contrast energy contributed significantly to the response at that temporal frequency. However, they found that amplitude of the response at 2F1+2F2 was approximately independent of spatial phase, and therefore Regan and Regan suggested that the response at 2F1+2F2 was a better measure of spatial frequency selectivity.

2F1+2F2 SNR was measured for each subject in each condition with the same methods used to estimate F1+F2 SNR. Only subjects not already declared outliers based on their F1+F2 results were included in this analysis. Figure 5.7 plots 2F1+2F2 SNR as a function of spatial frequency offset and age group. A comparison of Figures 5.3 and 5.7 indicates that 2F1+2F2 activity was weaker than F1+F2 activity. Nonetheless, there is significant 2F1+2F2 activity (i.e., SNR $> 1$) in all conditions for younger subjects, and in five of seven conditions in older subjects (1-tailed t-tests, $\alpha = 0.05$). The data from both age groups does seem to depend on spatial frequency offset, but the tuning is weak, and the Gaussian curve-fits are not as good as they were for F1+F2 activity. A 2 (age) by 7 (offset condition) ANOVA on these 2F1+2F2 SNR results found a significant main effect of age condition [$F(1,18) = 7.97$, $p < 0.05$], but no effect of condition [$F(6,108) = 1.74$, $p = 0.12$] and no age $\times$ condition interaction [$F(6,108) = 1.42$, $p = 0.21$]. Regarding the present investigation of whether spatial frequency selective mechanisms are more broadly tuned in older age, given the lack of an ANOVA interaction effect, and the narrower bandwidth of the best-fitting Gaussian to the mean older SNRs (Figure 5.7), there is no indication that older subjects' 2F1+2F2 activity is more broadly tuned than younger subjects.

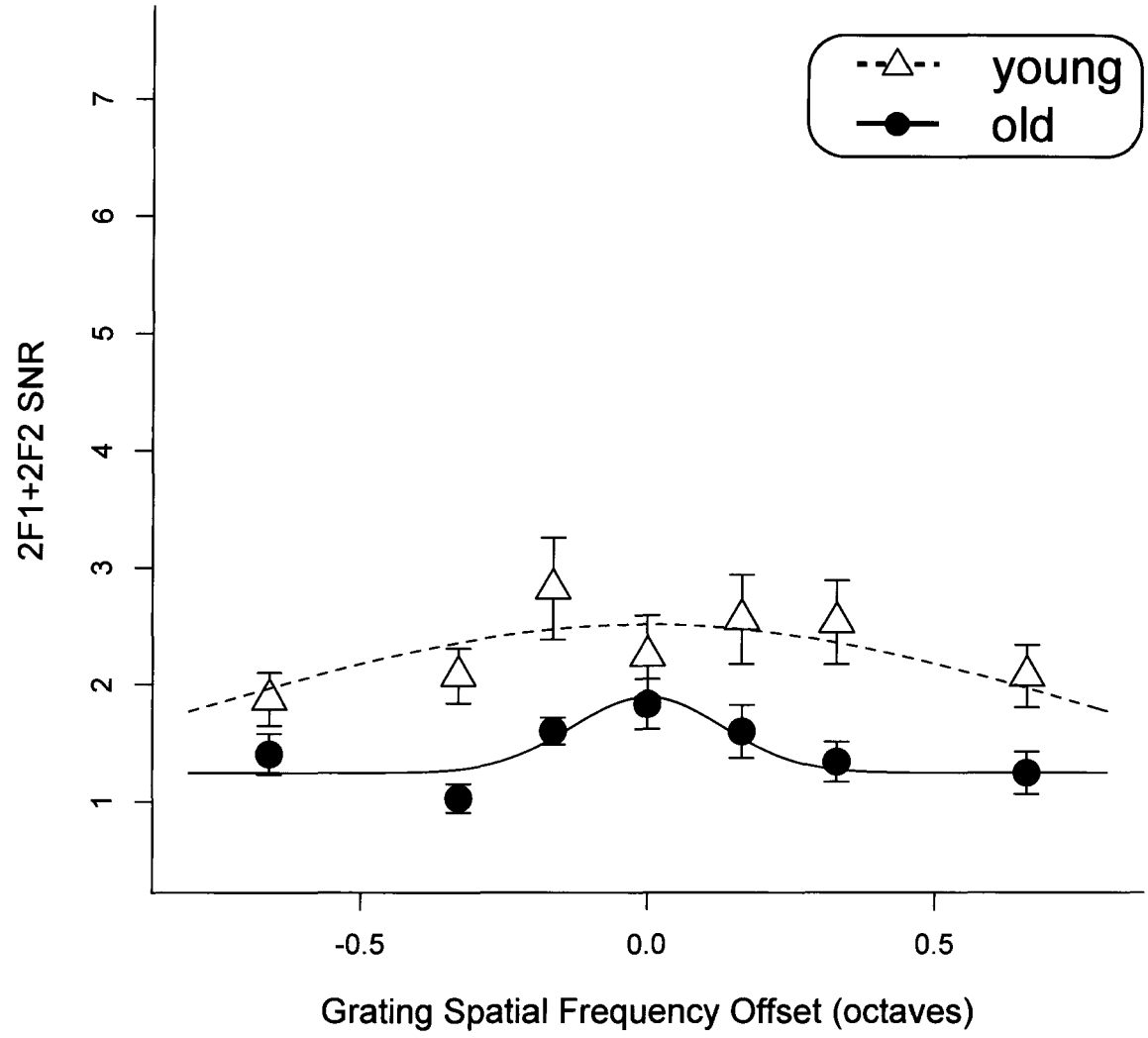


Figure 5.7: 2F1+2F2 tuning. Mean 2F1+2F2 SNRs for older and younger subjects are plotted as a function of target-mask spatial frequency offset condition. Error bars represent the standard errors of the means. Equation 5.1 was fit to the average SNRs for each age group; the solid and dashed lines represent the best-fitting result for older and younger subjects, respectively.

## 5.4 Discussion

**Cortical spatial frequency tuning is preserved with age** Single-cell studies of age-related changes in primate visual cortical neurons have found evidence of broader orientation tuning (Schmolesky et al., 2000; Leventhal et al., 2003; Yu et al., 2006) and decreases in the ratio of preferred spatial frequency to spatial resolution (Zhang et al., 2008). Leventhal et al. (2003) implicated reduced GABAergic inhibition – which is thought to be necessary for the degree of stimulus selectivity observed in V1 neurons – as the cause for this age-related decline. These findings raise the possibility that low-level visual mechanisms tuned for spatial frequency become detuned in older age, which could explain age-related deficits for complex form vision (e.g., Boutet and Faubert, 2006; Del Viva and Agostini, 2007; Roudaia et al., 2008). In the current study, we measured the effect of age on the tuning of the population response of spatial frequency-selective visual cortex neurons using intermodulation activity that arises in the ssVEP when two flickering stimuli are presented simultaneously (Regan and Regan, 1988; Candy et al., 2001). The tuning of `F1+F2` and `2F1+2F2` intermodulation activity did not differ between older and younger subjects, suggesting that cortical spatial frequency tuning is preserved in older age in humans. The current results are consistent with psychophysical studies of the spatial frequency selectivity of pattern masking (Govenlock et al., 2010).

Given reports of detuned single-cell neurophysiology (e.g., Zhang et al., 2008), but tuned behaviour (Govenlock et al., 2010), if the current experiment had found an effect of age on the average tuning of awake, behaving humans, this would have supported the idea that perception of spatial frequency, in older age, may adaptively rely on a subset of cells that retain fine tuning (i.e., outlying cells on the finely-tuned tail of a distribution that is detuned on average). Indeed, there is evidence for such subset-monitoring models of perception (Barlow, 1972, 2009) of, for example, visual motion (Newsome et al. 1990, 1995, but cf., Shadlen et al. 1996; Britten et al. 1996) and tactile (e.g., LaMotte and Mountcastle, 1975; Recanzone et al., 1992; Vallbo, 1995) perception. However, because we found no effect of age for the current measure of the population response for spatial frequency tuning in visual cortex, there is no need to favour such a subset-monitoring explanation for maintained psychophysical spatial frequency tuning in older age.

**Reconciling senescent primate V1 functional decline with maintenance of psychophysical and ssVEP spatial frequency tuning in older humans** There are at least two explanations for the discrepancy between the functional decline of senescent

primate single-cells, and the maintenance of tuning in older humans behaviourally and electrophysiologically (ssVEP). One possibility is that there is a interaction between age and the global anesthetic in the aforementioned single-cell studies that leads to a decline in the function of senescent single-cells that is not due to senescence, *per se*. Although the specific interaction is still debated, the sedatives and anesthetic used in those single-cell studies, typically ketamine and halothane, are known to interact with GABAergic mechanisms (e.g., Cheng and Brunner, 1981; Tanelian et al., 1993; Hevers et al., 2008). Because the biochemical action of anesthetics, and the relevant changes that occur in senescence, are both poorly understood, it is difficult to address this concern. However, both Wang et al. (2005) and Zhang et al. (2008) performed a control experiment and found that the level of anesthetic employed did not affect V1 or V2 neurons' functional selectivity, supporting the idea that their findings are due to senescence, rather than an interaction between senescence and the anesthetic agents.

Another possibility for this discrepancy is that older humans do have neurons that are otherwise detuned, but by virtue of focused attention or consciousness, older humans are adaptively able to tune their neurons in an on-line, ad hoc fashion. It is well established that the deployment of attention improves performance on perceptual tasks (e.g., Yeshurun and Carrasco, 1998). How these attentional benefits are instantiated neurophysiologically, and how they interact with older age, however, is not clear. In young adult primate models, attention does not seem to sharpen the tuning of visual neurons, but does increase the responsiveness of neurons, which can lead to better discriminatory performance in these neurons along the stimulus dimension to which they are selective (Treue and Maunsell, 1999; McAdams and Maunsell, 1999; McAdams and Reid, 2005). Further, in humans, attention does positively-modulate the amplitude of the ssVEP (e.g., Hillyard et al., 1997; Di Russo and Spinelli, 1999) and event-related potentials (ERPs) in response to visual stimuli (e.g., Müller and Hillyard, 2000), the magnitude of the BOLD response in V1 (Smith et al., 2006), and, perhaps most relevantly, the tuning of the V1 BOLD response with respect to stimulus spatial position (Fischer and Whitney, 2009).

Several studies have shown that underlying patterns of brain activity that are correlated with performance on simple visual tasks can differ significantly between older and younger subjects, even in the absence of age differences in behavioural measures of performance (McIntosh et al., 1999; Della-Maggiore et al., 2000; Bennett et al., 2001). In these studies, older subjects had significantly higher PET activation in frontal cortical regions than younger subjects. Younger and older subjects also exhibited different patterns of functional connectivity between frontal areas and visual cortex. These neural differences could reflect

age-related compensatory deployment of attention whereby higher brain areas may be brought online to compensate for declining function in primary visual cortex. If older humans' visual cortex neurons are detuned while in an unattended state as a function of senescence, but are tuned by focused attention when needed, then future experiments diverting subjects' deployment of attention while viewing the current steady-state stimulus might yield broader tuning functions in older subjects.

**Conclusion** Despite several reported functional declines of V1 and V2 neurons in single-cell studies of senescent primates, older age does not affect human psychophysical spatial frequency tuning (Govenlock et al., 2010), nor does it affect average neural spatial frequency tuning as measured with the ssVEP in the current study. Thus, the current results do not support the notion that awake, behaving, attending older humans have detuned neurons, and that they are able to compensate for this by selectively monitoring a subset of neurons that retain fine, young-like tuning. Rather, unless there is a to-be-determined interaction between senescence and anesthesia affecting the functional performance of visual neurons in the primate models of aging, it is possible that older humans are able to improve the tuning their spatial frequency-selective visual cortex neurons by virtue of focussed attention or consciousness.

**Acknowledgements**

This research was supported by the Canada Research Chairs program, of which PJB and ABS are members, a grant from the Canadian Institutes of Health Research (CIHR) to PJB and ABS, a Natural Sciences and Engineering Research Council of Canada Postgraduate Scholarship to SWG, and the CIHR Strategic Training Grant on Communication and Social Interaction in Healthy Aging. Portions of this work will be presented at the annual meeting of the Vision Sciences Society (Naples, FL U.S.A, May 2010).

# References

Anderson, S. J., Burr, D. C., 1985. Spatial and temporal selectivity of the human motion detection system. Vision Research 25 (8), 1147–1154.

Appelbaum, L. G., Wade, A. R., Pettet, M. W., Vildavski, V. Y., Norcia, A. M., 2008. Figure-ground interaction in the human visual cortex. J Vis 8 (9), 8.1–19.

Barlow, H. B., 1972. Single units and sensation: a neuron doctrine for perceptual psychology? Perception 1 (4), 371–94.

Barlow, H. B., 2009. Single units and sensation: a neuron doctrine for perceptual psychology? Perception 38 (6), 795–8.

Bennett, P. J., Sekuler, A. B., McIntosh, A. R., Della-Maggiore, V., 2001. The effects of aging on visual memory: Evidence for functional reorganization of cortical networks. Acta Psychologica 107 (1-3), 249–273, aLLISON.

Boutet, I., Faubert, J., 2006. Recognition of faces and complex objects in younger and older adults. Memory and Cognition 34 (4), 854–864.

Brainard, D. H., 1997. The psychophysics toolbox. Spat Vis 10 (4), 433–436.

Britten, K. H., Newsome, W. T., Shadlen, M. N., Celebrini, S., Movshon, J. A., 1996. A relationship between behavioral choice and the visual responses of neurons in macaque mt. Vis Neurosci 13 (1), 87–100.

Campbell, F. W., Cooper, G. F., Enroth-Cugell, C., Jul 1969. The spatial selectivity of the visual cells of the cat. J Physiol 203 (1), 223–35.

Candy, T. R., Skoczenski, A. M., Norcia, A. M., Jun 2001. Normalization models applied to orientation masking in the human infant. J Neurosci 21 (12), 4530–41.

Cheng, S. C., Brunner, E. A., Jul 1981. Inhibition of gaba metabolism in rat brain slices by halothane. Anesthesiology 55 (1), 26–33.

Clementz, B. A., Wang, J., Keil, A., Dec 2008. Normal electrocortical facilitation but abnormal target identification during visual sustained attention in schizophrenia. J Neurosci 28 (50), 13411–8.

Crum, R. M., Anthony, J. C., Bassett, S. S., Folstein, M. F., 1993. Population-based norms for the mini-mental state examination by age and education level. Journal of the American Medical Association 269, 2386–2391.

De Valois, R. L., Albrecht, D. G., Thorell, L. G., 1982. Spatial frequency selectivity of cells in macaque visual cortex. Vision Res 22 (5), 545–59.

Del Viva, M. M., Agostini, R., 2007. Visual spatial integration in the elderly. Investigative Ophthalmology and Vision Science 48 (6), 2940–2946.

Delahunt, P., Hardy, J., Werner, J., 2008. The effect of sensescence on orientation discrimination and mechanism tuning. Journal of Vision 8 (3), 1–9.

Della-Maggiore, V., Sekuler, A. B., Grady, C. L., Bennett, P. J., Sekuler, R., McIntosh, A. R., 2000. Corticolimbic interactions associated with performance on a short-term memory task are modified by age. Journal of Neuroscience 20, 8410–8416, aLLISON.

Di Russo, F., Pitzalis, S., Aprile, T., Spitoni, G., Patria, F., Stella, A., Spinelli, D., Hillyard, S. A., 2007. Spatiotemporal analysis of the cortical sources of the steady-state visual evoked potential. Human Brain Mapping 28, 323–334.

Di Russo, F., Spinelli, D., 1999. Physiological evidence for an early attentional mechanism in visual processing in humans. Vision Research 39, 2975–2985.

Ding, J., Sperling, G., Srinivasan, R., Jul 2006. Attentional modulation of ssvep power depends on the network tagged by the flicker frequency. Cereb Cortex 16 (7), 1016–29.

Ferster, D., Miller, K. D., 2000. Neural mechanisms of orientation selectivity in the visual cortex. Annu Rev Neurosci 23, 441–71.

Fischer, J., Whitney, D., 2009. Attention narrows position tuning of population responses in v1. Current Biology 19, 1356–1361.

Geisler, W. S., Albrecht, D. G., 1997. Visual cortex neurons in monkeys and cats: detection, discrimination, and identification. Vis Neurosci 14 (5), 897–919.

Gold, J. I., Shadlen, M. N., 2007. The neural basis of decision making. Annu Rev Neurosci 30, 535–74.

Govenlock, S. W., Sekuler, A. B., Bennett, P. J., in preparation. Orientation tuning in human visual cortex in normal aging. (cite VSS poster if necessary).

Govenlock, S. W., Taylor, C. P., Sekuler, A. B., Bennett, P. J., 2009. The effect of aging on the orientational selectivity of the human visual system. Vision Research 49, 164–172.

Govenlock, S. W., Taylor, C. P., Sekuler, A. B., Bennett, P. J., 2010. The effect of aging on the spatial frequency selectivity of the human visual system. Vision Research 17, 1712–1719.

Habak, C., Wilkinson, F., Wilson, H. R., 2008. Aging disrupts the neural transformations that link facial identity across views. Vision Res 48 (1), 9–15.

Herbert, A. M., Overbury, O., Singh, J., Faubert, J., 2002. Aging and bilateral symmetry detection. Journal of Gerontology Series B: Psychological Science and Social Sciences 57, P241–P245.

Hevers, W., Hadley, S. H., Lüddens, H., Amin, J., May 2008. Ketamine, but not phencyclidine, selectively modulates cerebellar gaba(a) receptors containing alpha6 and delta subunits. J Neurosci 28 (20), 5383–93.

Hillyard, S., Hinrichs, H., Tempelmann, C., Morgan, S., Hansen, J., Scheich, H., Heinze, H., 1997. Combining steady-state visual evoked potentials and fmri to localize brain activity during selective attention. Human Brain Mapping 5 (4), 287–292.

Kuffler, S. W., 1953. Discharge patterns and functional organization of mammalian retina. J Neurophysiol 16 (1), 37–68.

LaMotte, R. H., Mountcastle, V. B., May 1975. Capacities of humans and monkeys to discriminate vibratory stimuli of different frequency and amplitude: a correlation between neural events and psychological measurements. J Neurophysiol 38 (3), 539–59.

Legge, G., Foley, J. M., 1980. Contrast masking in human vision. Journal of the Optical Society of America. A, Optics, Image science, and Vision 70 (12), 1458–1471.

Leventhal, A. G., Wang, Y., Pu, M., Zhou, Y., Ma, Y., 2003. GABA and its agonists improved visual cortical function in senescent monkeys. Science 300, 812–815.

Maffei, L., Fiorentini, A., Jul 1973. The visual cortex as a spatial frequency analyser. Vision Res 13 (7), 1255–67.

Mantyjarvi, M., Laitinen, T., 2001. Normal values for the pelli-robson contrast sensitivity test. Journal of Cataract and Refractive Surgery 27 (2), 261–266.

Maxwell, S., Delaney, H., 2004. Designing Experiments and Analyzing Data: A Model Comparison Approach, 2nd Edition. Lawrence Erlbaum Associates, Mahwah, New Jersey.

McAdams, C. J., Maunsell, J. H. R., 1999. Effects of attention on the reliability of individual neurons in monkey visual cortex. Neuron 23, 765–773.

McAdams, C. J., Reid, R. C., 2005. Attention modulates the responses of simple cells in monkey primary visual cortex. J Neurosci 25 (47), 11023–33, dEDA.

McIntosh, A. R., Sekuler, A. B., Penpeci, C., Rajah, M. N., Grady, C. L., Sekuler, R., Bennett, P. J., 1999. Recruitment of unique neural systems to support visual memory in normal aging. Current Biology 9, 1275–1278, aLLISON.

Müller, M. M., Hillyard, S., Sep 2000. Concurrent recording of steady-state and transient event-related potentials as indices of visual-spatial selective attention. Clin Neurophysiol 111 (9), 1544–52.

Müller, M. M., Hübner, R., Mar 2002. Can the spotlight of attention be shaped like a doughnut? evidence from steady-state visual evoked potentials. Psychol Sci 13 (2), 119–24.

Müller, M. M., Malinowski, P., Gruber, T., Hillyard, S. A., Jul 2003. Sustained division of the attentional spotlight. Nature 424 (6946), 309–12.

Newsome, W. T., Britten, K. H., Salzman, C. D., Movshon, J. A., 1990. Neuronal mechanisms of motion perception. Cold Spring Harb Symp Quant Biol 55, 697–705.

Newsome, W. T., Shadlen, M. N., Zohary, E., Britten, K. H., Movshon, J. A., 1995. Visual motion: linking neuronal activity to psychophysical performance. In: Gazzaniga, M. S. (Ed.), The Cognitive Neurosciences. MIT Press: Cambridge MA, Ch. 25, pp. 401–414.

Parker, A. J., Newsome, W. T., 1998. Sense and the single neuron: Proving the physiology of perception. Annual Review of Neuroscience 21, 227–277.

Pelli, D., Robson, J., Wilkins, A., 1988. The design of a new chart for measuring contrast sensitivity. Clinical Vision Sciences 2 (3), 187–199.

Pelli, D. G., 1997. The videotoolbox software for visual psychophysics: Transforming numbers into movies. Spatial Vision 10, 437–442.

R Development Core Team, 2009. R: A Language and Environment for Statistical Computing. R Foundation for Statistical Computing, Vienna, Austria.
URL `http://www.R-project.org`

Recanzone, G. H., Merzenich, M. M., Schreiner, C. E., May 1992. Changes in the distributed temporal response properties of si cortical neurons reflect improvements in performance on a temporally based tactile discrimination task. J Neurophysiol 67 (5), 1071–91.

Regan, D., Regan, M., 1988. Objective evidence for phase-independent spatial frequency analysis in the human visual pathway. Vision Rsearch 28 (1), 187–191.

Regan, D., Regan, M. P., 1987. Nonlinearity in human visual resonses to two-dimensional patterns, and a limitation of fourier methods. Vision Rsearch 27 (12), 2181–2183.

Ringach, D. L., Bredfeldt, C. E., Shapley, R. M., Hawken, M. J., Feb 2002. Suppression of neural responses to nonoptimal stimuli correlates with tuning selectivity in macaque v1. J Neurophysiol 87 (2), 1018–27.

Rodieck, R. W., Stone, J., Sep 1965. Analysis of receptive fields of cat retinal ganglion cells. J Neurophysiol 28 (5), 832–49.

Roudaia, E., Bennett, P., Sekuler, A., 2008. The effect of aging on contour integration. Vision Research 48, 2767–2774.

Schmolesky, M. T., Wang, Y., Pu, M., Leventhal, A. G., 2000. Degradation of stimulus selectivity of visual cortical cells in senescent rhesus monkeys. Nature Neuroscience 3, 384–390.

Shadlen, M. N., Britten, K. H., Newsome, W. T., Movshon, J. A., Feb 1996. A computational analysis of the relationship between neuronal and behavioral responses to visual motion. J Neurosci 16 (4), 1486–510.

Smith, A., Cotillon-Williams, N., Williams, A., 2006. Attentional modulation in the human striate cortex: The time-course of the bold response and its implications. Neuroimage 29, 328–334.

So, Y. T., Shapley, R., Jan 1981. Spatial tuning of cells in and around lateral geniculate nucleus of the cat: X and y relay cells and perigeniculate interneurons. J Neurophysiol 45 (1), 107–20.

Stanford, T., Pollack, R. H., 1984. Configuration color vision tests: the interaction between aging and the complexity of figure-ground segregation. J Gerontol 39 (5), 568–571.

Stromeyer, C. F. r., Julesz, B., 1972. Spatial-frequency masking in vision: critical bands and spread of masking. Journal of the Optical Society of America. A, Optics, Image science, and Vision 62, 1221–1232.

Stromeyer, C. F. r., Klein, S., 1974. Spatial frequency channels in human vision as asymmetric (edge) mechanisms. Vision Research 14, 1409–1420.

Sutoyo, D., Srinivasan, R., Jan 2009. Nonlinear ssvep responses are sensitive to the perceptual binding of visual hemifields during conventional 'eye' rivalry and interocular 'percept' rivalry. Brain Res 1251, 245–55.

Tanelian, D. L., Kosek, P., Mody, I., MacIver, M. B., Apr 1993. The role of the gabaa receptor/chloride channel complex in anesthesia. Anesthesiology 78 (4), 757–76.

Treue, S., Maunsell, J. H., Sep 1999. Effects of attention on the processing of motion in macaque middle temporal and medial superior temporal visual cortical areas. J Neurosci 19 (17), 7591–602.

Vaegan, Rahman, A. M. A., Sanderson, G. F., Jul 2008. Glaucoma affects steady state vep contrast thresholds before psychophysics. Optom Vis Sci 85 (7), 547–58.

Vallbo, A. B., 1995. Single-afferent neurons and somatic sensation in humans. In: Gazzaniga, M. S. (Ed.), The Cognitive Neurosciences. MIT Press: Cambridge MA, Ch. 14, pp. 237–252.

Wang, Y., Wang, R., Gao, X., Hong, B., Gao, S., Jun 2006. A practical vep-based brain-computer interface. IEEE Trans Neural Syst Rehabil Eng 14 (2), 234–9.

Wang, Y., Zhou, Y., Ma, Y., Leventhal, A., 2005. Degradation of signal timing in cortical areas V1 and V2 of senescent monkeys. Cerebral Cortex 15 (15), 403–408.

Yeshurun, Y., Carrasco, M., 1998. Attention improves or impairs visual performance by enhancing spatial resolution. Nature 396 (6706), 72–5.

Yu, S., Wang, Y., Li, X., Zhou, Y., Leventhal, A. G., 2006. Functional degradation of extrastriate visual cortex in senescent rhesus monkeys. Neuroscience 140, 1023–1029.

Zhang, J., Wang, X., Wang, Y., Fu, Y., Liang, Z., Ma, Y., Leventhal, A. G., 2008. Spatial and temporal sensitivity degradation of primary visual cortical cells in senescent rhesus monkeys. European Journal of Neuroscience 28, 201–207.

Zhu, W., Xing, D., Shelley, M., Shapley, R., 2010. Correlation between spatial frequency and orientation selectivity in v1 cortex: Implications of a network model. Vision Research in press doi:10.1016/j.visres.2010.01.007.

# Chapter 6

# General Discussion

The research conducted for the current dissertation investigated the effect of normal aging on the selectivity of lower-level visual mechanisms that register information about the orientation and spatial frequency at which luminance changes across the visual scene. Given the inevitability of internal response variability, or noise, this selectivity is positively related to the amount of information that these mechanisms convey to higher-level visual processes that are responsible for the final stages of visual perception. This research was motivated by several reports of functional changes in senescent visual neurons that are thought to underlie these lower-level mechanisms (e.g., Schmolesky et al., 2000), as well as reports of age-related changes in the perception of complex visual forms (e.g., Habak et al., 2008), which could have been due to a decline in the informativeness of lower-level mechanisms. Over the course of several psychophysical and electrophysiological experiments, I found no indication that the selectivity of these orientation- and spatial frequency-selective mechanisms declines in normal aging.

## 6.1 Age-related compensatory reorganization

Given age-related declines for the perception of complex visual forms, the current results support the notion that higher-level mechanisms, but not lower-level mechanisms, are affected by age. This hypothesis raises questions about how it is possible for aging to affect some brain structures or processes, but not others. There are some instances of selective age-related loss: as mentioned previously, rods, but not cones, seem to be affected by age, and it is common for cells in the substantia nigra to degenerate in older

age (i.e., Parkinson's disease) whereas other brain structures seem to remain unaffected. However, more parsimoniously, and perhaps more in accord with the evolved nature of the brain[1], is the notion that the brain undergoes some amount of widespread, diffuse degradation into older age, both physiologically and anatomically.

In this scenario — the idea that the brain declines diffusely in older age — the fact that aging affects performance on complex but not simple tasks could be explained by the idea that higher-level processes and resources are brought to bear on simple tasks, to compensate for declines in low-level mechanisms. Indeed, several neuroimaging studies have shown that, given a simple visual task, although older and younger adults perform equivalently, older adults demonstrate significantly different patterns of underlying brain activity, which may be evidence for age-related compensatory reorganization (e.g., McIntosh et al., 1999; Bennett et al., 2001; Reuter-Lorenz and Lustig, 2005). If older adults are "mentally squinting," so to speak, and are bringing higher, more frontal brain resources to bear in order to compensate for declining lower-level mechanisms, then those higher level mechanisms—(a) because they are being co-opted to support lower-level mechanisms, and (b) having, themselves, been subject to some age-related decline—will have a lessened capacity to deal with complex visual tasks or stimuli. As it relates to the visual pathway, this hypothesis has been developed by Faubert (2002) and is supported by experiments in which an effect of older age emerges only when visual stimulus or task complexity exceeds some threshold, at which, it stands to reason, the compensatory action of higher-level mechanisms has been exhausted (e.g., Habak and Faubert, 2000; Faubert and Bellefeuille, 2002). In a general way, this hypothesis is supported an age-related decline for any complex visual perception. This hypothesis is also supported by the fact that adults report that visual perception becomes more effortful for complex stimuli and

[1]With respect to aging and evolution, Dawkins (1995), among others, has related a story paraphrased as follows: After several years of Model A and T automobile production, Henry Ford reportedly sent his engineers to examine cars that had outlived their usefulness and were resting in junkyards. The engineers were to report back on the matter of which parts were *not* responsible for the break-down of the cars. Those parts that were unaffected by older age, Ford argued, had in fact been made *too well.* The manufacturing resources (e.g., labour, design, the cost and quality of the materials) that had been committed to making those parts were to be reduced; the surplus resources were then to be reallocated to the parts of the car that were actually declining in older age so that the whole car might be made to last longer, given a constant total expenditure of resources. To the extent that evolution by natural selection also works economically, one might expect the different parts of the aged brain and body to decline at approximately the same rate. Any mutation that caused bodily resources to be reallocated from parts that were outlasting the rest of the organism to parts that were causing its demise would confer an adaptive advantage to that organism insofar as that organism might live longer to care for its descendants. This discussion, however, should be qualified by the notion that natural selection likely has not had sufficient opportunity to exert any influence on what we now call old age: humans did not typically live beyond the age of 30 or 40 until very recently in our evolutionary history.

tasks as they get older (Sekuler and Sekuler, 2000). For a review of this age-related compensatory reorganization theory as it relates not just to vision but to other mental faculties as well, see Reuter-Lorenz and Lustig (2005) and Park and Reuter-Lorenz (2009).

As discussed in previous chapters, one way that this compensation for an age-related decline in the function of lower-level mechanisms might be achieved is by an increasing reliance on what might be the compensatory action of focused attention in older age — which one might loosely equate with those higher-level mechanisms — to (A) improve the selectivity of their otherwise poorly-selective orientation- and spatial frequency-selective mechanisms, or to (B) selectively monitor a subset of the neurons comprising those low-level mechanisms that maintain high selectivity into older age. In single-cell physiological experiments, attention has been shown to affect the response properties of V4 (Haenny et al., 1988) and V1 (McAdams and Reid, 2005) neurons, although attention does not seem to affect the selectivity of those neurons, *per se* (McAdams and Maunsell, 1999). This latter null result may be due to a floor effect in younger adult, highly-selective neurons, though—the effect of attention on such single-cell selectivity has not yet been investigated in senescent animals. Several neuroimaging experiments with humans show attentional modulation of EEG (e.g., Hillyard et al., 1997; Müller et al., 1998; Di Russo and Spinelli, 1999; Müller and Hillyard, 2000; Müller et al., 2003, 2006) and BOLD (e.g., Smith et al., 2006; Fischer and Whitney, 2009) activity in the visual cortex. Behaviourally, attention is known to improve performance for a plethora of simple visual tasks (e.g., Yeshurun and Carrasco, 1998, 1999; Carrasco et al., 2000). In future experiments, if we increase the attentional load required of older subjects as they perform our behavioural tasks (in Chapters 2 and 3) or view our EEG stimulus (in Chapters 4 and 5), in case (A) (from above), we would observe a decline in both behavioural and ssVEP-measured selectivity, and in case (B), we would observe a decline in behavioural, but not ssVEP-measured selectivity.

## 6.2 Investigating intermediate-level visual mechanisms

Although the current dissertation found no evidence that selectivity of lower-level visual mechanisms for orientation and spatial frequency declines in normal aging, it is possible that an effect of aging emerges for what might be an immediately higher level mechanism in the visual processing hierarchy, wherein localized orientation and spatial frequency information is integrated across space, and across orientations and spatial

frequencies. This integration contributes to the perception of textures and contours that define figure-ground boundaries and also characterize the interiors of the figure or ground regions of the visual scene. In experiments that might be considered an extension of those included in this dissertation, I have begun to investigate the effect of older age on the integration of localized orientation signals.

Orientation grouping is the position-specific integration of spatially-disparate, localized orientation signals, which contributes to the perception of contours and curvature (Wang and Hess, 2005). Orientation pooling is the position-*in*specific integration of localized orientation signals, and contributes to texture perception (e.g., Dakin, 2001). This pooling falls within a category of visual mechanisms that compute summary statistics of the visual periphery such as the mean and variance of orientation, spatial frequency, and size information. Along with characterizing the shape and structure of visual objects and backgrounds, the output of these integration mechanisms are thought to help determine the direction and amplitude of saccadic eye movements when an observer is viewing a novel or changing visual scene (e.g., Alvarez and Oliva, 2008).

Recent work from our lab has suggested that orientation-grouping declines in older age (Roudaia et al., 2008). This decline could be due to a decline in grouping mechanisms (i.e., the intergration of local orientation signals in a position-specific manner), or it could be due to an age-related decline in the ability to integrate local orientation signals, *perse* (i.e., pooling, the integrations of local orientation signals irrespective of their spatial position). To test how age affects pooling, following Dakin (2001) I have attempted to characterize the ability of older subjects to estimate the mean orientation of a set of spatially-disparate, variably oriented, peripheral orientation signals (Govenlock et al., 2009). In one experiment I varied the number of signals available, and in a second experiment I varied the orientation variability of these signals. Using an equivalent noise approach in order to delineate the effects of additive, internal noise (i.e., the extent to which each signal is corrupted internally) from calculation efficiency (i.e., how many of these signals subjects actually utilize), I found no effect of age on either measure. In fact, there is some indication that older subjects perform the task marginally better than younger subjects in some conditions. These results suggest that orientation pooling mechanisms are preserved in older age. Future experimentation ought to test whether pooling is preserved with respect to other sorts of statistics that may be summarized from multiple peripheral signals, such as the mean size or spatial frequency of peripheral signals, as well as estimates of the variability of such signals.

This well-maintained or perhaps even improved ability to pool information across space in older age is advantageous for some perceptual tasks, but may have its drawbacks too. Crowding is the effect whereby a signal in the periphery is less discriminable when it is flanked by distracting stimuli than when it is presented in isolation. Crowding may be thought of as obligatory, maladaptive pooling (Parkes et al., 2001). In ongoing work, I am measuring the effect of older age on the crowding of orientation signals in the near periphery. Early results indicate that older subjects exhibit significantly more crowding in the periphery than do younger subjects, suggesting that the aging visual system becomes more obligated to pool together peripheral visual signals. Considered in the context of age-related compensatory reorganization (Faubert, 2002), that older adults performance declines for grouping and crowding, but not pooling, suggests that grouping and crowding involve more complex computations than pooling.

## 6.3 Increased noise and decreased alpha-band activity in the aged occipital EEG spectrum

In each of the aforementioned single-cell studies on the physiology of senescent primate and feline V1 and V2 neurons, alongside observations of reductions in the selectivity of those neurons for the orientation, spatial frequency, and direction of motion of visual stimuli, those same senescent neurons also consistently exhibited a marked increase in spontaneous firing rates (Schmolesky et al., 2000; Leventhal et al., 2003; Hua et al., 2006; Yu et al., 2006; Hua et al., 2008; Zhang et al., 2008). This increase in spontaneous firing rate in senescence may be conceptualized as internal noise that is added to the neural representation of visual stimuli as it transverses areas V1 and V2. In agreement with this finding, psychophysical studies reporting an age-related decline in for some visual perceptual tasks have attributed that decline to an increase in additive, internal noise (Pardhan 2004; Betts et al. 2007; Bennett et al. 2007, but cf. Pardhan et al. 1996; Bennett et al. 1999).

Although in the current dissertation we did not find an age-related decrease in stimulus-selectivity—which was our primary focus—we did discover support for an age-related increase in spontaneous firing rates in visual cortex neurons. In Chapters 4 and 5 we designed stimuli that elicited EEG activity at very precise, prescribed frequencies. However, when considering the occipital EEG frequency spectra in its entirety, it did

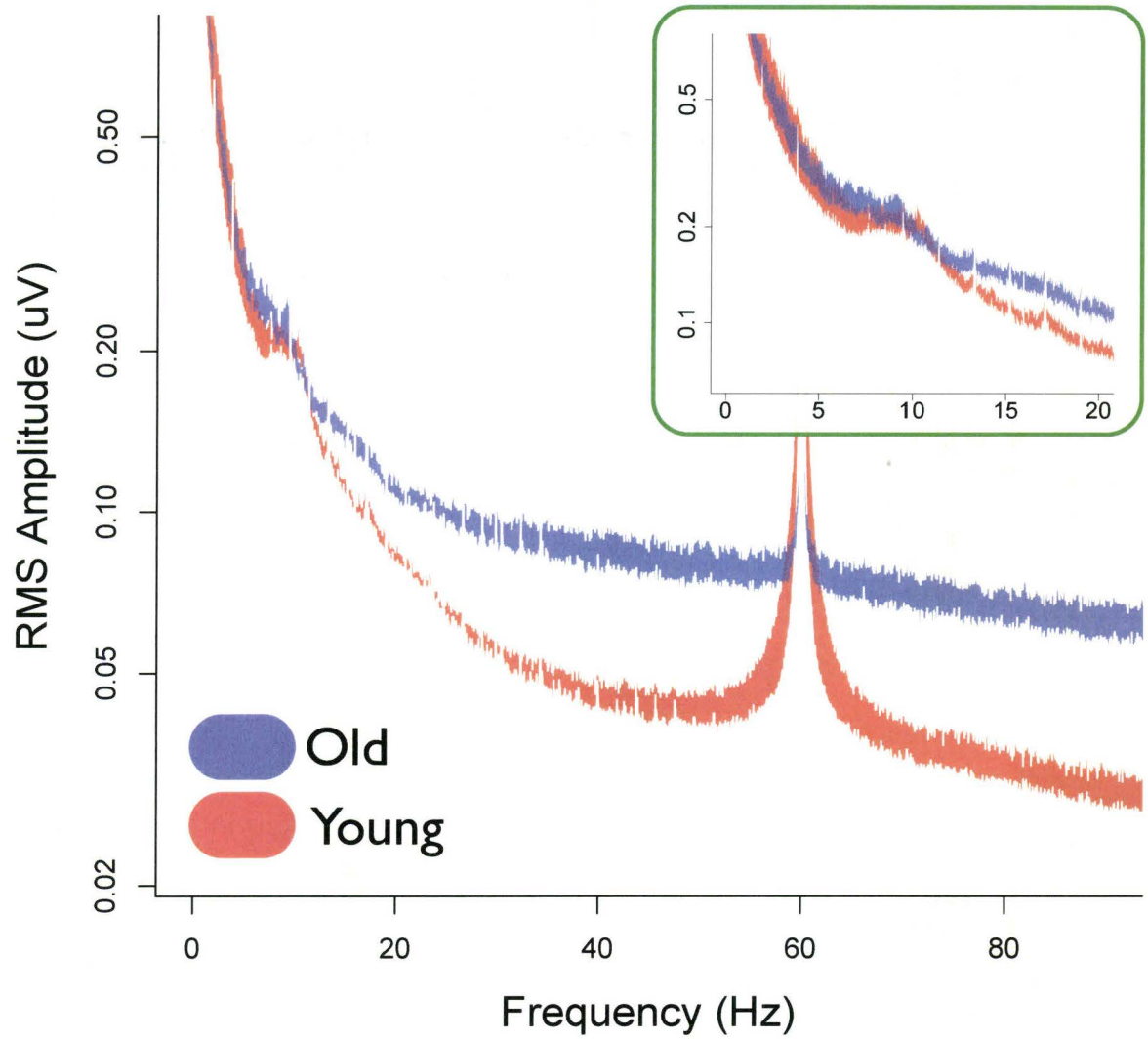


Figure 6.1: EEG frequency amplitude spectra as a function of age. These data are collapsed across Chapters 4 and 5 and across all grating-offset conditions in those experiments. The blue/darker band depicts ± 1 standard error of the mean of older subjects' activity at each frequency; the red/lighter band represents ± 1 standard error about the means in younger subjects. Older subjects demonstrate higher amplitude at frequencies greater than about 15Hz. Older subjects demonstrate relatively weaker alpha (nominally 8 to 12 Hz) energy, as well as a "slowing" of alpha energy (i.e., a shift to lower frequencies). Inset: a closer view of lower frequencies.

not escape our notice that older subjects yielded more energy at frequencies unrelated to our stimulus frequencies. Plotted in Figure 6.1 are the EEG amplitude spectra recorded from subjects in Chapters 4 and 5 as a function of age, averaged across all conditions and all subjects, for their respective electrode-of-interest in those chapters, which was an electrode over or near the occipital pole. EEG amplitude was, on average, higher in older subjects at all frequencies greater than approximately 15 Hz. This increased amplitude may reflect higher spontaneous firing rates of visual cortex neurons in older adults.

Several considerations are warranted, however, before we draw the conclusion that there is more neural activity in the aged visual cortex. First, actual neuronal spiking data from senescent primate single-cells ought to be obtained in order to model and predict where an age-effect should be found in frequency-space, and how strong the effect should be. Second, a better understanding of how volume conduction—the way in which cerebrospinal fluid, mater, skull, and scalp conspire to spread, attenuate, and otherwise pervert the electrical signal produced by neural dipoles before they are recorded by scalp electrodes—changes in older age is needed. Third, an increase in EEG amplitude at mid to high frequencies might not be maladaptive noise: recent developmental work comparing children to young adults suggests that a developmental increase in mid to high frequency EEG amplitude might, instead, be interpreted as an adaptive increase in brain complexity that enhances cognitive and perceptual abilities (e.g., Anokhin et al., 1996; McIntosh et al., 2008). Fourth, subjects in each age group should be considered individually because the distribution of subjects' EEG spectra, for older subjects in particular, may be highly variable and non-normal. Finally, although it seems unlikely that the age-related difference in EEG power was due to our stimuli or task, some additional subjects from each age group ought to be run to verify that this difference persists during resting states, when subjects are either fixating a small, static target, or resting awake with their eyes closed—in which case, this result could be related to what, in fMRI research, is called the "default network;" in disagreement with the current results, Damoiseaux et al. (2008) found that resting-state BOLD activity is reduced in normal aging.

Another feature of the EEG spectra plotted in Figure 6.1 is a weaker energy peak in the alpha band (i.e., frequencies between approximately 8 and 12 Hz) in older subjects. This feature is more discernible when considering the individual subjects' spectra (not shown). Relatively high energy in the alpha band, compared to flanking bands, is characteristic of human EEG (Barlow, 1993). The functional relevance of this activity has been the topic of much research, and is still debated, but seems generally related to attentiveness: Alpha activity is inversely related to wakefulness, increases over occipital sites when subjects

close their eyes, is inversely related to the extent to which subjects are attending to their external environment (Ray and Cole, 1985), and the phase of ongoing alpha oscillations affects the detectability of near-threshold visual stimuli (e.g., Mathewson et al., 2009).

Previous research has reported that, in older age, alpha power is generally weaker, that alpha activity "slows" (i.e., its peak energy shifts to lower frequencies), and that the distribution of alpha power over the scalp shifts from posterior to anterior sites (Niedermeyer, 1997). The current data, therefore, replicate the previous finding of reduced alpha energy in older age, but with a much higher frequency resolution. It is possible that some older subjects' alpha peaks shifted to lower frequencies, whereas others' did not, resulting in group-averaged activity in which it appears that older subjects have weaker alpha activity. Therefore, in future analyses I intend to characterize the effect of age on alpha energy by considering intersubject variability. Insofar as the allocation of attention is known to affect alpha, further experimentation may be required to demonstrate that the current effect of age on alpha was not due an group differences in the deployment of attention.

## 6.4 Using fMRI to investigate orientation selectivity

In Chapters 4 and 5 we employed an EEG technique that may have allowed us to measure the selectivity of the neuronal population response for orientation and spatial frequency in older humans. Both to compliment those results, and, as the case may be, to circumvent a reinterpretation of those results as being due to luminance-selective mechanisms as opposed to orientation or spatial frequency-selective mechanisms (see Discussion sections of those chapters), I have initiated an fMRI project designed to measure such selectivity in the visual cortex of older adults. Sponsored by the CIHR strategic training grant on Social Interaction and Communication in Healthy Aging that my supervisors and I have been involved with, in the summer of 2009 I was generously hosted by Dr. Chris Baker in the Lab of Brain and Cognition at the National Institute of Mental Health (NIMH) at the intramural research campus of the National Institutes of Health (NIH) in Bethesda, Maryland. Similar to the CIHR, the NIH is the research arm of the US Government's Public Health Service. Under the supervision of Dr. Baker, I spent approximately 400 hours learning to design, conduct, and analyze fMRI experiments. Although my expertise is still very much in development, I have since obtained approval from the McMaster Research Ethics Board (REB) and the St. Joseph's Healthcare

Hamilton REB and recently piloted the project here in Hamilton in collaboration with another graduate student in Dr.'s Bennett and Sekuler's lab, Lindsay Farber.

Motivated particularly by the single-cell findings of marked decline in orientation-selectivity in senescent primate V1 and V2 neurons (Schmolesky et al., 2000; Yu et al., 2006), we are employing multivariate pattern analysis techniques that have been used to investigate orientation-selectivity in younger adults (Kamitani and Tong, 2005; Haynes and Rees, 2005). This sort of technique was originally applied to fMRI data by Haxby et al. (2001), among others, in order to test the extent to which blood oxygenation-level dependence (i.e., the BOLD signal) can be used to discriminate the brain's response to different categories or instances of visual objects, and is useful when the patterns of brain activity in question are distributed and spatially overlapping. A multivariate approach can be usefully brought to bear on the issue of orientation-selectivity as follows: neurons preferring a particular orientation are clustered into localized hypercolumns in V1, but many hypercolumns prefer that particular orientation, and they are distributed throughout V1 in a retinotopic manner (Hubel and Wiesel, 1968). A purely horizontal stimulus will elicit activity from all hypercolumns selective for horizontal, which are also responsive to region of the retina on which that stimulus falls. Hypercolumns, spanning about 500$\mu$m across the human cortical surface, are too small to localize within a single functional MRI voxel, which, for currently technical reasons, have a resolution limit of about 2mm$^3$. Thus, voxels are too big to isolate and study the response of a single hypercolumn. However, due to the heterogenous, pseudo-random distribution of hypercolumns, by chance alone, voxels may tend to be biased to contain more hypercolumns selective for one orientation than another. Therefore, a horizontal stimulus will elicit some heterogenous pattern of BOLD activity, and a vertical stimulus will tend to elicit some distinct pattern of BOLD activity. Because hypercolumns are selective for orientation in a bandpass manner, patterns of brain activity for disparately-oriented stimuli will be at least somewhat discriminable, as has been found in young adults (Kamitani and Tong, 2005; Haynes and Rees, 2005); activity elicited by stimuli of nearby orientations are difficult to discriminate, and activity elicited by stimuli of very different orientations is easier to discriminate. If, however, the neurons comprising these hypercolumns become, in the extreme, non-selective for orientation, then a horizontal stimulus will activate all hypercolumns, a vertical stimulus will also activate all hypercolumns, and the patterns of BOLD activity elicited by these two stimuli will be completely indiscriminable from one another.

The multivariate statistical techniques that can be used to discriminate these patterns of BOLD activity include, among others, principle components analysis (PCA), support-

vector machines (SVM), and, most simply, cross-correlation techniques. We will be utilizing the lattermost technique, at least initially: The correlations between patterns of activity elicited by repeated presentations of the same orientation should be higher than the correlations between activity elicited by nearby orientations, which should in turn be higher than correlations between activity elicited by very different orientations. The rate of decline in this correlation as the orientation difference between the stimuli is increased will be taken as a proxy for the orientation-selectivity of visual cortex neurons, *en masse*.

This fMRI-measure of the orientation selectivity of the population response of visual cortical neurons could both corroborate and complement the measurements I have obtained using the ssVEP. The spatial resolvability of the BOLD signal will allow me to assess orientation tuning as a function of visual area (i.e., V1, V2, and V4), whereas it is relatively difficult to isolate the sources of EEG activity, and, because the stimulus will be a single oriented-grating, this fMRI-measure will not be attributable, whether in whole or in part, to a dynamic stimulus luminance or contrast-energy signal (see Discussion section of Chapter 4 and Results section of Chapter 5).

## 6.5 Alternate explanations

Aside from age-related compensatory reorganization or deployment of focused attention, two other possible explanations for the tuning discrepancy found between the primate studies and the current human studies involve cross-species age estimation, and whether the visual stimulus involves motion. Leventhal and colleagues tested older rhesus monkeys between the ages of about 26 and 30 years. In the wild, rhesus monkeys do not typically live past 20. In captivity, about 25% of rhesus monkeys live past the age of 25, and very few live past 30 (Schmolesky et al., 2000). Matching humans in terms of their biological age to the rhesus monkeys in those studies can be an imprecise process. As such, the samples of older humans that participated in the current experiments may not have been as advanced, in terms of age, as the monkeys in the single-cell studies. It is possible, therefore, that greater age differences in orientation- and spatial frequency-selectivity might have emerged if we had tested older human subjects. Arguing against this idea, however, is the finding that psychophysical spatial frequency tuning did not correlate with age in our sample of older subjects (see final paragraph of Section 3.3.2 in Chapter 3). If selectivity does broaden in the oldest of humans, one might expect at least a trend in that direction in the current samples of older humans.

Another possible explanation for this primate-human discrepancy is the fact that Leventhal and colleagues employed *drifting* stimuli when characterizing the orientation- and spatial frequency-selectivity of senescent neurons, whereas in the current thesis I employed static stimuli. It is possible that an effect of age emerges for pattern mechanisms (i.e., those sensitive to orientation and spatial frequency) particularly when those mechanisms are confronted with pattern motion. Indeed, Bennett et al. (2007) found an effect of older age in humans on psychophysical direction-of-motion selectivity using random-dot displays, and Leventhal and colleagues report in several papers that direction-of-motion selectivity also declines in visual cortex neurons in senescent primates (e.g., Schmolesky et al., 2000). Therefore, if Leventhal and colleagues repeated their experiments with static stimuli they may not observe age-related declines in orientation- or spatial frequency-selectivity, and if I repeated the current experiments with drifting stimuli I may observe declines in orientation- and spatial frequency-selectivity. The effect of older age on the interaction between pattern- and motion-selective mechanisms is a topic requiring further research.

Visual neurons in the lateral geniculate nucleus are anatomically and functionally segregable into the magnocellular (M), parvocellular (P), and koniocellular (K) pathways. The neurons in these pathways respond to different types of visual stimuli: M neurons, for example, tend to respond best to motion, high temporal frequencies, and low spatial frequencies, whereas P neurons tend to respond best to color, low temporal frequencies, and high spatial frequencies (Livingstone and Hubel, 1988; Shapley, 1990). The current experiments used brief, low-frequency stimuli that may have preferentially activated the M pathway, and so may have been insensitive to age-related changes in the P and K pathways. In other words, varying the spatial, temporal, and chromatic aspects of the stimuli may reveal larger age differences in orientation- and spatial-frequency selectivity.

## 6.6 Conclusion

Despite reports of marked functional declines in senescent primate V1 and V2 neurons—neurons that are thought to underly the function of low-level visual mechanisms that are selective for orientation and spatial frequency—older human adults do not demonstrate evidence for declines in the selectivity of these low-level mechanisms, either psychophysically or with EEG. This maintenance of selectivity in older humans may be due to age-related compensatory activity that may be engaged by focused attention or consciousness, faculties that were denied the anesthetized primates. Thus, the current dissertation

contributes to our growing understanding of how the brain adaptively responds to the stresses of older age.

# References

Alvarez, G. A., Oliva, A., Apr 2008. The representation of simple ensemble visual features outside the focus of attention. Psychol Sci 19 (4), 392–8.

Anokhin, A. P., Birbaumer, N., Lutzenberger, W., Nikolaev, A., Vogel, F., Jul 1996. Age increases brain complexity. Electroencephalogr Clin Neurophysiol 99 (1), 63–8.

Barlow, J. S., 1993. The electroencephalogram: Its patterns and origins. MIT Press: Cambridge MA.

Bennett, P. J., Sekuler, A. B., McIntosh, A. R., Della-Maggiore, V., 2001. The effects of aging on visual memory: Evidence for functional reorganization of cortical networks. Acta Psychologica 107 (1-3), 249–273.

Bennett, P. J., Sekuler, A. B., Ozin, L., 1999. Effects of aging on calculation efficiency and equivalent noise. Journal of the Optical Society of America. A, Optics, Image science, and Vision 16, 654–658.

Bennett, P. J., Sekuler, R., Sekuler, A. B., 2007. The effects of aging on motion detection and direction identification. Vision Research 47, 799–809.

Betts, L. R., Sekuler, A. B., Bennett, P. J., 2007. The effects of aging on orientation discrimination. Vision Research 47, 1769–1780.

Carrasco, M., Penpeci-Talgar, C., Eckstein, M., Jan 2000. Spatial covert attention increases contrast sensitivity across the csf: support for signal enhancement. Vision Research 40 (10-12), 1203–15.

Dakin, S. C., 2001. Information limit on the spatial integration of local orientation signals. J Opt Soc Am A Opt Image Sci Vis 18 (5), 1016–1026.

Damoiseaux, J. S., Beckmann, C. F., Arigita, E. J. S., Barkhof, F., Scheltens, P., Stam, C. J., Smith, S. M., Rombouts, S. A. R. B., Aug 2008. Reduced resting-state brain activity in the "default network" in normal aging. Cereb Cortex 18 (8), 1856–64.

335 Dawkins, R., 1995. River Out of Eden: A Darwinian View of Life. Basic Books: New
336 York.

337 Di Russo, F., Spinelli, D., 1999. Electrophysiological evidence for an early attentional
338 mechanism in visual processing in humans. Vision Research 39 (18), 2975–85.

339 Faubert, J., Sep 2002. Visual perception and aging. Can J Exp Psychol 56 (3), 164–76.

340 Faubert, J., Bellefeuille, A., Feb 2002. Aging effects on intra- and inter-attribute spatial
341 frequency information for luminance, color, and working memory. Vision Res 42 (3),
342 369–78.

343 Fischer, J., Whitney, D., 2009. Attention narrows position tuning of population responses
344 in v1. Current Biology 19, 1356–1361.

345 Govenlock, S. W., Sekuler, A. B., Bennett, P. J., 2009. The effect of aging on the spatial
346 pooling of local orientation signals. Journal of Vision (VSS conference abstract) 9.

347 Habak, C., Faubert, J., 2000. Larger effect of aging on the perception of higher-order
348 stimuli. Vision Res 40 (8), 943–50.

349 Habak, C., Wilkinson, F., Wilson, H. R., 2008. Aging disrupts the neural transformations
350 that link facial identity across views. Vision Res 48 (1), 9–15.

351 Haenny, P. E., Maunsell, J. H. R., Schiller, P. H., 1988. State dependent activity in
352 monkey visual cortex. Exp Brain Res 69 (245–259).

353 Haxby, J. V., Gobbini, M. I., Furey, M. L., Ishai, A., Schouten, J. L., Pietrini, P., Sep 2001.
354 Distributed and overlapping representations of faces and objects in ventral temporal
355 cortex. Science 293 (5539), 2425–30.

356 Haynes, J.-D., Rees, G., May 2005. Predicting the orientation of invisible stimuli from
357 activity in human primary visual cortex. Nat Neurosci 8 (5), 686–91.

358 Hillyard, S., Hinrichs, H., Tempelmann, C., Morgan, S., Hansen, J., Scheich, H., Heinze,
359 H., 1997. Combining steady-state visual evoked potentials and fmri to localize brain
360 activity during selective attention. Human Brain Mapping 5 (4), 287–292.

361 Hua, T., Kao, C., Sun, Q., Li, X., Zhou, Y., Jan 2008. Decreased proportion of gaba
362 neurons accompanies age-related degradation of neuronal function in cat striate cortex.
363 Brain Res Bull 75 (1), 119–25.

Hua, T., Li, X., He, L., Zhou, Y., Wang, Y., Leventhal, A. G., 2006. Functional degradation of visual cortical cells in old cats. Neurobiology of Aging 27, 155–162.

Hubel, D. H., Wiesel, T. N., Mar 1968. Receptive fields and functional architecture of monkey striate cortex. J Physiol 195 (1), 215–43.

Kamitani, Y., Tong, F., May 2005. Decoding the visual and subjective contents of the human brain. Nat Neurosci 8 (5), 679–85.

Leventhal, A. G., Wang, Y., Pu, M., Zhou, Y., Ma, Y., 2003. GABA and its agonists improved visual cortical function in senescent monkeys. Science 300, 812–815.

Livingstone, M., Hubel, D., 1988. Segregation of form, color, movement, and depth: anatomy, physiology, and perception. Science 240 (4853), 740–9.

Mathewson, K. E., Gratton, G., Fabiani, M., Beck, D. M., Ro, T., Mar 2009. To see or not to see: prestimulus alpha phase predicts visual awareness. J Neurosci 29 (9), 2725–32.

McAdams, C. J., Maunsell, J. H. R., 1999. Effects of attention on the reliability of individual neurons in monkey visual cortex. Neuron 23, 765–773, dEDA.

McAdams, C. J., Reid, R. C., 2005. Attention modulates the responses of simple cells in monkey primary visual cortex. J Neurosci 25 (47), 11023–33.

McIntosh, A. R., Kovacevic, N., Itier, R. J., 2008. Increased brain signal variability accompanies lower behavioral variability in development. PLoS Comput Biol 4 (7), e1000106.

McIntosh, A. R., Sekuler, A. B., Penpeci, C., Rajah, M. N., Grady, C. L., Sekuler, R., Bennett, P. J., 1999. Recruitment of unique neural systems to support visual memory in normal aging. Current Biology 9, 1275–1278.

Müller, M. M., Anderson, S., Trujillo, N. J., Valdes-Sosa, P., Malinowski, P., Hillyard, S. A., 2006. Feature-selective attention enhances color signals in early visual areas of the human brain. Proceedings of the National Academy of Sciences: USA 103, 14250–14254.

Müller, M. M., Hillyard, S., Sep 2000. Concurrent recording of steady-state and transient event-related potentials as indices of visual-spatial selective attention. Clin Neurophysiol 111 (9), 1544–52.

Müller, M. M., Malinowski, P., Gruber, T., Hillyard, S. A., Jul 2003. Sustained division of the attentional spotlight. Nature 424 (6946), 309–12.

394 Müller, M. M., Picton, T. W., Valdes-Sosa, P., Riera, J., Teder-Salejarvi, W. A., Hillyard,
395 S. A., 1998. Effects of spatial selective attention on the steady-state visual evoked
396 potential in the 20-28 hz range. Cognitive Brain Research 6, 249–261.

397 Niedermeyer, E., Jun 1997. Alpha rhythms as physiological and abnormal phenomena.
398 Int J Psychophysiol 26 (1-3), 31–49.

399 Pardhan, S., 2004. Contrast sensitivity loss with aging: sampling efficiency and equivalent
400 noise at different spatial frequencies. J Opt Soc Am A Opt Image Sci Vis 21 (2),
401 169–175.

402 Pardhan, S., Gilchrist, J., Elliott, D. B., Beh, G. K., 1996. A comparison of sampling
403 efficiency and internal noise level in young and old subjects. Vision Res 36 (11),
404 1641–1648.

405 Park, D. C., Reuter-Lorenz, P., 2009. The adaptive brain: aging and neurocognitive
406 scaffolding. Annu Rev Psychol 60, 173–96.

407 Parkes, L., Lund, J., Angelucci, A., Solomon, J. A., Morgan, M., Jul 2001. Compulsory
408 averaging of crowded orientation signals in human vision. Nat Neurosci 4 (7), 739–44.

409 Ray, W. J., Cole, H. W., May 1985. Eeg alpha activity reflects attentional demands, and
410 beta activity reflects emotional and cognitive processes. Science 228 (4700), 750–2.

411 Reuter-Lorenz, P. A., Lustig, C., 2005. Brain aging: Reorganizing discoveries about the
412 aging mind. Curr Opin Neurobiol 15 (2), 245–251.

413 Roudaia, E., Bennett, P., Sekuler, A., 2008. The effect of aging on contour integration.
414 Vision Research 48, 2767–2774.

415 Schmolesky, M. T., Wang, Y., Pu, M., Leventhal, A. G., 2000. Degradation of stimulus
416 selectivity of visual cortical cells in senescent rhesus monkeys. Nature Neuroscience 3,
417 384–390.

418 Sekuler, R., Sekuler, A. B., 2000. Visual perception and cognition. In: Evans, J. G.,
419 Williams, T. F., Beattie, B. L., Michel, J. P., Wilcock, G. K. (Eds.), Oxford Textbook
420 of Geriatric Medicine. Oxford University Press, New York, pp. 874–880.

421 Shapley, R., 1990. Visual sensitivity and parallel retinocortical channels. Annu Rev Psychol
422 41, 635–58.

423 Smith, A., Cotillon-Williams, N., Williams, A., 2006. Attentional modulation in the human
424 striate cortex: The time-course of the bold response and its implications. Neuroimage
425 29, 328–334.

426 Wang, Y. Z., Hess, R. F., 2005. Contributions of local orientation and position features
427 to shape integration. Vision Research 45 (11), 1375–1383.

428 Yeshurun, Y., Carrasco, M., 1998. Attention improves or impairs visual performance by
429 enhancing spatial resolution. Nature 396 (6706), 72–5.

430 Yeshurun, Y., Carrasco, M., Jan 1999. Spatial attention improves performance in spatial
431 resolution tasks. Vision Research 39 (2), 293–306.

432 Yu, S., Wang, Y., Li, X., Zhou, Y., Leventhal, A. G., 2006. Functional degradation of
433 extrastriate visual cortex in senescent rhesus monkeys. Neuroscience 140, 1023–1029.

434 Zhang, J., Wang, X., Wang, Y., Fu, Y., Liang, Z., Ma, Y., Leventhal, A. G., 2008. Spatial
435 and temporal sensitivity degradation of primary visual cortical cells in senescent rhesus
436 monkeys. European Journal of Neuroscience 28, 201–207.